UNIVERSITY OF TRENTO

Department of Cellular, Computational and Integrative Biology

Alpha-1 adrenergic receptors as new targets in Neuroblastoma

PhD Degree in Biomolecular Sciences

Tutor:
Professor Alessandro Quattrone

PhD candidate:
Francesca Broso

ACADEMIC YEAR: 2019/2020

ORIGINAL AUTHORSHIP

Declaration:

I, Francesca Broso, confirm that this is my own work and the use of all material from other sources has been properly and fully acknowledged.

TABLE OF CONTENTS

ABSTRACT

High-risk neuroblastoma (NB) is an aggressive childhood tumor that originates from progenitor neural crest cells. Even if the therapeutic protocol for NB is articulate and aggressive, the outcome remains dismal, with the 5-year disease-free overall survival below rating 50%. A novel drug combination strategy can possibly provide a new solution to this unmet therapeutic need. 13-cis retinoic acid (13-cis-RA, isotretinoin) is an anti-proliferative and pro-differentiative agent currently used in the post-consolidation phase of NB therapy. To identify molecules able to potentiate the anti-proliferative activity of 13-cis-RA, NB cells were treated with a library of 169 naturally occurring polyphenols in combination with the retinoid. This *in vitro* screen led to the identification of isorhamnetin as a synergistic partner of 13-cis-RA, producing an 80% reduction in cell viability. At the molecular level, this synergistic effect is followed by a marked increase in the expression of a member of the catecholamine receptor superfamily: the adrenergic receptor alpha-1B (ADRA1B) suggesting that this receptor might represent a key mediator of the synergistic effect of 13-cis-RA and isorhamnetin observed *in vitro*. This finding redirected our attention to the class of adrenergic receptors (ARs) as novel targets in NB. To investigate the role of ADRA1B in the synergism, we generated CHP134 NB cell lines knocked-out (KO) for the receptor and observed that exposure of CHP134 KO cell to 13-cis-RA leads to a reduction of cell viability and neural differentiation. We, therefore, substituted the genetic KO strategy with the alpha-1B adrenergic antagonist, L765,314, obtaining the same results. Subsequently, we extended the analysis on the role of adrenergic receptors (AR) performing a biased screen using two libraries of AR-ligands. The screen results confirm that the molecules working as alpha-1-ARs antagonists are those that greatly increase cell sensitivity to 13-cis-RA with reduction of cell viability and increase in differentiation. We confirmed our observation in NB xenograft mice models *in vivo*, treating mice with a combination of 13-cis-RA and the FDA approved alpha-1 AR antagonist doxazosin. The proposed pharmacological treatment was effective in slowing tumor growth, leading to tumors of smaller size. From our results, we can conclude that the deletion or inhibition

of alpha-1-AR sensitizes NB cells to 13-Cis-RA, both in terms of induction of apoptosis and neural differentiation.

Since NB is a catecholamine-rich tumor, we propose that antagonization of alpha-1-AR disrupts the established autocrine pro-survival circuit generated by catecholamines in NB and restores the ability of the cells to follow the pro-differentiative and pro-apoptotic programs endorsed by 13-cis-RA. Considering the druggable nature of the alpha-1-AR receptors, we indicate this class of receptors as a novel pharmacological target for the treatment of neuroblastoma.

INTRODUCTION

1. Neuroblastoma

Neuroblastoma (NB) is a neuroendocrine extracranial solid tumor of the sympathetic nervous system. NB is a childhood tumor: almost 90% of NBs are diagnosed before 5 years of age, the average age at diagnosis is 22 months (Esiashvili *et al*, 2009) and the majority of the patient is under 15 years. With an annual incidence of 7-12 new cases per million children (Maris, 2010), NB accounts for 7-8% of all paediatric malignancies which makes NB the third most common tumor of childhood after leukaemia and brain tumors; globally, 15% of children who die of cancer have NB (Maris *et al*, 2007; Kaatsch, 2010; Maris, 2010). Clinically NB is a heterogeneous disease both in terms of manifestation and prognosis. In some cases, it completely regresses spontaneously with full recovery, while in other cases the outcome is unfavourable. Around 50% of the diagnosed patients present a clinically aggressive form of NB with relapse occurring in more than 50% of them (Maris, 2010). Most NBs (~65%) develop in the abdomen at the level of the sympathetic ganglia and/or of the adrenal medulla. Often, metastases are found already at diagnosis (Brodeur, 2003; Maris, 2010).

1.1 Cellular origin

Despite NB progression has been extensively studied, there is still debate about the early stages of its pathogenesis. NB is an elusive cancer deriving from the transient population of the neural crest (NC) cells (Anderson & Axel, 1986; Brodeur, 2003) that, during embryonic development, delaminates from the neural tube undergoing epithelial to mesenchymal transition (Simões-Costa & Bronner, 2015). As such, NB can be considered a developmental tumor caused by an early impairment of the NC cells differentiation program, resulting in poorly differentiated stromal Schwann and neuroblastic cells.

The NC cells, depending on their localization along with the cranium to sacrum anterior-posterior axis, give rise to a variety of cell types including ganglia, cartilage and bones, thymus, melanocytes, adrenal medulla and part of the heart and septum. Till recently, NB was believed to emerge from the trunk NC cells, and particularly from the

sympathoadrenal (SA) sub-lineage, from which the neurons of sympathetic ganglia and the chromaffin cells (ChCs), composing the adrenal medulla, are derived (Huber *et al*, 2009).

In 2017, Furlan *et al*. proposed a new model for adrenal medulla cellular origin (Furlan *et al*, 2017). Furlan and co-workers demonstrated that, in mice, the chromaffin cells of the adrenal medulla are not all deriving from the SA precursors, but the majority of them (about 80%) originate from the Schwann cell (SC) precursors (Furlan *et al*, 2017). Thus, the adrenal medulla is composed of cells of different origins: 20% derived from SA precursors and 80% from SC precursors (Figure 1). The direct consequence of this theory on the origin of the cells composing the adrenal medulla is that NB could originate from two distinct lineages that separate early during embryonic development: SA precursor that gives rise to the para-sympathetic ganglia and a limited portion of the adrenal medulla, and SC precursors that after migration give rise not only to the sympathetic neurons of the ganglia but also to most of the chromaffin cells composing the adrenal medulla (Figure 1). The early split of the NC precursors in the two sub-lineages, SCP and SAP, could explain the observed heterogeneity of NB.

This model has been recently debated by a novel study performed by single-cell RNAseq analysis on human samples of adrenal glands collected at different developmental stages by Jansky *et al*. In their work, they identify neural crest-derived SCP population as the founder of both adrenal chromaffin cells and medullar neuroblasts (Jansky *et al*, 2021). The discrepancy among the mentioned studies could be due to differences in differentiation timing between mice and humans and it highlights the need for more studies on adrenal gland development to better understand the cellular origin of NB.

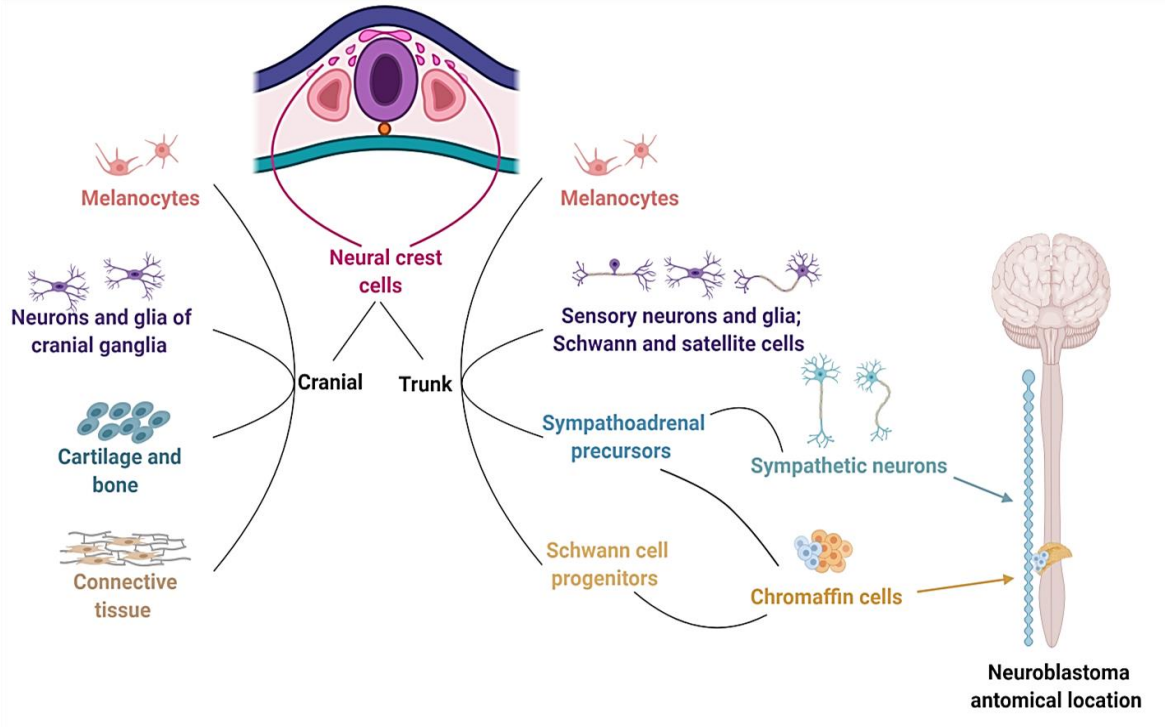

Figure 1. Cellular origin of sympathetic neurons and chromaffin cells according to Furlan *et al*. 2017. The model shows the developmental path of adrenal gland and sympathetic ganglia that are the main anatomical locations of NB. According to this study, the SA precursors give origin to sympathetic ganglia and to 20% of chromaffin cells while the other 80% derives from the SC precursors. According to this model, NB could originate from two subcellular origin lineages.

1.2 Genetic lesions

Neuroblastoma is mainly a sporadic tumor with just 1-2% of the cases ascribed as familial; in these few cases, the inheritance is autosomal dominant with incomplete penetrance (Claviez *et al*, 2004). The most frequent genetic alteration found in NB is the focal amplification of the MYCN (MYCN amplification, MNA) gene, present in 22% of the NB cases and associated with high-risk NB with poor prognosis (Brodeur *et al*, 1984; Seeger *et al*, 1985). The MYCN transcription factor is involved in the control of proliferation, apoptosis, stem-like state and neoplastic transformation (Ruiz-Pérez *et al*, 2017). MYCN expression is detected during the first phases of embryogenesis and is maintained in new-born mice in the kidney, hindbrain, and forebrain, while later in adulthood the expression of MYCN is lost (Zimmerman *et al*, 1986). In humans, the expression of MCYN was found to be present in undifferentiated neural cells of the

fetuses of 12-24 weeks (Grady *et al*, 1987). The embryonic expression of MYCN collimates with its role in pluripotency maintenance, inhibition of differentiation and promotion of proliferation also observed in NB cell lines (Wakamatsu *et al*, 1997; Kang *et al*, 2006; Cotterman & Knoepfler, 2009). Nonetheless, less mature NB cells express higher levels of MCYN and MYCN expression is down-regulated by retinoic acid-induced differentiation of NB cells lines (Thiele *et al*, 1985).

Another gene associated with NB manifestation is *PHOX2B* (Mosse *et al*, 2004; Trochet *et al*, 2004) encoding for a homeodomain transcription factor involved in the promotion of cell cycle arrest and the determination of autonomic peripheral nerve cells from NC cells (Pattyn *et al*, 1999; Trochet *et al*, 2005). As such, a mutation in *PHOX2B* can contribute to the perturbation of sympathoadrenal lineage differentiation leading to NB onset *PHOX2B* (Mosse *et al*, 2004; Trochet *et al*, 2004).

The *ALK* gene (anaplastic lymphoma receptor tyrosine kinase), is another well recognized oncogenic driver of NB; it presents either somatic activating mutations or copy number alteration in about 9-14% of NB cases (George *et al*, 2008; Janoueix-Lerosey *et al*, 2008; Mossé *et al*, 2008; Ogawa *et al*, 2011). During embryo development, ALK is expressed in the sympathoadrenal lineage of NC cells (Iwahara *et al*, 1997; Degoutin *et al*, 2009) where it is involved in the decision between proliferation and differentiation through the activation of multiple signal transduction pathways such as the MAPK-ERK and PI3K-AKT pathways (Souttou *et al*, 2001). When ALK mutation or amplification is concomitant to MYCN amplification the disease is very aggressive and often associated with a lethal outcome (Berry *et al*, 2012).

Mutations in α-thalassemia/mental retardation syndrome X-linked, ATRX, are also correlated with sporadic neuroblastoma (Molenaar *et al*, 2012). The *ATRX* gene encodes for an SWI/SNF chromatin-remodelling ATP-dependent helicases important for the maintenance of guanine-(G)-rich DNA stretches like those present at the centromeres and the end of telomeres (Clynes & Gibbons, 2013; Clynes *et al*, 2015). There is no a clear correlation between ATRX mutations and the onset of NB, but the presence of variations

on the *ATRX* gene is highly associated with age at diagnosis and prognosis with a recurrence of 44% of ATRX mutation in patients older than 12 years with very poor prognosis (Cheung *et al*, 2012). Interestingly the MYCN amplification and *ATRX* genetic lesions appear to be mutually exclusive leading to synthetic lethality in mice (Zeineldin *et al*, 2020). The existing connection between NB and ATRX mutations points out the role of telomere maintenance in NB, and in general in cancers. Thus, it is not surprising that the TERT gene (telomerase reverse transcriptase), is overexpressed in 30% of NB and is a marker of reduced event-free survival (Hiyama *et al*, 1995; Coco *et al*, 2012).

Another oncogenic maker of NB is LIN28B. LIN28B is an RNA binding protein frequently activated in NB that exerts its oncogenic activity through the suppression of biogenesis of microRNAs of the Let-7 family (Molenaar *et al*, 2012). The let-7 family members are tumor suppressors thanks to their silencing action on key oncogenes like MYCN, RAS and CDK6 (Johnson *et al*, 2007; Kumar *et al*, 2007; Yong & Dutta, 2007). The suppression of Let-7 miRNAs by LIN28B results in increased expression of the MYCN protein (Molenaar *et al*, 2012). Other markers of poor prognosis in NB are the abnormal number of chromosomes (aneuploidy) (Look *et al*, 1984), and large segmental chromosomal lesions (Schleiermacher *et al*, 2010). The most frequent segmental chromosomal alterations are deletions of chromosomal regions (LOH) harbouring tumor suppressor genes, such as 1p loss ($1p^-$) (Maris *et al*, 1995; Caron *et al*, 1996), 11q loss ($11q^-$) (Attiyeh et al. 2005), 3p loss ($3p^-$) (Spitz *et al*, 2003) and gain of the regions 17q ($17q^+$) (Bown *et al*, 1999).

1.3 Classification

Neuroblastoma is a tumor characterized by high clinical heterogeneity which poses some problems in the classification and stratification of patients into risk categories, essential to tailor treatments and make a prognosis. Thus, a big effort has been done to establish risk stratification schemes considering all the prognostic factors available. There are two main approaches to stratify NB: the old International Neuroblastoma Staging System (INSS) (Table 1) and the new International Neuroblastoma Risk Group staging system

(INRGSS) (Table 2). The INSS is considering surgical and pathological criteria like the presence of infiltrations and lateralization of the tumor to categorize the disease in five stages: 1, 2, 3, 4 and 4S (Brodeur *et al*, 1988). NB tumors classified as 4S (S for "Special") according to the INSS staging are those NBs of patients under 12 months that show metastatic spread limited to liver, skin and moderate bone marrow infiltration and are characterized by a very favourable prognosis with a high rate of spontaneous tumor regression. Many studies have been done to try to elucidate this phenomenon, for example, it has been observed that the NB cells derived from 4S patients express high levels of the neurotrophin receptor TrKA (tropomyosin receptor kinase A) and as such are more responsive to the ligand NGF (nerve growth factor) leading to neural differentiation (Nakagawara *et al*, 1993; Nakagawara & Brodeur, 1997). Anyway, a clear and defined mechanism through which the tumor regression frequently occurs in this tumor type has not been found yet (Brodeur & Bagatell, 2014).

Table 1. International Neuroblastoma Staging System (INSS)

Stage	***Definition***
1	Localized tumor with complete gross excision, with or without microscopic residual disease; representative ipsilateral lymph nodes negative for tumor microscopically
2A	Localized tumor with incomplete gross excision; representative ipsilateral non-adherent lymph nodes negative for tumor microscopically
2B	Localized tumor with or without complete gross excision; representative ipsilateral non-adherent lymph nodes positive for tumor. Enlarged contralateral lymph nodes must be negative microscopically.
3	Unrespectable unilateral tumor infiltrating across the midline, with or without regional lymph node involvement; or localized unilateral tumor with contralateral regional lymph node involvement or midline tumor with bilateral extension by infiltration or by lymph node involvement
4	Any primary tumor with dissemination to distant lymph nodes, bone, bone marrow, liver, skin and/or other organs
4S	Localized primary tumor (as defined for stages 1, 2A or 2B), with dissemination, limited to skin, liver, and/or bone marrow. Limited to infants < 1 year of age and bone marrow with <10% tumor cell involvement

The new INRGSS classification, developed in 2004 and based on the analysis of 8800 cases of NB, relies on imaging criteria to stratify the disease into four risk groups: very low, low, intermediate and high (Cohn *et al*, 2009) (Table 2).

Table 2. International Neuroblastoma Risk Group Staging System (INRGSS)

Stage	***Definition***
L1	Localized tumor not involving vital structures and defined by the list of image-defined risk factors and confined to one body compartment
L2	Localized tumor with the presence of one or more image-defined risk factors
M	Metastatic disease (except stage MS)
MS	Metastatic disease in children younger than 18 months of age at diagnosis with metastases limited to the skin, liver, and or bone marrow

This new staging system allowed the implementation of INRG classification system (Table 3) that combines the INRGSS with other seven prognostic risk factors: age, histologic category, the grade of tumor differentiation, MYCN status (amplified, MNA vs non-amplified), 11q aberration and ploidy (Look *et al*, 1984) to classify NB into 16 different pre-treatment groups (Pinto *et al*, 2015).

Table 3.International Neuroblastoma Risk Group (INRG) classification system. *except GN (ganglioneuroma) maturing, GNB (ganglioneuroblastoma) intermixed

INRG stage	***Patient age (months)***	***Tumor Histology***	***Tumor differentiation***	***MYCN amplification***	***11q aberration***	***DNA ploidy***	***Pre-treatment risk group***
L1/L2	Any	GN Maturing, GNB intermixed	Any	Any	Any	Any	Very Low
L1	Any	Any*	Any	No	Any	Any	Very Low
MS	<18	Any	Any	No	No	Any	Very Low
L2	<18	Any*	Any	No	No	Any	Low
L2	≥18	GNB nodular, neuroblastoma	Differentiating	No	No	Any	Low
M	<18	Any*	Any	No	Any	Hyperdiploid	Low
L2	<18	Any	Any	No	Yes	Any	Intermediate
L2	≥18	GNB nodular, neuroblastoma	Differentiating	No	Yes	Any	Intermediate
L2	≥18	GNB nodular, neuroblastoma	Poorly differentiated or undifferentiated	No	Any	Any	Intermediate
M	<18	Any	Any	No	Any	diploid	intermediate
L1	Any	Any*	Any	Yes	Any	Any	High
L2	Any	Any	Any	Yes	Any	Any	High
M	<18	Any	Any	Yes	Any	Any	High
M	≥18	Any	Any	Any	Any	Any	High
MS	<18	Any	Any	Yes	Any	Any	High
MS	<18	Any	Any	Any	Yes	Any	High

1.4 Neuroblastoma cell lines

Being a highly heterogeneous disease it is not surprising that also among the established NB cell lines great variability exists. Three distinct NB cell line cellular phenotypes have been identified and characterized: neuroblastic N-type, substrate adherent S-type and intermediate I-type.

N-type cells appear small and rounded with weak adhesion to cell culture vessels and neurites like processes, thus are considered as precursors of the sympathoadrenal cell lineage of the neural crest, and express enzymes for the biosynthesis and uptake of norepinephrine (TH, and DBH) (Ciccarone *et al*, 1989; Ross *et al*, 2003). The N-type cells are fast proliferating cells with high tumorigenic potential and can be induced to differentiate toward the neural phenotype (Piacentini *et al*, 1996; Spengler *et al*, 1997).

On the contrary, the S-type NB cells, are considered to be the precursors of the non-neural lineage of NC cells, so they are the multipotent precursors to Schwann cells, melanocytes and glial cells (Ciccarone *et al*, 1989). At the phenotypic level, the S-type cells display a large and flattened appearance like epithelial or fibroblast cells and adhere easily to the cell-culture substrate. The S-type NB cells are characterized by the expression of vimentin, fibronectin and collagens, which are typically expressed by Schwann cells, melanocytes and mesenchymal cells while lacking neural properties (Ciccarone *et al*, 1989). S-type cells are poorly tumorigenic in nude mice (Piacentini *et al*, 1996; Spengler *et al*, 1997).

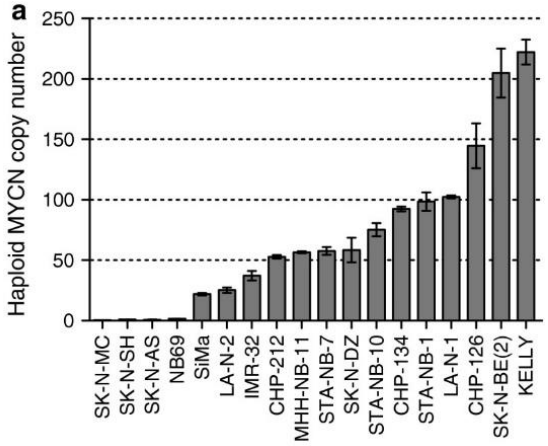

Figure 2. MYCN levels in parental NB cell lines. Haploid MYCN DNA copy number obtained by qPCR. Image form Image from (Sidarovich *et al*, 2014)

Finally, I-type cells are morphologically and biochemically considered to be intermediate to N- and S-type cells.

I-type cells may be a multipotent stem cell or an intermediate stage in the trans-differentiation between N- and S-type cells (Ross *et al*, 1983, 1995; Ciccarone *et al*, 1989).

NB cell lines can also be classified according to the amplification status of the *MCYN* locus but this is not strictly related to the morphological appearance of NB cells neither to their ability to differentiate or tumor aggressiveness (Edsjö *et al*, 2004). This supports the already mentioned heterogeneity of neuroblastoma and further points out the difficulties in finding a highly efficient therapeutic protocol.

1.5 Neuroblastoma therapy

The treatment protocol used for NB is tailored to the INSS, so it varies according to the risk classification.

As already mentioned, infants with INSS stage 4S often show spontaneous regression and as such the patient do not need any treatment (Kholodenko *et al*, 2018).

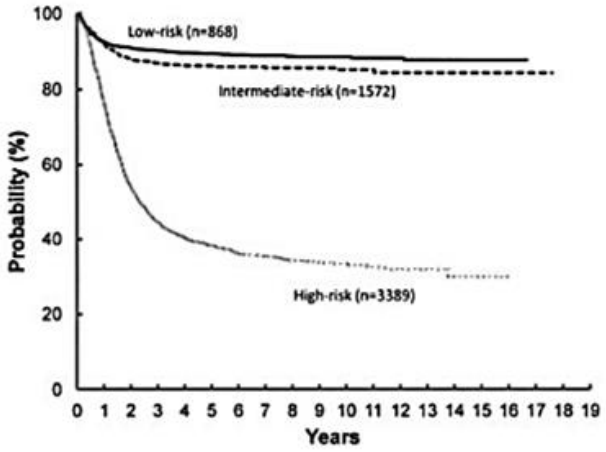

Figure 3. Event free survival (EFS) based on Children's Oncology Group stratification. Kaplan-Meir survival curves were calculated for children enrolled in the Children's oncology Group, Children's Group and Pediatric Oncology Group Neuroblastoma studies. Image from: Julie R. Park, Rochelle Bagatell, and Michael Hogarty. Children's Oncology Group's 2013 Blueprint for Research: Neuroblastoma. Pediatric Blood Cancer, 2012, DOI 10.1002/pbc.24433.

Low-risk patients with tumor confined to one compartment of the body and on lymph nodes infiltration are treated by surgical resection and, eventually, also chemotherapy just for those who show relapse. Thanks to these treatments, the 5-year overall survival (OS) probability of these patients rates 99% (Strother *et al*, 2012) (Figure 3).

The intermediate-risk NB patients are treated with a combination of surgical resection and multidrug chemotherapy; in this case, the 5-year OS is almost 96% (Figure 3). Unfortunately, 50% of children

diagnosed with NB present metastatic high-risk tumors (Kholodenko *et al*, 2018). Currently, these patients are treated with one of the most aggressive treatment protocols used in paediatric oncology that is divided into three phases: induction, consolidation and maintenance (Smith & Foster, 2018) (Figure 4). The induction phase aims to first reduce the tumor mass by chemotherapy and surgery. The following consolidation phase includes high dose chemotherapy combined with autologous hematopoietic stem cells rescue and finally, radiotherapy directed to body sites still showing active disease, to eliminate any residual disease. Finally, the maintenance phase is carried out to reduce as much as possible the eventuality of relapse, by inducing cell differentiation with 13-cis retinoic acid (13-cis-RA) and by immunotherapy with anti-ganglioside 2 antibodies (GD2) (Smith & Foster, 2018). Despite these treatments, children with high-risk NB have still very unfavourable outcomes: up to 60% of patients experience relapses and the 5-year disease-free survival rates between 25% and 35% (Figure 3) (Park *et al*, 2013).

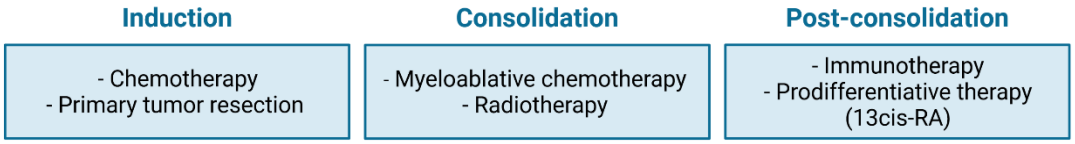

Figure 4. Workflow of neuroblastoma therapy. The treatment protocol for NB is composed of three subsequent phases: induction, consolidation, and post-consolidation. For each phase is reported the administered treatment.

1.5.1 13-cis-Retinoic Acid

Interest in differentiating agents for the NB treatment first came from the clinical observation of spontaneous maturation of the INSS stage 4S NBs. Retinoids have been studied in cancer therapy, for their ability to block proliferation and induce differentiation. Retinoic acid (RA), the main biologically active component of vitamin A (retinol) is known to reverse malignant cell growth *in vivo* and *in vitro* of several types of tumors (Bushue & Wan, 2010), and is well known for its role as anteroposterior determinant during embryonic development (Duester, 2008).

The multiple effects of retinoids are mediated by the classical pathway involving two classes of nuclear receptors: retinoic acid receptors (RARs: α, β and γ) and retinoid X receptors (RXRs) (Bayeva *et al*, 2021). RA is transported into the nucleus by the cellular RA-binding protein (CRABP) and delivered to RAR/RXRs receptors, which, after hetero-oligomerization, function as ligand-dependent transcription factors to inhibit cells growth, induce cells cycle arrest and promote cell differentiation (Di Masi *et al*, 2015a; Bayeva *et al*, 2021) (Figure 5). Another possibility is the so-called non-genomic pathway, in which the RA is bound by non-classical receptors such as ER, and PPAR gamma. These non-genomic pathways exert a strong anti-apoptotic and proliferative effect, anyway, given the stronger affinity of RA for RARs than for other receptors, the classical pathway has a dominant role over the non-genomic pathways (Di Masi *et al*, 2015a) (Figure 5).

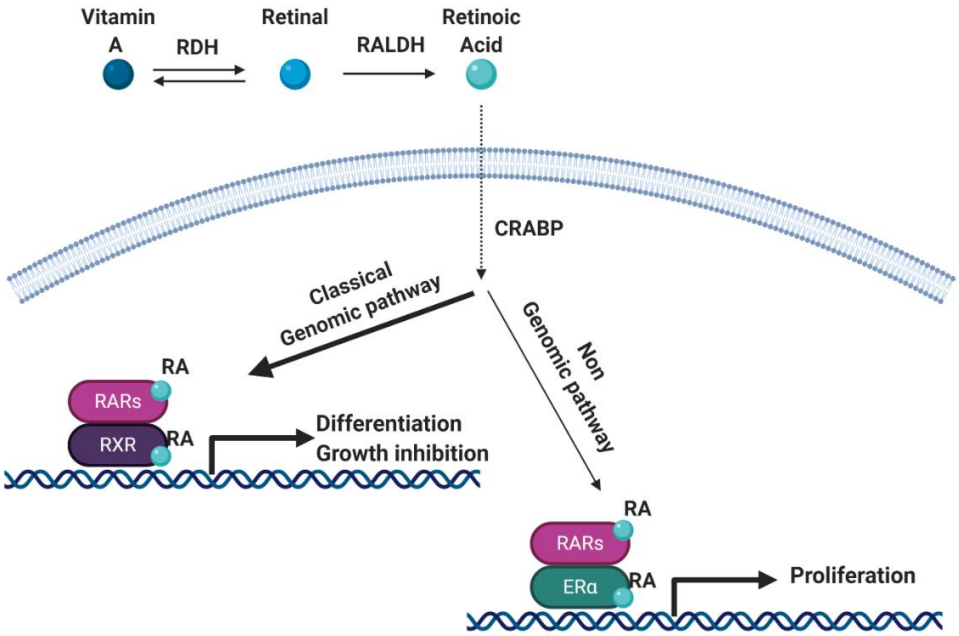

Figure 5. Retinoic Acid signaling pathway. RA binding protein transports RA into the nucleus, where RA binds to its receptors (RAR/RXRs), which function as ligand dependent transcription factors to promote inhibition of cells growth, cells cycle arrest and cell differentiation In alternative RA binds to ER receptor for the activation of non-genomic pathway for promotion of proliferation (Di Masi *et al*, 2015; Bayeva *et al*, 2021). RDH= Retinol Dehydrogenase, RALDH= Retinaldehyde Dehydrogenase, CRABP= Cellular Retinoic Acid Binding Protein, RARs=Retinoic Acid Receptos, RXR=Retinoic X Receptor, ER=Estrogen Receptor, RA=Retinoic Acid

The RAR and RXR family of retinoic acid receptors are expressed in several human NB cell lines (Li *et al*, 1994), and RA can inhibit proliferation and promote neurite outgrowth in several human NB cell lines *in vitro* and *in vivo* (Sidell *et al*, 1982, 1983; Phhlman *et al*, 1984; Abemayor, 1992; Mena *et al*, 1994). RA exist in three isomeric forms: all-trans RA (ATRA), 13-cis-RA (isotretinoin) and 9-cis-RA. Due to its favourable pharmacokinetic profile, lower toxicity and higher stability with respect to other isoforms, 13-cis-RA is the preferred one for NB therapy (Matthay *et al*, 1999; Ponthan *et al*, 2001; Veal *et al*, 2013).

Several pharmacokinetic studies have demonstrated that the peak blood drug levels achieved in NB patients receiving 13-cis-RA administered as high-dose pulse therapy, is above the 5μM (Villablanca *et al*, 1995) which is in line with the concentration required to inhibit the growth of NB cells *in vitro* (Reynolds *et al*, 1994). A trial showed that 13-cis-RA improved event-free survival in advanced stage NB patients when given after either autologous bone marrow transplantation or non-myeloablative chemotherapy. However, approximately 50% of patients develop resistance or are unresponsive to 13-cis-RA therapy, emphasizing the need for novel approaches (Matthay *et al*, 1999).

At the molecular level, the exposure of NB cell lines to 13-cis-RA has been reported to associate with a down-regulation of *MCYN* (Thiele *et al*, 1985; Gaetano *et al*, 1991) and with an increased expression of "classical" and "newly" identified neural differentiation markers such as Trk (Tropomyosin receptor kinase A), βIII-tubulin, Map2 (microtubule associate protein), TH (tyrosine hydroxylase), NeuN (Neural nuclear protein), GAP43 (growth-associated protein), p-ERK (extracellular signal-regulated kinase), pAKT (protein kinase B) and p21 (Qiao *et al*, 2012; Bayeva *et al*, 2021) and neurites-like outgrowth. The 13-cis-RA induced differentiation is also accompanied by a decreased expression of the neuroblastoma driver PHOX2B which goes along with a diminished self-renewal capacity and inhibition of tumorigenicity (Yang *et al*, 2016).

A role for the transcription factor SOX9 (SRY-Box Transcription Factor 9) as a mediator of 13-cis-RA induced growth inhibition has been reported in breast cancer, where it has been observed that RARs agonists induce *SOX9* expression (Afonja *et al*, 2002). The same

group demonstrated that the activation of *SOX9* transcription by RA leads to its binding to the enhancer of the transcription factor gene *HES-1* (Hairy and enhancer of split-1) with consequent promotion of its expression (Müller *et al*, 2010). *HES-1* is highly expressed in neo-epithelial and epithelial cells during embryo development and loss of *HES-1* in mice leads to defects in neural tube formation, indicating its role in the regulation of neurogenesis (Ishibashi *et al*, 1995). Importantly, studies on NB differentiation demonstrate that transient activation of HES-1 plays a pivotal role in promoting sympathetic neural differentiation of SH-SY5Y and SK-N-BE NB cells lines (Grynfeld *et al*, 2000; Axelson, 2004).

RA effects are caused by the activation of downstream signalling pathways (Figure 5), therefore, some compounds that are able to interact with these cascades can influence RA final action. For example, MEK inhibitors decreased the pro-differentiative effects of ATRA in SHSY5Y NB cells. On the contrary, inhibition of PKC (protein kinase C) resulted in the promotion of neurite formation (Delaune *et al*, 2007).

Finally, it is clear that the response to RA treatment largely varies across NB cell lines with some showing resistance to 13-cis-RA, which could explain the lack of complete response in patients (Gaetano *et al*, 1991; Cohen *et al*, 1995; Di Francesco *et al*, 2007; Bayeva *et al*, 2021).

1.6 Catecholamines in Neuroblastoma

Neurotransmitters are endogenous chemical messengers used by the cells of the nervous system to communicate among them and to communicate with other target cells spread all around the body. The components of the sympathetic peripheral nervous system such as the postganglionic neurons of the sympathetic ganglia and the chromaffin cells of the adrenal medulla, secrete specific neurotransmitters known as catecholamines, which are: dopamine (DA), noradrenaline (NA or norepinephrine, NE) and adrenaline (ADR, or epinephrine, E). NE and E neurotransmitters, exert their effects on target cells by binding to different adrenergic receptors (ARs).

Generally, the adrenoceptors are expressed in several tissue and organs, where they are involved in the control of important functions such as vasodilation\vasoconstriction, rate and strength of cardiac muscle contraction, digestion, respiration, metabolism, and endocrine functions. The importance of catecholamine metabolisms in NB is widely recognized as it can be classified as a neuroendocrine tumor. Almost 90% of NBs secretes high levels of catecholamines and their metabolites are detectable in patient's urine samples (Maris 2010). For this reason, the serum and/or urinary level of catecholamine metabolites like vanillyl mandelic acid (VMA), homovanillic acid (HVA) and dopamine (DA) has been introduced as diagnostic and prognostic parameters (Maris, 2010).

A high level of urinary dopamine has been associated with INSS stage 4 NBs, while the favourable 4S stage is characterized by low levels of DA and high levels of VMA (Strenger *et al*, 2007). The high ratio VMA/HVA is a predictor of good prognosis and is indicated as a parameter for the classification of high risk and low-risk NBs (Brodeur *et al*, 1993). Patients with stages 3 and 4 NB have higher levels of DA compared to lower stages patients (Nakagawara *et al*, 1988; Strenger *et al*, 2007). More recently the metabolite normetanephrine (MNA) has been evaluated and found to correlate with the NB stages: low levels are found in stage 1 patients with increasing levels toward the 4 stage and lower levels in 4S (Verly *et al*, 2017).

2. Adrenergic receptors signalling

ARs are members of the class of the guanine nucleotide-binding G-protein coupled receptors, so are receptors able to activate heterotrimeric G proteins after the binding of the ligand. The ARs are divided into three subfamilies: the α_1, α_2 and β based on different pharmacological features and catecholamine affinity, the type of G protein-associated and thus the type of secondary messenger targeted and the effect on it (Table 4) (Figure 6). Each subfamily is composed of several subtypes: α_{1A}, α_{1B} and α_{1D}, α_{2A}, α_{2B} and α_{2C}, β_1, β_2, and β_3 (Ruffolo *et al*, 1991; Stein, 2012).

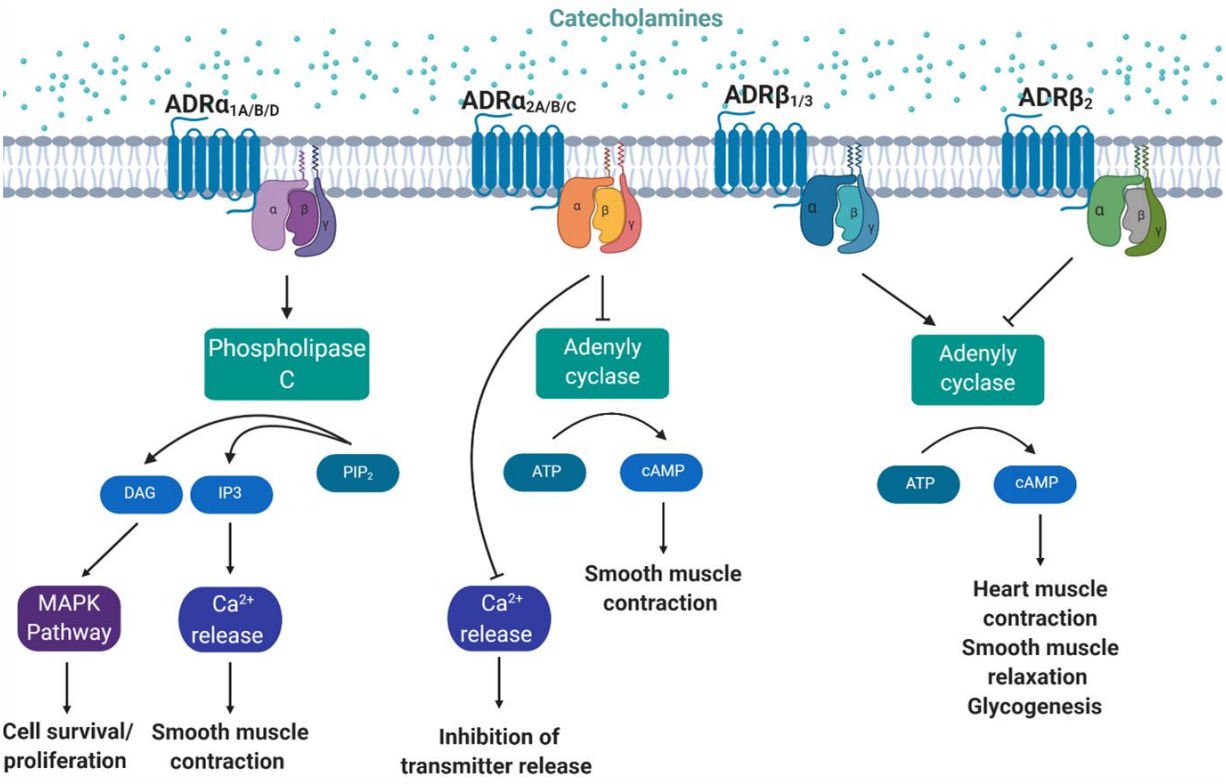

Figure 6. Signal transduction pathways of adrenergic receptors. The α1-ARs are coupled with G_q G proteins and their signalling pathway starts with the activation of the phospholipase C for the hydrolysis of phosphatidylinositol 4,5 bisphosphate (PIP_2) which in tuns generates the second messenger inositol (1,4,5 triphosphate) (IP3) and diacylglycerol (DAG). PIP3 is then responsible for the release of Ca^{2+} from the intracellular stores that will act synergistically with DAG in the activation of protein kinase c (PKC). The α2-ARs are coupled with $G_{\alpha i}$ proteins, their activation provokes reduction of cAMP (cyclic adenosine monophosphate) and Ca^{2+} levels that lead to smooth muscle contraction and suppression of NA and ADR release. β1/2-ARs coupled with $G_{\alpha s}$ which promote the action of adenylyl cyclase with consequent increase in cAMP and positive chronotropic and inotropic effect at cardiac level and increase in lipolysis. On the other hand, β3-ARs action is mediated by $G_{\alpha s}$ and $G_{\alpha i}$, the last mediates inhibition of cAMP production and thus smooth muscle relaxation (Ruffolo *et al*, 1991; Stein, 2012).

Table 4. Adrenergic receptors subtypes characteristics. For each receptor is reported the type of coupled G-protein and the effect on the second messenger

Receptor	*Affinity*	*G protein*	*Effect on the second messenger*
α_{1A} α_{1B} α_{1D}	NA>ADR	G_q	Activation of PLCγ
α_{2A} α_{2B} α_{2C}	NA>ADR	$G_{i\alpha}$	Decrease of AMPc
β_1 β_2 β_3	NA=ADR	$G_{s\alpha}$	Increase of AMPc

Adrenergic receptor agonists and antagonists are used for therapeutic porpoise for decades. In general, adrenergic drugs are used as bronchodilators, vasopressors, and cardiac stimulators. For example, the alpha-blockers work by inhibiting the uptake of circulating catecholamines and thus leading to a lowering of blood pressure because of smooth muscle relaxation; while the beta-adrenergic antagonists are commonly used to control cardiac arrhythmias and angina pectoris (Miller & Cumpston, 2014; Dézsi & Szentes, 2017).

2.1 Adrenergic signalling in the control of cancer cell proliferation

As part of the G-protein coupled receptors superfamily, the adrenoceptor has been recognized as a modulator of pivotal pathways involved in the regulation of cell growth and proliferation.

Originally, in 1991, Allen and colleagues demonstrated that transfection of the α_{1B}-adrenergic receptor into Rat-1 and NIH3T3 fibroblasts, and consequent treatment with a receptor agonist, lead to the formation of foci, signs of the high rate of cell proliferation. The transfected fibroblast also showed a gain of tumorigenic ability when injected into mice (Allen *et al*, 1991). These data indicate that the gene encoding for α_{1B}-AR acts as a proto-oncogene, and was further confirmed by mutagenesis experiments in which activating mutations at specific sites (288, 290 and 293) augment the number of formed foci without agonist stimulation (Allen *et al*, 1991). *In vivo* studies on α_{1B}-AR confirmed

its role in the control of cell proliferation; transgenic mice with the constitutively active form of α_{1B}-ARs expressed specifically in the heart exhibit cardiac hypertrophy with defect of heart contraction (Milano *et al*, 1994).

Several studies focused on the downstream pro-proliferative signalling pathways modulated by different ARs families. It has been demonstrated that α_1-ARs stimulate the MAPK pathways (Hu *et al*, 1999), and in particular, studies on rat pheochromocytoma cells line PC12, establish that α_{1A}-AR acts on all the three major subfamilies of MAPK (JNKs, p38 and ERKs), α_{1B}-AR activates p38 and ERKs, while α_{1D}-AR exerts its action just through the ERKs (Zhong & Minneman, 1999). In contrast, another study with NIH3T3 cells demonstrated that α_{1A} and $\alpha_{1B,}$ but not α_{1D}, stimulates the MAPK, PI3K and RAS pathways (Hu *et al*, 1999).

Studies employing AR-agonists and antagonists further demonstrated their involvement in the modulation of cancer progression. For instance, challenging PC-2 and PC-3 cell lines with the α2-ARs antagonist yohimbine leads to inhibition of cell proliferation (Shen et al. 2008); the blockage of β2-AR or β2-AR with antagonists induces apoptosis and stops the proliferation of NB cell lines *in vitro* and *in vivo* (Wolter *et al*, 2014) via suppression of the mTOR pathway (Deng *et al*, 2019); the non-selective α1-antagonists doxazosin has been reported to promote cell death in glioblastoma cell lines through the inhibition of the PI3K/AKT pathway and the increase in TP53 protein levels (Gaelzer *et al*, 2016).

All these data are in line with the observation that both E and NE have pro-proliferative effects when added to cells in culture. Xin-you and colleagues demonstrated that the exposure of pancreatic cancer cells to NE stimulates cell proliferation, with an increase in the S-phase population, and induction of phosphorylation of the MAPK p38 (Huang *et al*, 2011). A study on breast cancer cell lines reports that addition to culture media of NE, E or α2-ARs agonists stimulate cell proliferation and the effect is reversed by the antagonist rauwolscine (Vázquez *et al*, 2006). Also, β-ARs have been implicated in breast cancer progression; the treatment of MDA-MB-231, ER-negative breast cancer cell line,

with NE, augments the migration and adhesion of the cancer cells to endothelial cells, and that this effect is mediated by the β1-AR (Strell *et al*, 2012).

2.2 Adrenergic signalling in the control of neurogenesis

Recently, taking advantage of the existing AR modulators, studies have been published addressing the role of adrenergic receptors in neural differentiation.

In 2009, Gupta et al. demonstrated that neurospheres isolated from α1A-AR expressing mice present lower cloning efficiency and mainly originate neural germ layer cells (Gupta *et al*, 2009). α2-ARs has been shown to induce neural differentiation also in rat pheochromocytoma PC-12 cells following a subtype-specific agonist stimulation (Lymperopoulos *et al*, 2006). In this case, the induction of neural differentiation by alpha-2-Ars resulted to be sustained by the activation of CREB (cAMP response element-binding protein) mediated by GRK-2 (TrkA-activated GPCR kinase) (Karkoulias *et al*, 2020).

On the other hand, other studies demonstrate that blockage instead of activation of α-ARs promotes neural differentiation. For example, the α1-AR antagonist tamsulosin has been demonstrated to sustain neurogenesis by activation of PKC/CREB and PI3K/Akt pathways in old rats(Kim *et al*, 2017), and the α2-AR antagonist dexefaroxan was shown to be able to promote hippocampal neurogenesis (Rizk *et al*, 2006).

The opposing effect has been also reported not only in terms of activation and inhibition but also among the different sub-families of ARs. For example, the activation of different adrenergic receptor subtypes has been reported to have a divergent effect on hippocampal neurogenesis: the stimulation of α2-AR decreases the hippocampal neurogenesis, while β-AR activation improves the activity of hippocampal precursors cells (Jhaveri *et al*, 2014).

All these observations indicate that the role of adrenergic receptors in neural differentiation can vary according to the activated\inhibited receptor subtype and to the target tissue. Even though there is not a clear picture of the role of all the ARs in induction/inhibition of neurogenesis, all the reported studies suggest that ARs are interesting targets whose role in NB differentiation is worth investigating.

2.3 Crosstalk of 13-cis-RA and adrenergic signalling

Due to the role of RA as an activator of pathways involved in the control of cell proliferation and differentiation in tissues relevant for the adrenergic signalling (i.e. cardiac (Nakajima, 2019) and sympathetic nervous system (Chandrasekaran *et al*, 2000)), some studies have been carried out to assay the presence of a cross-talk between the RA and AR signalling. For example, it has been demonstrated that the biosynthetic and transport pathways for RA are both deregulated in cardiomyocytes of adrenergic-deficient mice (*Dbh*$^{-/-}$) (Osuala *et al*, 2012). As a consequence of the adrenergic deficiency and alteration of RA pathways, the *Dbh*$^{-/-}$ mice embryos die at E10.5 by heart failure indicating that RA could be a mediator of adrenergic action in early phases of heart development (Osuala *et al*, 2012).

An interplay between adrenergic signalling and RA has also been reported in some types of cancer. A study on teratocarcinoma stem cells demonstrated that the endodermal differentiation pursuit by these cells upon RA exposure is accompanied by an increase in the expression of β-AR and modulation of G-proteins expression levels (Galvin-Parton *et al*, 1990). This finding was further confirmed by the identification of the RA-responsive domain in the promoter of the β1-AR gene (Bahouth *et al*, 1998). Furthermore, it has been reported that in lung cancer cells, RA is involved in the modulation of cAMP levels; the exposure of the cells to either 13-cis-RA or 9-cis-RA lead to an increase in intracellular levels of cAMP the secondary messenger of alpha-2-AR and beta-AR (Al-Wadei & Schuller, 2006).

All these studies indicate the presence of crosstalk between the AR and the RA signalling pathways and since both are involved in the control of cancer proliferation (See section 1.5.1 and section 2.1) this interplay can open new routes for the setup of novel therapy via the co-modulation of these two signalling cascades.

3. Flavonoids

In the last 15 years, research for new drugs to be used in oncology has refocused on natural products. Flavonoids are plant secondary metabolites characterized by a low molecular weight phenolic structure with a diphenyl propane (C6C3C6) skeleton. The diphenyl propane skeleton is shared by all flavonoids but they can be classified into six classes depending on the carbon of the C ring on which the B ring is attached and the degree of unsaturation and oxidation of the C ring: anthocyanins, chalcones, flavanone, flavones, flavonols and isoflavonoids (Panche *et al*, 2016).

All these compounds have been subjected to wide experimentation, to check their possible roles in human health. Flavonoids have been demonstrated to exhibit a broad spectrum of biological activities beneficial for human health serving as anti-oxidants (Procházková *et al*, 2011), anti-microbial, anti-viral, anti-inflammatory, cardio-protective (Hertog *et al*, 1993), neuroprotective (Gutierrez-Merino *et al*, 2011) and anti-cancer compounds (Rodríguez-García *et al*, 2019). Initially, the beneficial biological functions of flavonoids have been ascribed to their antioxidant properties; anyway, more recently their role as a modulator of key signalling pathways has emerged, with the regulation of inflammation and cell proliferation (Ramos, 2008).

For example, they can modulate the PI3K/AKT/mTOR pathway to induce cell cycle arrest, apoptosis and autophagy in breast cancer cell lines (Zhang *et al*, 2018). Other pivotal cancer-related pathways reported to be modulated by flavonoids are the NFkB(Li & Sarkar, 2002), the MAPK (Huang *et al*, 2005) the Notch (Wang *et al*, 2006) and the WNT pathways (Kawahara *et al*, 2009; Sarkar *et al*, 2009; Amado *et al*, 2011). Flavonoids can

induce cell cycle arrest, by increasing levels of CDIs (Cyciline dependent kinase inhibitors) and inhibiting cyclins, and apoptosis, through cytochrome-c release, activation of caspases and down- or up-regulation of Bcl-2 family members (Ramos, 2008). The role of flavonoids has been also recognized in inhibition of survival/proliferation signals (AKT, MAPK, NF-κB, etc.) and inflammation (COX-2, TNF secretion, etc.), as well as suppression of key proteins involved in angiogenesis and metastasis in cellular and animal cancer models (Ramos, 2008).

The anti-cancer properties of flavonoids have been evaluated also on NB cells. For example, it has been shown that the flavonoids isoliquiritigenin and epigallocatechin can induce growth arrest and cell death in SH-SY5Y cells (Escobar *et al*, 2019) (Wan *et al*, 2021).

AIM OF THE STUDY

This thesis project aims at the identification of a new therapeutic strategy for neuroblastoma. Currently, the therapeutic protocol for NB foresees the tumor resection followed by chemotherapy and a final pro-differentiative treatment with 13-cis-RA. This last step of the protocol is of pivotal importance to reduce the tumor proliferative potential and to avoid tumor relapse. Thus, the goal of this study is to identify a compound that can improve the anti-proliferative and pro-differentiative effect of 13-cis-RA. The alpha-adrenergic receptors are a member of the G-protein-coupled receptors (GPCRs) family and as such, they are involved in the control of essential cellular functions like cell proliferation. Moreover, a role in neural differentiation and a cross-talk with retinoic acid signalling has been proposed for this class of receptors (see sections 2.2 and 2.3) in other types of malignancies. Starting from these considerations we investigated the role of ARs in modulating the cellular response to the treatment with 13-cis-RA in terms of inhibition of proliferation and increase of differentiation.

STARTING RESULTS

To identify a molecule able to potentiate the anti-proliferative effects of 13-cis-RA, a high throughput screening was performed challenging CHP134 neuroblastoma cells with a low dose of retinoic acid in combination with a library of 169 natural compounds (Figure 7 A). Setting the threshold to 80% growth inhibition, the screening highlighted 10 ten natural compounds representing different chemical or sharing strong structural similarities able to increase the anti-proliferative role of 13-cis-RA (Figure 7 B). Further analysis on these hits pointed out that 13-cis RA and isorhamnetin combination showed the most synergistic effect on the inhibition of CHP134 cell growth. Evaluating different combinations of drug concentrations, the rate 1:3 between the retinoid and isorhamnetin, resulted to be the more effective with significant reduction of cell viability already at 5μM of 13-cis-RA and 15μM of isorhamnetin (Figure 7 C-D).

The reported synergistic effect was observed in different neuroblastoma cell lines, regardless of the status of MYCN amplification status (Figure 8 A-D).
We tested the drugs combination also on CHP134 3D spheroids used to mimic tumour-like cell aggregates; when used together, 13-cis-RA and isorhamnetin lowered cell viability (Figure 9 B) and induced cell death of the cellular spheroids already after 48h as showed by the sytox dye staining (Figure 9 A).

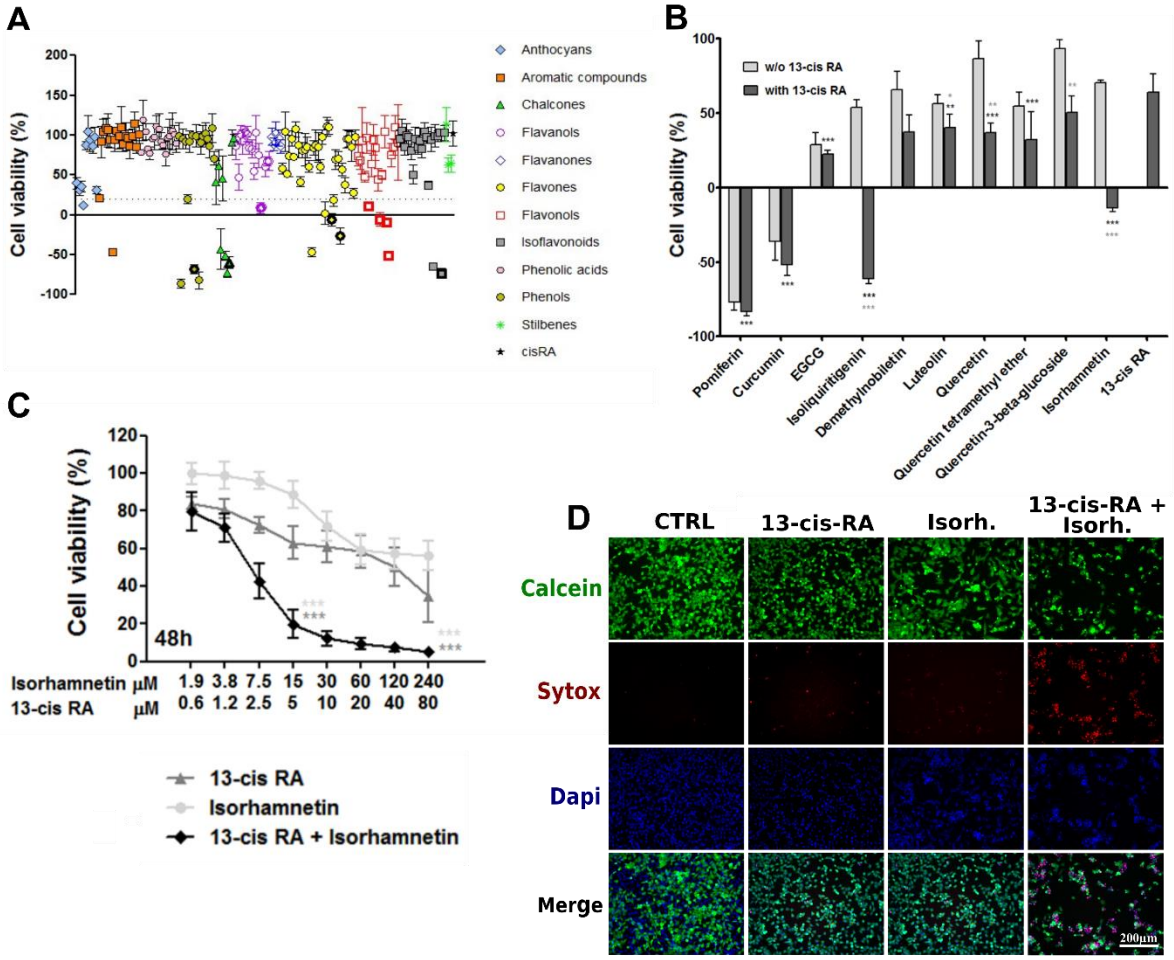

Figure 7. 13-cis-RA and the flavonoid isorhamnetin have a synergistic impact on NB cells viability. (A) Results of the high throughput screening; cell viability CHP134 cells treated with 169 natural compounds library (10µM) and 0.05 µM 13-cis-RA for 48h is represented as the percentage of viable cells relative to 0.1% DMSO-treated controls considering time-zero measurement. Ten compound combinations inhibiting more than 80% of cell growth (lower dotted line), were selected for validation (in bold). **(B)** CHP134 cells were treated with ten hits (10µM) alone or in presence of 13-cis-RA (5µM) for 48h. Cell viability represents the percentage of viable treated cells compared to viable cells before treatment starts. Statistically significant differences between double treatment and 13-cis-RA treatment (black asterisks) and natural compound treatment (grey asterisks) were calculated according to a two-tailed unpaired t-test. **(C)** Cell viability of CHP134 cells exposed for 48h to 2-fold serial dilutions of isorhamnetin and 13-cis-RA at 1:3 ratio. Data are normalized on DMSO treated cells. Statistically significant differences between double treatment and 13-cis-RA treatment (black asterisks) and natural compound treatment (grey asterisks) were calculated according to two-way ANOVA followed by Dunnett's multiple comparisons tests. **(D)** Representative images of the effect of single and combined treatments for 48h on CHP134 cells. Cells were stained with the live cell labelling dye, calcein (green) and the dead cell marker Sytox (red). Cells imaged with 20X long WD objective. (A-B-C). Data obtained by Dr Pamela Gatto.

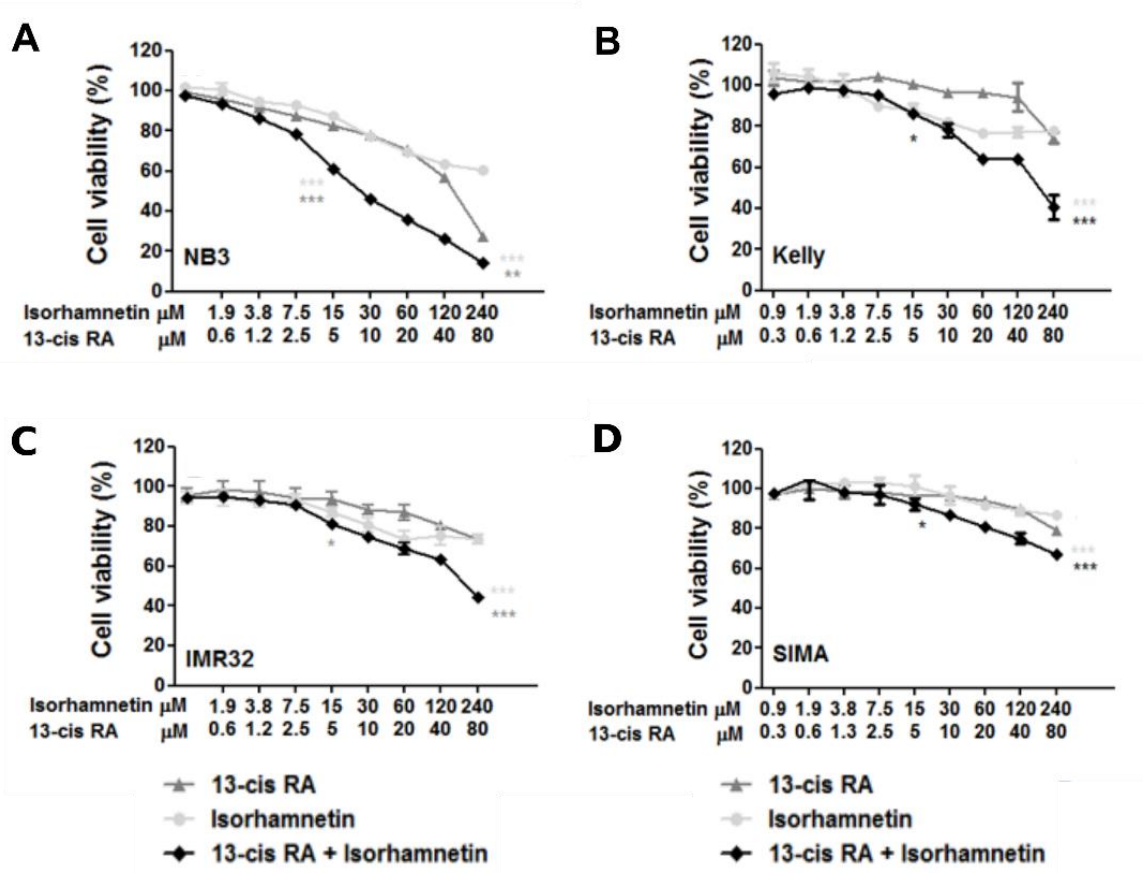

Figure 8. The combination of isorhamnetin and 13-cis-RA is effective and synergistic in several neuroblastoma cell lines. Cell viability of **(A)** NB3, **(B)** Kelly, **(C)** IMR32 and **(D)** SIMA treated with a range of 2-fold serial dilution of isorhamnetin and 13-cis-RA for 48h. Statistically significant differences between double treatment and 13-cis RA treatment (dark grey asterisk) and natural compound treatment (light grey asterisk) were calculated according to two-way ANOVA followed by Dunnett's multiple comparisons tests. Data obtained by Dr Pamela Gatto.

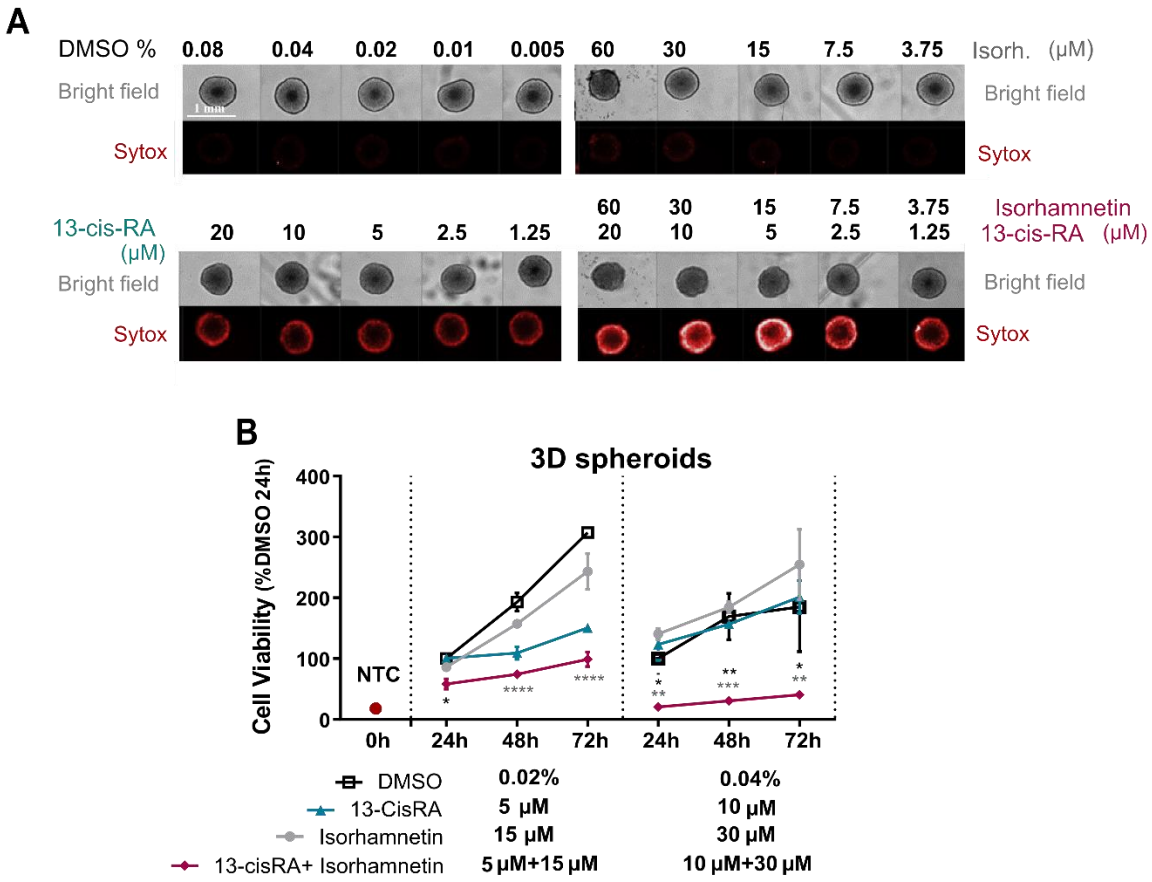

Figure 9. The combination of 13-cis-RA and isorhamnetin lowers the cell viability of NB spheroids. **(A)** Images of 3D spheroid (CHP134 cell line) treated with 13-cis-RA and isorhamnetin alone or in combination. After 48h the spheroids were stained with the death cell marker Sytox and imaged with 10X long WD objective**. (B)** Cell viability of 3D spheroids after 24h, 48h, and 72h from the start of indicated treatments. The data are displayed as the percentage of vehicle-treated controls at 24h post-treatment start. Statistically significant differences between double treatment and 13-cis-RA treatment (black asterisks) and natural compound treatment (grey asterisks) were calculated according to two-way ANOVA followed by Dunnett's multiple comparisons tests.

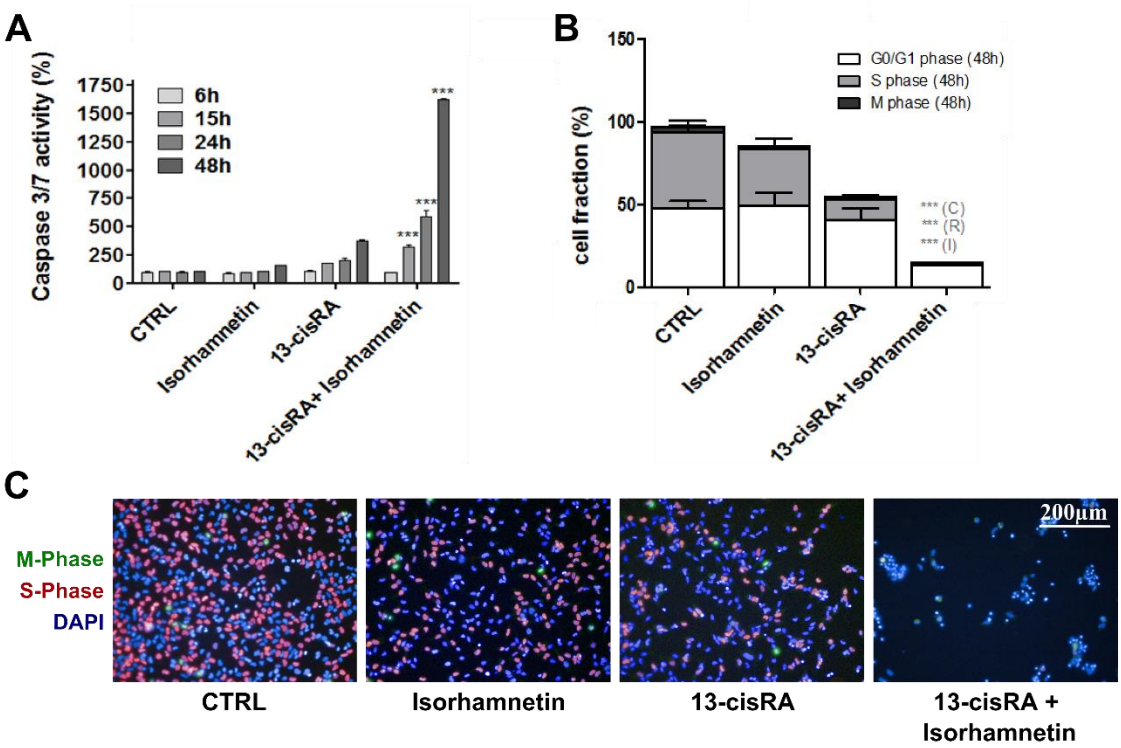

Figure 10. 13-cis-RA in combination with isorhamnetin deregulates the cell cycle and induces apoptosis. (A) Caspase activity determination in CHP134 cells treated with either DMSO, 13-cis-RA (5µM) isorhamnetin (15µM) or their combination for 6h, 15h 24h and 48h. Caspase-3 and -7 activities were normalized on cell viability. **(B)** Analysis of the treatment's effect on cell cycle progression was performed by high content image analysis of cells stained as reported in material and method. The percentage of cells in various phases is expressed relative to the total number of cells. All the reported statistically significant differences between double treatment and 13-cis RA treatment (R), natural compound treatment (I) and control (C) were calculated according to one-way ANOVA followed by Tukey multiple comparisons. **(C)** Representative images of treated cells fixed and stained as follows: cells in the S phase were detected with Click-iT EdU Alexa Fluor 594 imaging assay and cells in the M phase were displayed with primary anti-phospho-histone H3 antibody and Alexa Fluor 488 secondary antibody. Cells imaged with 20X long WD objective**.** Data obtained by Dr Pamela Gatto.

Investigating the cellular mechanisms behind the reduction of cell viability induced by the drug combination, we reported that the use of isorhamnetin and 13-cis-RA in concert is effective in the induction of apoptosis (Figure 10 A) and blockage of cell cycle progression (Figure 10 B). To explore the molecular players involved in the synergism a gene expression analysis has been done by microarray on polysomal RNA of differentially treated cells. This analysis revealed the occurrence of 214 differentially expressed genes in the cells treated with 13-cis-RA and isorhamnetin combination relative to single

treatments. In detail, the microarray gene expression analysis pointed out that combination treatment of 13-cisRA plus isorhamnetin led to coherent perturbations of gene expression including negative regulation of cell proliferation and lipid and drug metabolism, activation of specific neural cell differentiation and migration gene pathway, up-regulation of specific G protein-coupled receptor downstream signalling, cell cycle arrest and apoptosis gene sets.

Further validation of the microarray data pointed out that the reduction of cell viability prompted by the combination of isorhamnetin and 13-cis-RA is specifically accompanied by a marked increase in the expression of the adrenergic receptor alpha 1-B (Figure 11).

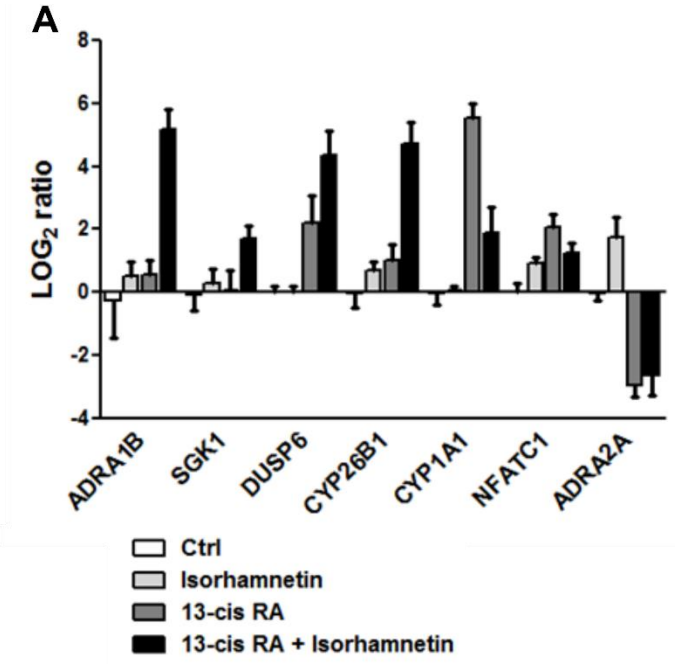

Figure 11. The exposure of NB cell to isorhamnetin and 13-cis-RA leads to variation in gene expression. (A) Validation of the microarray gene expression analysis by TaqMan real-time qPCR. The validation was performed on the top 10 genes that resulted as modulated in the cells treated with the drug combination. (13-cis-RA, 5 μM plus isorhamnetin 15μM) Data obtained by Dr Pamela Gatto and Dr Toma Tabaldi

ADRA1B (ADRα1B) belongs to the superfamily of G-protein coupled receptors and to the subfamily of adrenergic receptors (AR) that are catecholamine receptors expressed in the sympathetic nervous system (SNS). Of note, the adrenergic receptor alpha2A (ADRA2A), another member of the AR-Family, also resulted to be modulated by our treatments: its expression was inhibited by the presence of 13-cis-RA either alone or in combination with isorhamnetin (Figure 11). These two receptors, even if are members of the same family, are involved in different signal transduction pathways (Figure 6).

Interestingly, the SNS other than the expression tissue of AR, is also the anatomical location of NB onset and high levels of catecholamines are found in NB patient's samples with a prognostic/diagnositc value. With these considerations in mind and the knowledge that the adrenergic receptors have a role in the modulation of pivotal pathways involved in the control of proliferation and neural differentiation, we decided to direct our attention to this class of receptors. Moreover, the druggable nature of ARs makes these receptors an interesting target to be explored in NB for drug repurposing efforts. Given the specific overexpression of ADRA1B only in the combined treatment with 13-cis-RA and isorhamnetin, we decided to move on focusing in particular on the role of this alpha-AR.

RESULTS

1. Knock-out or pharmacological blockage of ADRA1B sensitize NB cells to 13-cis-RA treatment

To study the role of ADRA1B in the mediation of the synergistic effect of 13-cis-RA and isorhamnetin, we decided to generate NB cell line KO for this adrenergic receptor.

Exploiting the CRISPR/Cas9 technology, we knocked out ADRA1B from CHP134 and SK-N-AS NB cells (Figure 12 A, Figure 13 A). We selected these two cell lines since the first one is sensitive to 13-cis-RA and to the combination of the retinoid with isorhamnetin (Figure 7 C), while the second line is known to be refractory to 13-cis-RA and as such its cell viability is not affected by the co-treatment with the flavonoid (Figure 14 A). The generated ADRA1B KO cells were then challenged with 13-cis-RA and isorhamnetin either alone or in combination. Evaluating the expression of ADRA1B in WT and KO cHP134 cells, we reported that upon the exposure to either DMSO or 13-cis-RA or isorhamnetin the mRNA is detectable at very high Ct values (~36-37), indicating low expression of the receptor in these conditions. On the other hand, when we challenged the cells with the combination of 13-cis-RA and isorhamnetin, we observed a shift toward lower Ct values representing overexpression of ADRA1B only in WT cells, while in KO cells the mRNA quantity remains very low (Figure 12 B). The induction of the expression increases along with the prolongation of the treatment period.

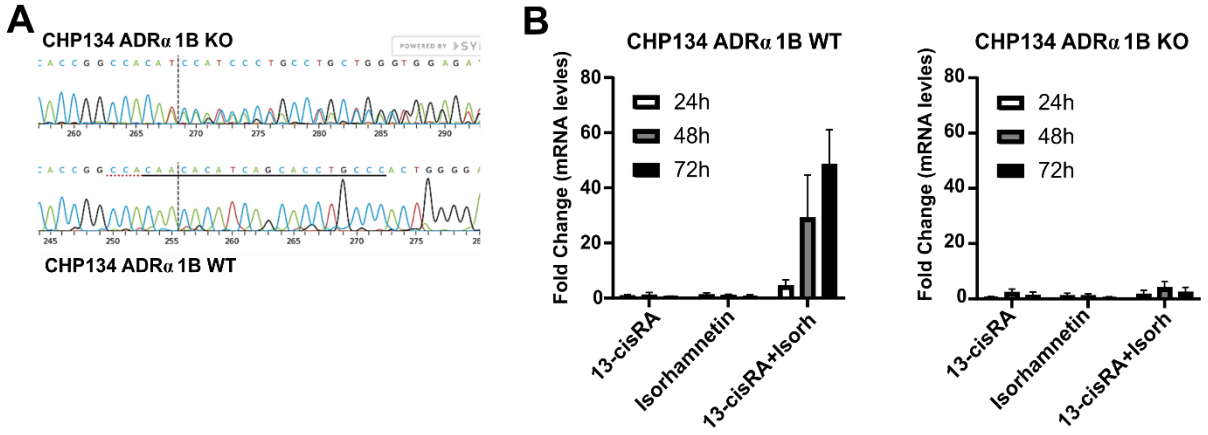

Figure 12. Genetic KO of ADRA1B in CHP134 cells (A) Sanger sequencing chromatogram of the DNA locus of *ADRA1B* targeted by designed CRISPR/Cas gRNA. The upper part of the panel is referred to KO cells, while the lower part represents the chromatogram of control cells. **(B)** Real-time qPCR of ADRA1B in WT and ADRA1B KO cells treated for 24h, 48h and 72h with 13-cis-RA (5μM) and isorhamnetin (15μM) alone or in combination. Data are normalized on DMSO treated cells for each time point.

The increase of the amount of mRNA of ADRA1B was not observed in SK-N-AS cells, where its expressions remained very low regardless of the type of treatment (Figure 13 B). This observation is in line with the refractory of this cell line to 13-cis-RA and its combination with isorhamnetin (Figure 14 A).

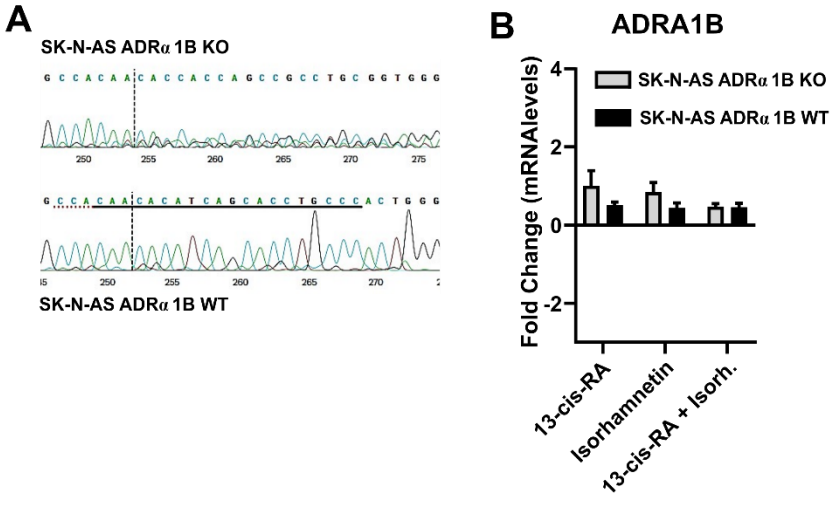

Figure 13. Genetic KO and expression of ADRA1B in SK-N-AS cells. (A) Sanger sequencing chromatogram of the DNA locus of *ADRA1B* targeted by designed CRISPR/Cas gRNA. The upper part of the panel is referred to as KO cells, while the lower part represents the chromatogram of control cells. **(B)** Real time qPCR of ADRA1B in SK-N-AS treated for 48h with 13-cis-RA (5μM), isorhamnetin (15μM) alone or in combination. Data are normalized in DMSO treated cells.

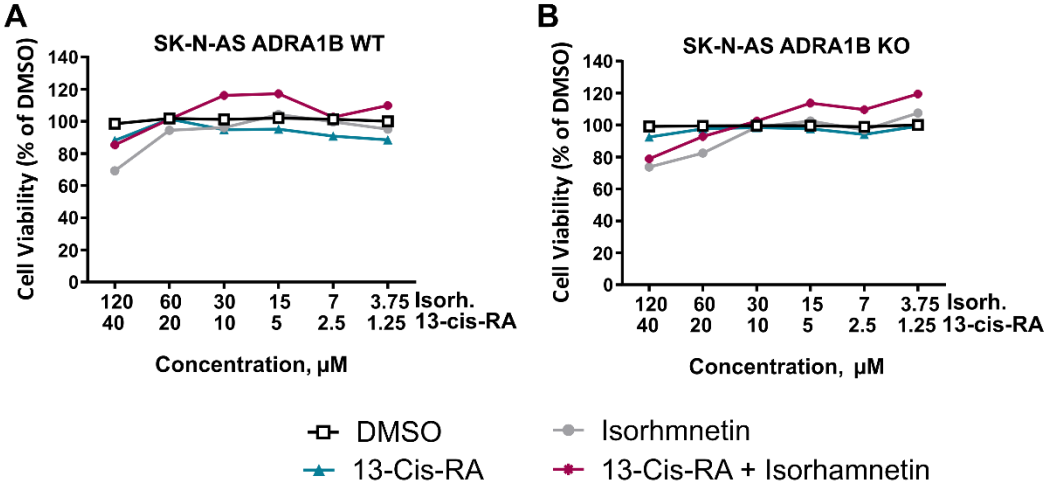

Figure 14. SK-N-AS are unresponsive to treatment with 13-cis-RA and isorhamnetin. Cell viability of SK-N-AS cells. (A) WT and **(B)** KO for ADRA1B exposed for 48h to serial dilutions of 13-cis-RA and isorhamnetin alone or in combination. Reported data are normalized on DMSO treatment. (SD are not shown to have a clearer graph).

Interestingly, we observed that the CHP134 ADRA1B KO cells undergo a high reduction of cell viability not only when faced with the combination of 13-cis-RA and isorhamnetin, but also in presence of the retinoid alone (Figure 15 A-B). This sensitization over the 13-cis-RA was not detected in ADRA1B KO SK-N-AS cells that remained insensitive to the treatment (Figure 14 B).

To further validate this result, we selected the highly selective ADRA1B antagonist L765,314 (Patane *et al*, 1998) to be administered to NB cells along with 13-cis-RA to mimic the effect of the genetic KO of ADRA1B. Thus, we treated the cells with the antagonist alone or in combination with either 13-cis-RA or isorhamnetin and with the sum of the two. The combined treatment of CHP134 NB cells with the alpha-1B-AR antagonist and the retinoid leads to a decrease in cell viability, which resembles what was observed in KO cells challenged with 13-cis-RA, with an IC50 of 20uM for L765,314 in combination with 13-cis-RA (Figure 15 B-C-D, Figure 16 A). The use of L765,314 alone or in combination with isorhamnetin does not lead to any consistent change in cell viability compared to cells exposed to the single compounds (Figure 15 C-D). in detail, we just observed a mild reduction of cell viability in ADRA1B KO cells exposed to L765,314 together with isorhamnetin respect to cells exposed to isorhamnetin alone with a mean difference of only 13.17. This result can be due to some off-targets effect of L765,314 that could also explain the slight decrease of cell viability registred when the antagonist was given alone both in WT and KO cell line (DMSO vs L765,314 mean diff of 13.63 in WT and of 22 in KO cells) (Figure 15 C-D).

We applied the same treatment scheme to other cell lines, focusing our attention on the effect on cell viability of the 13-cis-RA used together with the ADRA1B inhibitor. All the tested cell lines showed augmented sensitivity to retinoid-induced loss of cell viability when the 13-cis-RA is administered along with L765,314 (Figure 16 B). In detail, we observed that the cell line previously reported as sensitive to the synergism of 13-cis-RA and isorhamnetin show a comparable level of reduction of cell viability when the flavonoid is substituted by the alpha-1B-AR antagonist L765,314 (Figure 8 and Figure 16 B: Kelly, SIMA, IMR32, NB3).

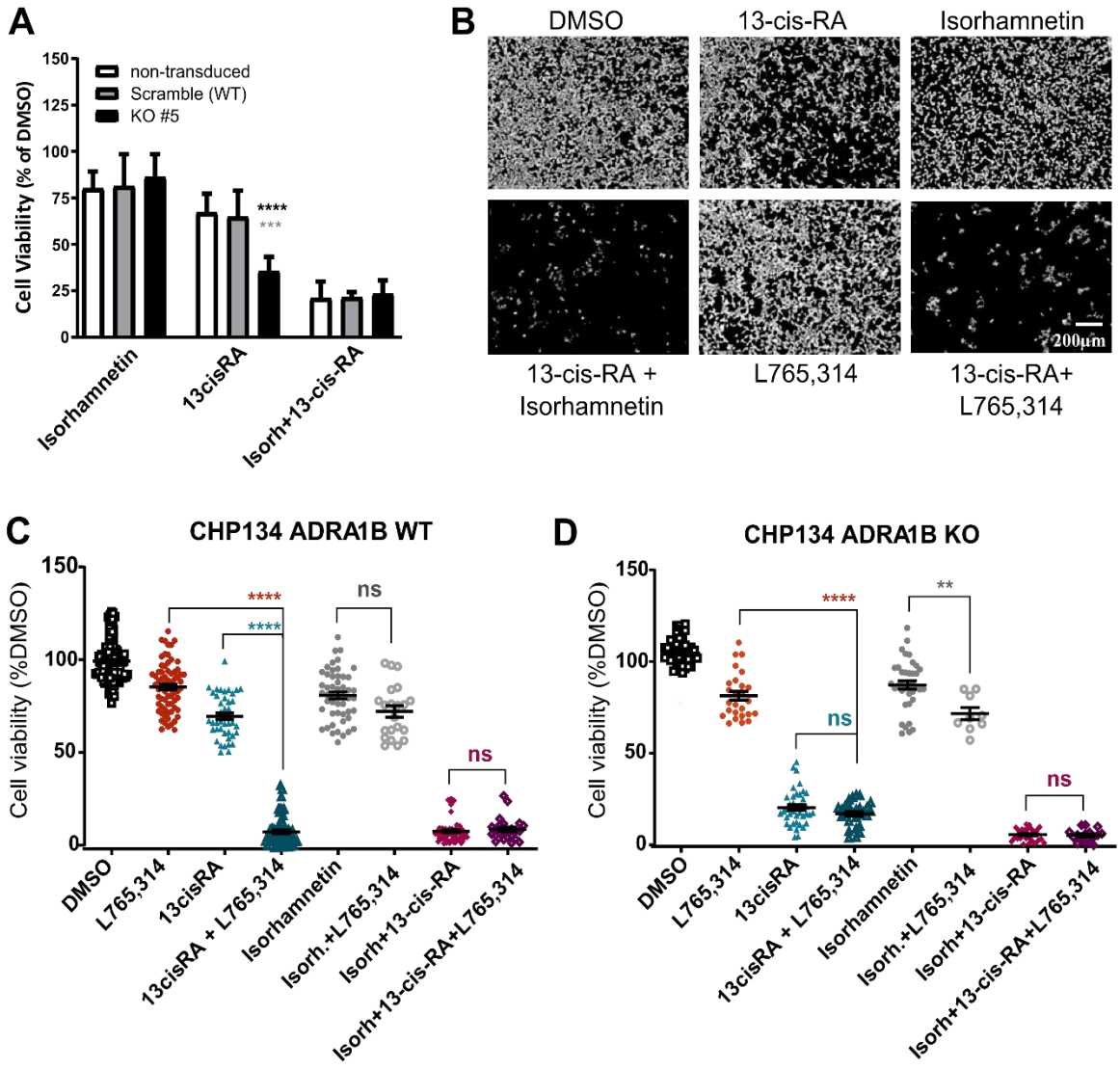

Figure 15. Genetic KO or antagonization of ADRA1B sensitizes CHP134 cells to 13-cis-RA treatment. **(A)** Cell viability assay on CHP134 either non-traduced or infeced with CRISPR/Cas9 vector contiaing gRNA to target *ADRA1B* site (KOcells) or a scramble gRNA (scramble). Statistically significant differences between KO and non-trasduced cells (black asterisks) and cells transduced with scramble CRISPR/Cas9-V1 plasmid (grey asterisks) were calculated according to one-way ANOVA followed by uncorrect Fisher LSD test. **(B)** Representative images of the effect of pharmacological blockage of ADRA1B by L765,314 (20µM) on cell response to 13-Cis-RA (5µM) and isorhamnetin (15µM) exposure for 72h. Cells imaged in digital phase contrast channel with 10X long WD objective**. (C)(D)** Cell viability of WT (scr) and ADRA1B KO cells after exposure for 72h to indicated compounds. Statistical analysis was performed by one-way ANOVA followed by Bonferroni's multiple comparisons test. All presented data were normalized on vehicle-treated cells.

In SK-N-AS cells, we observed a slight decrease of cell viability in the presence of L765, 314 relative to control cells, which is reflected in the combinatorial treatment with 13-cis-RA; the addition of the 13-cis-RA does not augment the loss of cell viability, which is in line with expected resistance to retinoic acid of this cell line (Figure 16 B; SK-N-AS). The mild effect of L765,314 was present with a lower extent also in SK-N-AS ADRA1B KO cells indicating some off-target effects like observed in the CHP134 cell line (Figure 15 C-D).

We further tested the co-treatment with the alpha-1B antagonist and 13-cis-RA also on non-NB cell lines: MCF10A (breast epithelial) and CCD18-Co (colon fibroblast). The colon fibroblasts-derived cells showed a little responsiveness to the treatments with 13-cis-RA combined with either isorhamnetin or L765,314, while the MCF10A cells resulted completely non-responsive with no decrease of cell viability upon administration of the tested compounds either alone or in concert.

In summary, these data indicate that the genetic KO or the pharmacological blockage of the adrenergic receptor alpha 1B leads to a sensitization of NB cells to 13-cis-RA, leading to an overall reduction of the cell viability. Therefore, it is likely that the observed synergistic effect between 13-cis-RA and isorhamnetin was mediated at least in part by the action of isorhamnetin as an antagonist of the ADRA1B receptor.

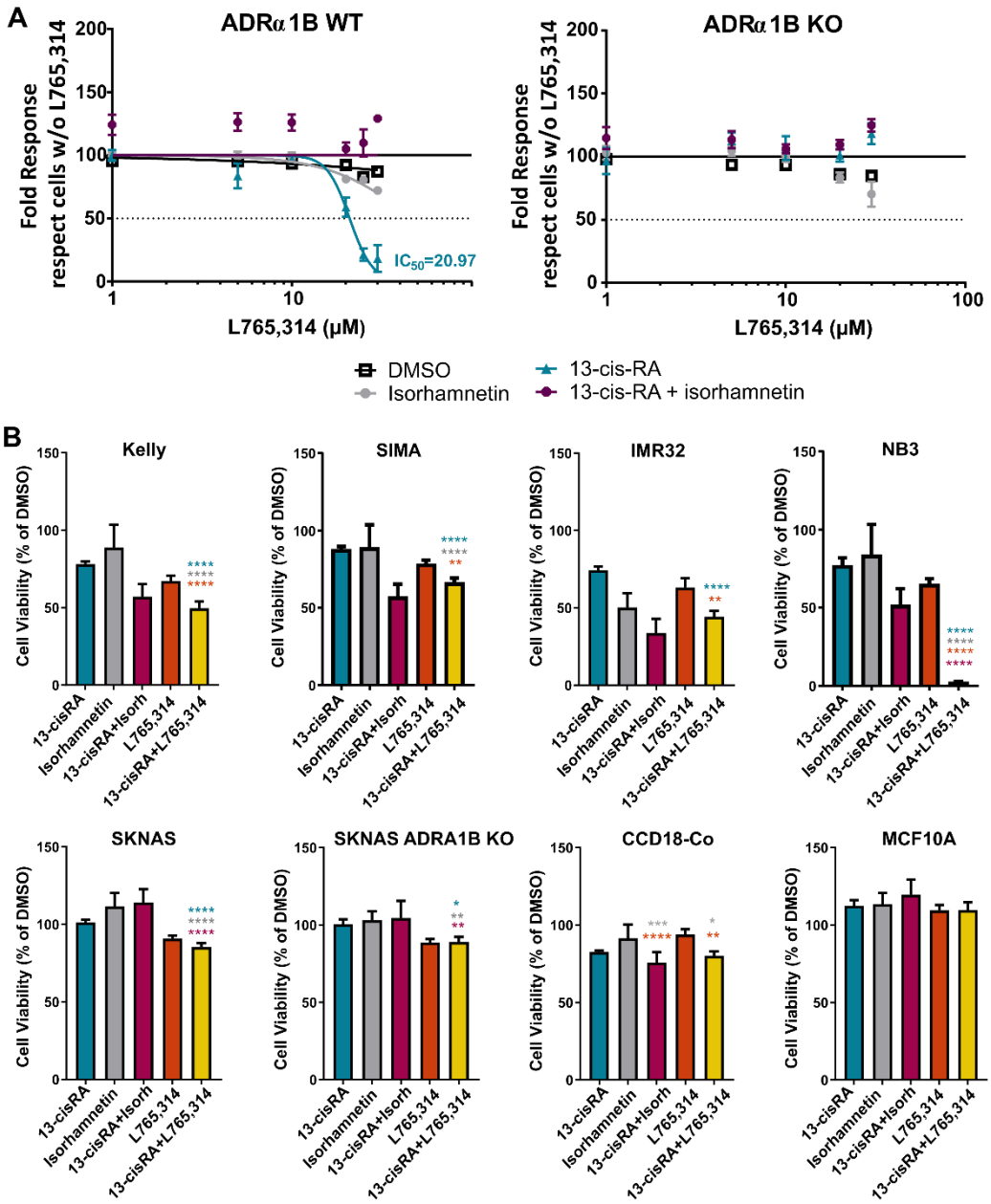

Figure 16. L765,314 sensitize cells to the 13-cis-RA treatment of several NB cell lines. (A) Dose-response curve of CHP134 cells WT and KO for ADRA1B treated with 13-cis-RA (5μM), isorhamnetin (15μM), 13-cis-RA/isorhamnetin plus/minus the ADRA1B inhibitor L765,314. Data were normalized on DMSO control and then the difference (fold) in cell viability upon addition of L765,314 was calculated. **(B)** Cell viability of different NB and non-NB cells (CCD18-co, MCF10A) upon the indicated treatments: 13-cis-RA (5μM), isorhamnetin (15μM), L765,314 (20μM). Data are displayed as the percentage of vehicle-treated control. Statistically significant differences between L765,314 plus 13-cis-RA (L+RA) treatment and 13-cisRA (RA)alone or in combination with isorhamnetin (RA+ISO) and L765,314 (L) alone, were calculated by one-way ANOVA followed by Dunnett's multiple comparisons tests. The statistical significances are reported following the graph colour code: RA+L vs RA, teal green asterisks, RA+L vs ISO grey asterisks, RA+L vs RA+ISO violet asterisks, RA+L vs L orange asterisks.

2. NB cells lacking ADRA1B are more sensitive to 13-cis-RA induced apoptosis and differentiation.

The activation of the retinoic acid pathway resulted in the decrease of cell viability through the induction of apoptosis and differentiation (Figure 5). Thus, we wanted to assay the extent of these cellular events in RA-sensitive NB cells challenged with 13-cis-RA and expressing or not the ADRA1B receptor, to start understanding if these two cell programs are the drivers of the observed reduction of cell viability, and to what extent these programs depend on ADRA1B.

For the analysis of apoptosis induction, we used the CellEvent™ Caspase-3/7 Green Detection Reagent that allows real-time monitoring of apoptosis in live cells: apoptotic cells with activated caspase-3/7 show bright green-fluorescent nuclei. The ADRA1B KO and WT CHP134 cells were exposed to 13-cis-RA and isorhamnetin alone or in combination for 72h during which the caspase signal was registered at fixed time points. To evaluate the rate of apoptosis induction, the percentage of assay positive cells were normalized over time zero, i.e., the number of green-fluorescent cells detected before drug administration. In the treatment with the drug combination, 13-cis-RA with isorhamnetin, we observed a consistent rise in the percentage of the green-fluorescent cells over time as a consequence of caspase 3/7 activation. The detected signal reached higher values in KO cells with respect to WT (Figure 17 A). A consistent induction of apoptosis has been also registered in ADRA1B KO cells exposed to the retinoid alone at even greater values of what observed in WT cells challenged with isorhamnetin and 13-cis-RA (Figure 17 A) After 48h of treatment the majority of KO cells exposed to the retinoid were found positive for the CellEvent™ Caspase-3/7 Green Detection Reagent (Figure 17 B). In conclusion, the apoptosis analysis reveals that the lack of ADRA1B is of favour to undertake the pro-apoptotic fate induced by 13-cis-RA.

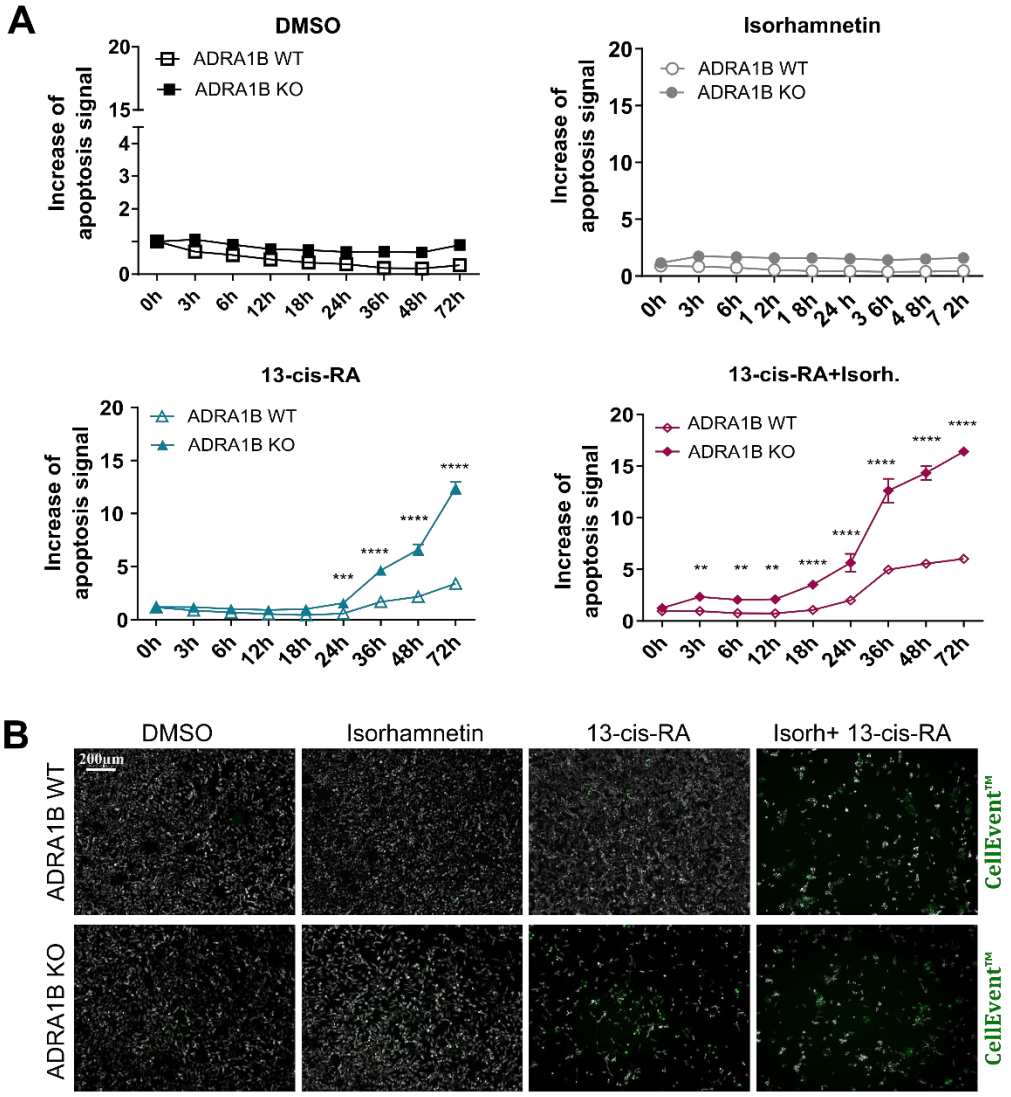

Figure 17. The KO of ADRA1B renders NB cells more prone to 13-cis-RA pro-apoptotic effect. (A) Timeline of the induction of apoptosis in cells exposed to the compounds for a total of 72h. Data are expressed as fold to increase respect to time 0 and normalized over the total number of cells for each time point. Statistically significant differences between treatments effects (WT vs ADRA1B KO) were calculated according to two-way ANOVA followed by Bonferroni's multiple comparison test. **(B)** Representative images of cells treated with 13-cis-RA (5µM) and isorhamnetin (15µM) alone or in combination for 48h and stained with CellEvent™ Caspase-3/7 Green Detection Reagent. Cells imaged by 10X high NA objective in DPC and 488 channels.

To evaluate if the decrease of cell viability of ADRA1B KO cells is also due to augmentation of the 13-cis-RA induced neural differentiation process, we performed a neurite phenotypical analysis. CHP134 cells either WT or KO for ADRA1B were treated with the isorhamnetin and 13-cis-RA alone or together, ad imaged every 24h for a total of 144h.

The obtained images were analysed by high content analysis approach to identify and measure the length of neurite protrusions, which are a marker of neuronal differentiation (Figure 18 A).

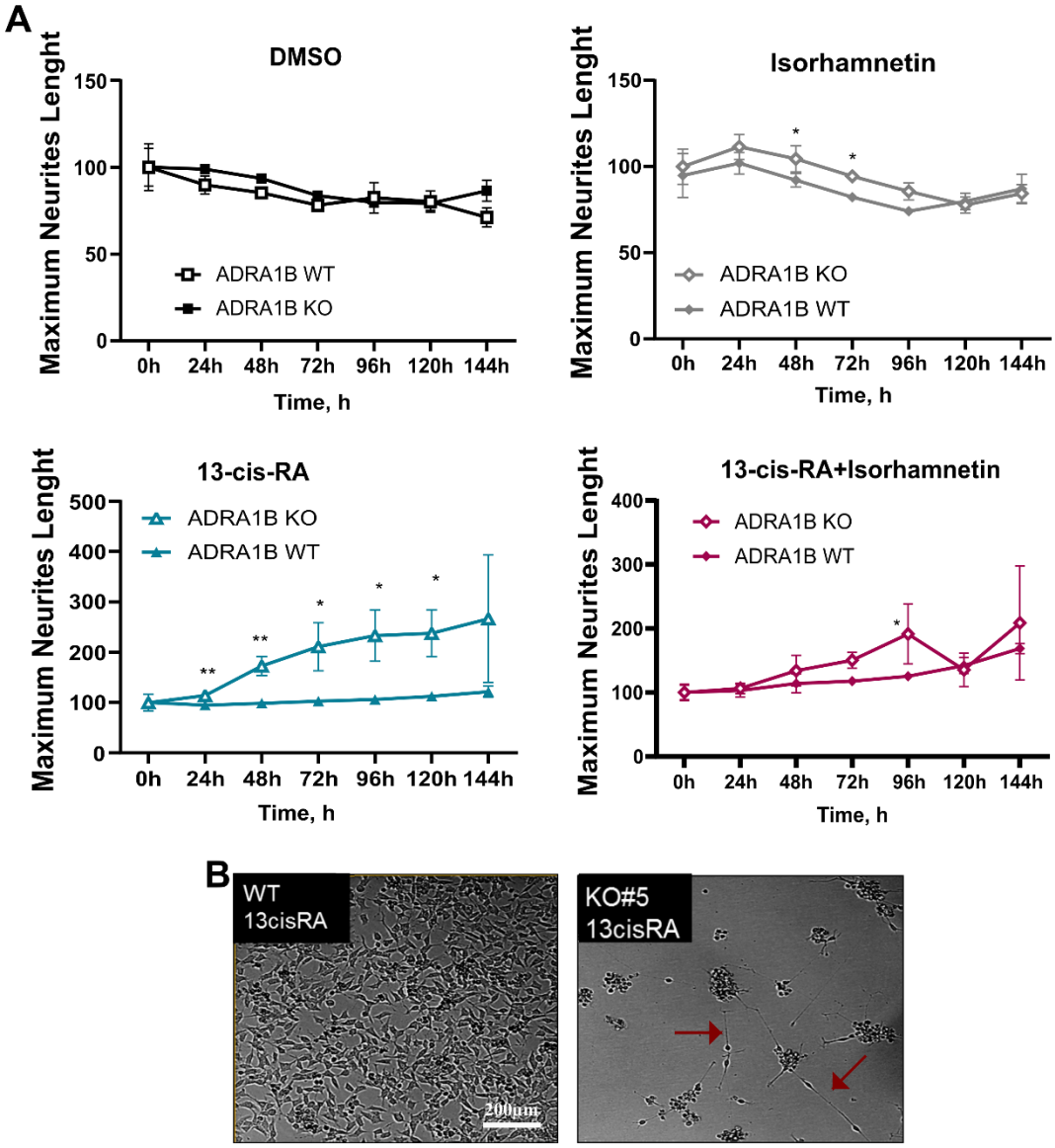

Figure 18. ADRA1B KO gmakes CHP134 cells more prone to 13-cis-RA pro-differentiative effect. **(A)** Quantification of maximum neurite length observed in CHP134 cells WT or KO for ADRA1B treated with 13-cis-RA, isorhamnetin alone and in combination for a total time of 144h. Cells were imaged every 24h. Statistically significant differences between treatments in the two different cell lines (WT and ADRA1B KO) were calculated according to two-way ANOVA followed by Bonferroni's multiple comparison test. **(B)** Representative images of ADRA1B WT and KO NB cells exposed for 72h to 13-cis-RA. Cells imaged by 20X LWD objective.

The images clearly showed that after exposure to 13-cis-RA the remaining KO cells extrude longer neurite-like branches with respect to WT (Figure 18 B). The quantification of maximum neurites length confirmed the observation: the cells lacking the receptor and challenged with 13-cis-RA for at least 48h protrude longer neurite-like protrusions relative to WT (Figure 18 A) indicating the is engaged the neural differentiation process.

3. CHP134 ADRA1B KO cells express higher levels of neural differentiation markers

To further examine the extent of the differentiation process started by 13-cis-RA in ADRA1B KO cells, we decided to assay the expression of some well-characterized differentiation markers used in NB, both at mRNA and protein level. . We treated ADRA1B WT and KO cells with 13-cis-RA, isorhamnetin and the combination of the two molecules for 48h. We reported an increase in the amount of mRNA of some differentiation-associated genes like TH, Beta3-tubulin, Sox9 and its downstream target Hes1, in cells exposed to 13-cis-RA either alone or in combination with isorhamnetin (Figure 19 A-B). The increase of gene expression of these neural differentiation markers was statistically significantly higher in the ADRA1B KO cells compared to the WT. We also detected in KO cells a higher amount of GAP43, beta3-tubulin and Sox9 proteins after the incubation with isotretinoin alone or together with isorhamnetin. On the other hand, we detected a reduction in the protein signal of the NB oncogenic driver PHOX2B in samples incubated with 13-cis-RA especially in ADRA1B KO genetic background where a greater decrease was observed (Figure 19 A-B). Furthermore, we assayed the expression level of MCYN which is known to be downregulated by 13-cis-RA. The MCYN expression resulted to be decreased in all the samples treated with isotretinoin; the downregulation is augmented in the presence of isorhamnetin and cells lacking ADRA1B. The exacerbation of the decrease of MCYN mRNA and protein amounts related to the presence of 13-cis-RA is also obtained co-treating cells with L765,314, reaching similar levels of what observed in KO cells treated with 13-cis-RA alone (Figure 19 C).

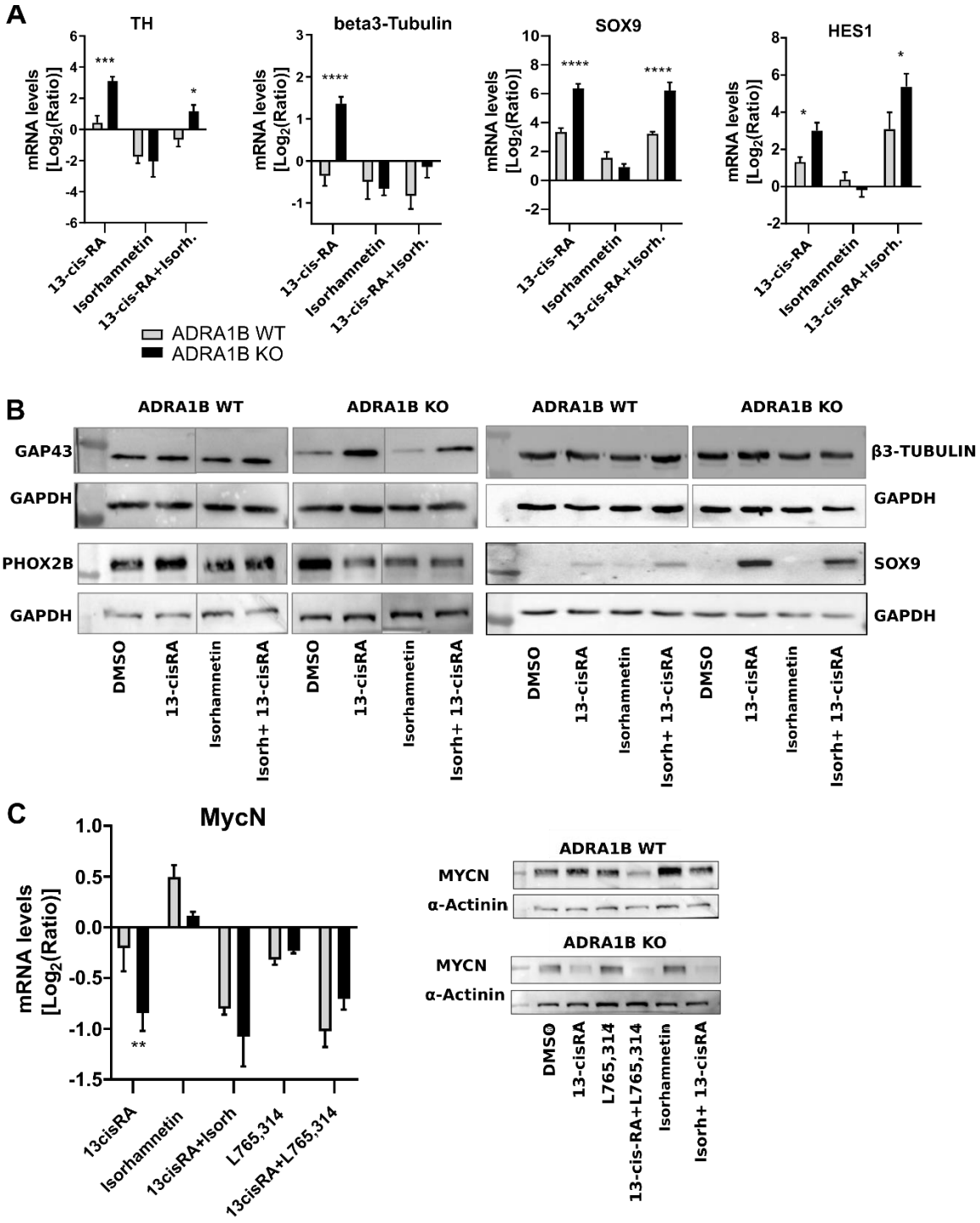

Figure 19. CHP134 KO for ADRA1B, upon exposure to 13-cis-RA, express higher levels of neural differentiation markers. (A) RT-qPCR of neural differentiation markers TH, Beta3-tubulin, Sox9 and Hes1 on samples of CHP134 cells either WT or KO for ADRA1B upon treatment with 13-cis-RA (5μM) and isorhamnetin (15μM) alone or in combination. Data were normalized on DMSO treated samples. Statistical evaluation between WT vs KO samples for each treatment condition was done by a Two-way ANOVA test followed by Bonferroni's multiple comparisons test. **(B)** Western blot analysis of neural differentiation markers: GAP43, PHOX2B, beta3-Tubulin and Sox9 on protein lysates of CHP134 cells WT and KO for ADRA1B treated with indicated compounds for 48h. **(C)** Analysis of the expression of MCYN by RT-qPCR and WB in WT and KO cells after 48h of indicated treatment

These deregulations of MYCN, TH, Beta3-tubulin, Sox9, Hes1 and GAP43 expression, were not detected in SK-N-AS WT or KO for ADRA1B, which is in agreement with the unresponsiveness of this NB cell line to treatments (Figure 20 A-C).

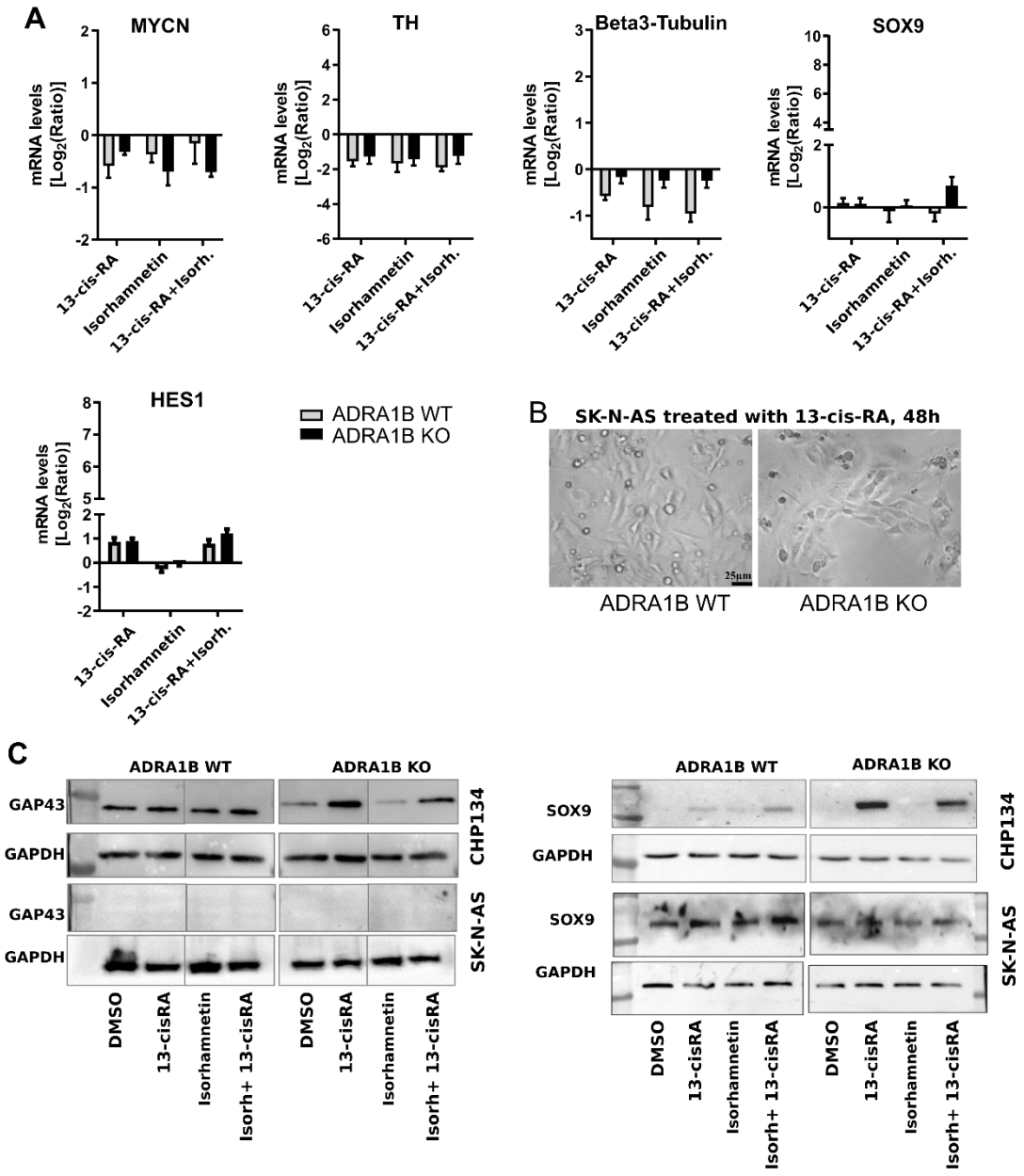

Figure 20. Treatment of WT or ADRA1B KO SK-N-AS cells with 13-cis-RA and isorhamnetin does not lead to variation in neural differentiation markers expression. (A) RT-qPCR of neural differentiation markers MCYN, TH, Beta3-tubulin, Sox9 and Hes1 on SK-N-AS cells either WT or KO for ADRA1B upon treatment with 13-cis-RA (5µM) and isorhamnetin (15µM) alone or in combination. Statistical comparison has been done comparing WT vs KO samples for each treatment condition by two-way ANOVA test followed by Bonferroni multiple comparisons test. **(B)** Images of SK-N-AS exposed for 48h to 13-cis-RA. Cells imaged with 5X magnification**. (C)** Western blot analysis of neural differentiation markers: GAP43, and Sox9 on protein lysates of SK-N-AS cells WT and KO for ADRA1B treated with indicated compounds for 48h. WBs for the same proteins on CHP134 lysates are reported for comparison.

The results presented up to here indicate that the lack of or inhibition of ADRA1B leads to sensitization of CHP134 NB cells to both anti-proliferative and pro-differentiative effects of 13-cis-RA.

4. Screening of a focused library of ARs ligands highlights alpha-AR as good targets in NB

Since the involvement of ARs in the control of cell proliferation and differentiation is well known (see sections 2.1 and 2.2), and since the druggable nature of these receptors poses some interesting advantages in the view of clinical application, we decided to perform a wider evaluation of the AR-ligands that can be potentially indicated as novel enhancers of the state of the art pro-differentiative therapeutic protocol for NB.

To this aim, we set up a screening with a focused library of 201 adrenergic receptor ligands used at two concentrations (20μM or 40μM) alone or in compresence of 13-cis-RA at 5μM. The cells were treated for 72h and then the cell viability was evaluated. The assay of the quality of the screening was previously evaluated by calculating the Z-factor showing the separation between the distributions of the positive (13-cis-RA plus isorhamnetin) and negative controls (DMSO) (Figure 21 B). The Z-factor equal to 0.68 which is above the cut-off 0.5, is an indicator of an excellent assay.

Screening raw data were processed performing normalization of all samples to the average of on-plate vehicle-treated controls with the open-source platform KNIME. The screening results are summarized in Figure 21 A. For hit selection, the following criteria were applied: first, compounds that at 20μM and 40μM alone reduced the cell viability to 0- 50% were filtered out; then compounds that at 20μM and/or at 40μM in combination with 13-cis-RA caused a decrease of cell viability greater than that of 13-cis-RA alone (by 30% at least) were further selected. The molecules that fulfil these requirements are reported in Table 5.

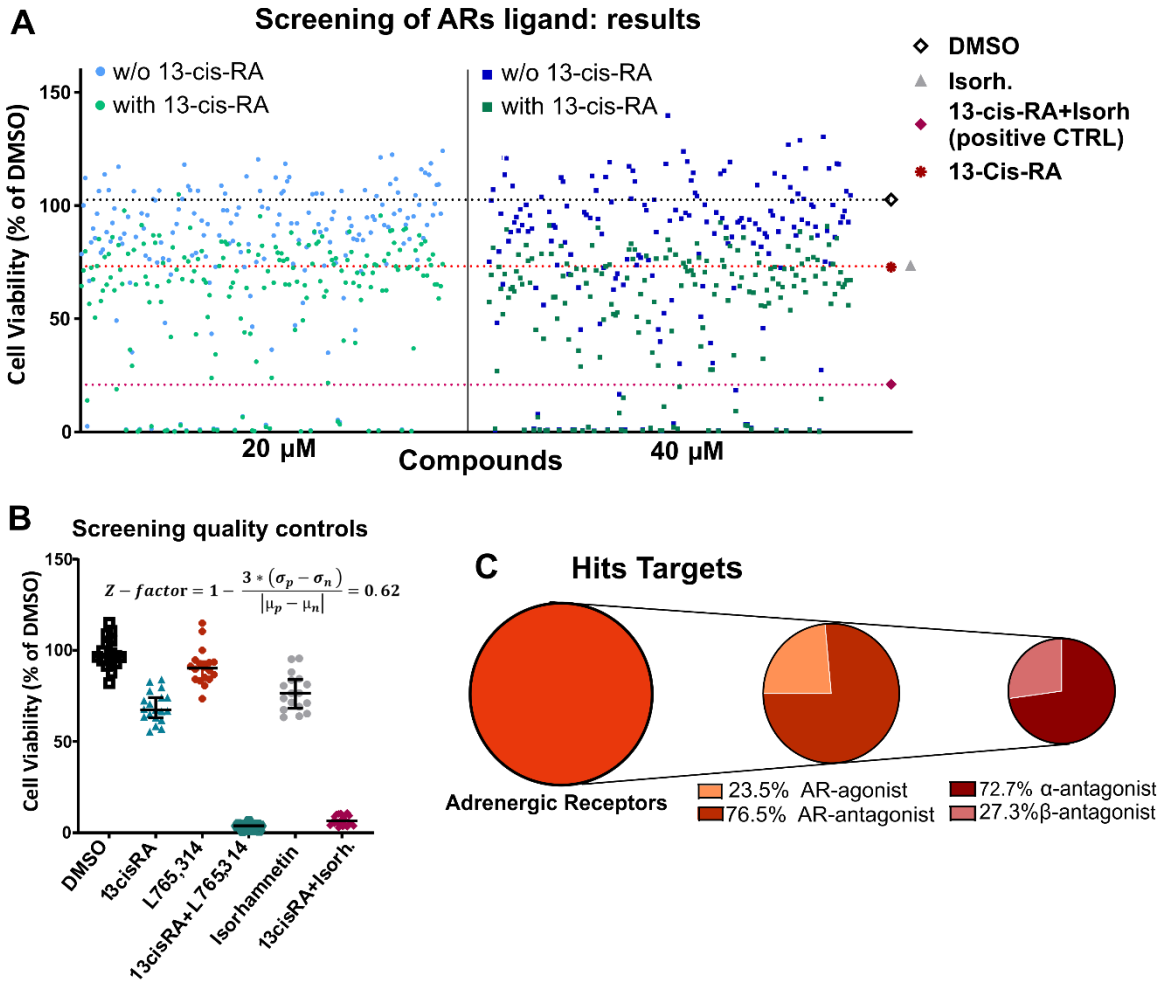

Figure 21. Results of the high-throughput screening with adrenergic receptors ligands. (A) Cell viability of CHP134 was assayed after 72h of treatment with 201 catecholamines receptors agonists and antagonists at 20µM (lighter dots) and 40µM (darker squares) alone and in combination with 13-cis-RA (5µM). Each point represents the mean of two technical replicates. Data are normalized on the mean cell viability of vehicle-treated cells. The yellow dotted line represents the chosen cytotoxicity level (i.e., cell viability reduction ≥ 50%). The black, red, and purple dotted lines indicate the mean cell viability of cells treated with DMSO (negative control), 13-cis-RA (5µM) and the combination 13-cis-RA (5µM) and isorhamnetin (15µM) (i.e., the positive control) respectively. **(B)** Cell viability values of the screening experimental control conditions. For the Z-factor calculation, 13-cis-RA plus isorhamnetin was the positive control, while DMSO was the negative control. **(C)** Hits' targets analysis focusing on the sub-classification of agonist vs antagonist and then on receptor subfamily.

Table 5. Screening hits and corresponding IC50. For each selected hit we report here the calculated IC50 when given alone or in combination to 13-cis-RA to NB cell for 72h.

	IC50 µM		
Drug name	**+13-cis-RA**	**Drug alone**	**Target**
AH 11110 HCl	10,29	134,9	α1B- AR antagonist
CGP 20712A 2HCl	28,58	1814	β1- AR antagonist
Imipramine HCl	32,24	43,63	AR antagonist
Doxepin HCl	33,98	43,65	α1- AR antagonist
Isoproterenol HCl	36,15	52,82	β1/2-adrenergic agonist
Amitriptyline HCl	36,18	26,27	α1- AR antagonist
Phenoxybenzamine HCl	36,83	39,72	α1 AR antagonist
Carazolol	37,32	89,11	β1-adrenergic antagonist
Corynanthine	42,33	41,27	α1/2- AR antagonist
ICI-118,551 HCl	45,27	44,95	β2- adrenergic agonist
Bopindolol malonate	55,47	23,64	β1-AR antagonist
Dobutamine HCl	57,50	86,51	β1/2- adrenergic agonist
Maprotiline HCl	59,97	96,74	α1- AR antagonist
Nicardipine HCl	71	94,52	AR antagonist
Trimipramine maleate	71,02	42,56	α1/2- AR antagonist
Ifenprodil hemitartrate	145,90	44,79	α1- AR antagonist
Dipiveferin HCl	1781	1677	Adrenergic receptor agonist

Of note, 13 out of 17 (76%) of selected hits are adrenergic receptor antagonist and specifically, among those that have specificity for either the alpha or beta-AR, 8 out of 11 (73%) are specific ligands of the alpha-1 subfamily (Figure 21 C). The hits were validated by performing dose-response curves of CHP134 cells treated with 2-fold serial dilutions of the AR-ligand, (from 80µM or 40µM till 2.5µM), in the presence or

absence of 13-cis-RA (5μM). After 72h of treatment cell viability was assessed. The hits-validation results are reported in (Figure 22). Applying a nonlinear regression model, we calculated the IC50 (inhibitory concentration) for each molecule alone or in combination with 13-cis.RA. The obtained IC50 values are reported in Table 5.

Some of the evaluated hits present a shift of IC50 toward lower values when administered together with 13-cis-RA, indicating potentiation of the growth inhibitory capacity of the 13-cis-RA. The hits showing this behaviour are the following: AH11110A HCl, GCP20712A 2HCl, imipramine, doxepin HCl, isoproterenol HCl, phenoxybenzamine HCl, carazolol, dobutamine HCl, maprotiline HCl and nicardipine HCl. Most of these compounds (8/10) are adrenergic receptor antagonists and, 4 out of 8 are specific alpha1-AR antagonists (Table 5). Only 2, isoproterenol HCl and dobutamine HCl are AR-agonist, but both are specific for the subfamily of β-AR.

The hit showing the lowest IC50 when employed along with 13-cis-RA is AH1110A HCl which is an ADRA1B antagonist. We tested the efficacy of AH1110A HCl plus 13-cis-RA on other NB cells lines; Kelly, Sima, IMR-32, NB3 and SK-N-AS. All the tested NB cell lines showed a reduction of cell viability when incubated with AH1110A HCl and 13-cis-RA already using the alpha-1B antagonist at 15μM. No reduction of cell viability was detected in cells treated with AH1110A HCl alone. The SK-N-AS only show unresponsiveness to all the assayed drug treatments, which is expected due to their intrinsic resistance to retinoic acid (Figure 23).

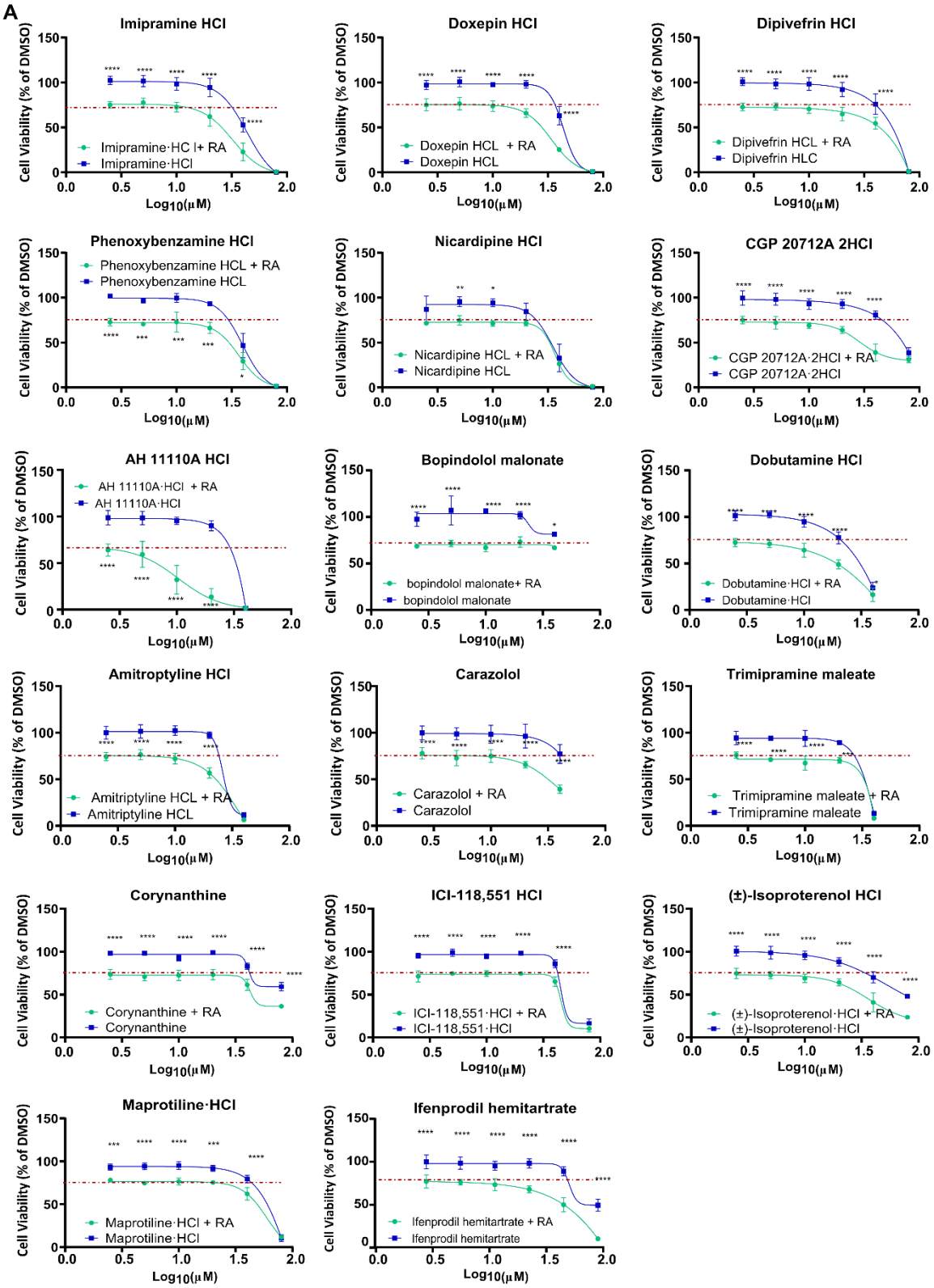

Figure 22. Hits validation of the adrenergic receptor ligand screening. (A) Cell viability of CHP134 cells after 72h of treatment with 2-fold serial dilutions of selected screening hits administered to cells alone (blue curves) or in combination with 13-cis-RA (5μM) (light green curve). The red dotted line represents the mean cells-viability of CHP134 cells exposed to 13-cis-RA alone for 72h. Data are normalized on DMSO treated cells. Statistical analysis was done with Two-way ANOVA test followed by Sidak's multiple comparison test.

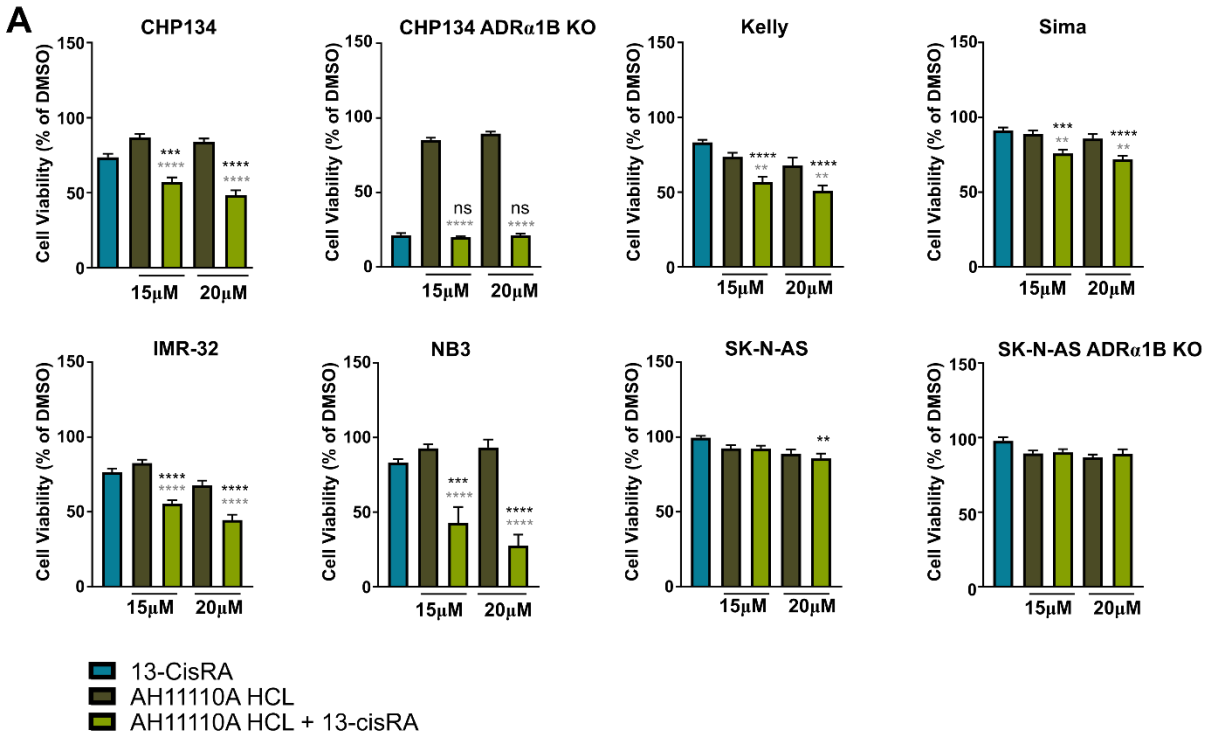

Figure 23. Combined treatment with AH1110A and 13-cis-RA is effective in the reduction of cell viability of several 13-cis-RA-sensitive NB cells. (A) Cell viability of indicated NB cell exposed to two concentrations of AH1110A alone or in combination with 13-cis-RA (5μM) for 72h. Statistically significant differences between treatments with AH1110A plus 13-cis-RA and either 13-cis-RA (black asterisks) or AH1110A alone (grey asterisks) were calculated by one-way ANOVA followed by Dunnett's multiple comparisons test.

Considering these data and the previous results on ADRA1B KO cells, we decided to focus our attention on the class of alpha-adrenergic receptor antagonists for further experiments. We selected 5 out of the 8 AR-antagonists showing a low and consistent shift of the IC50 when administered together with 13-cis-RA. Thus, the selected hits for further analysis were: AH1110A HCL, CGP 20127A 2HCl, imipramine HCl, doxepin HCl and carazolol.

5. Adrenergic receptors antagonization promotes NB cells differentiation

Since we observed an enhanced expression of differentiation markers and concomitant downregulation of PHOX2B and MYCN in ADRA1B KO or L765,314 treated WT cells exposed to 13-cis-RA, (Figure 19 C), we decided to perform neurite outgrowth assay by high content image analysis (HCA) of cells exposed to the selected AR-antagonists together with 13-cis-RA.

The CHP134 NB cells were treated with 2-fold serial dilutions of the following ARs-antagonist: AH1110A HCL, CGP 20127A 2HCl, imipramine HCl, doxepin HCl and carazolol administered either alone or concomitantly with 13-cis-RA. The cells were imaged after 120h of treatment. The acquired images were analysed with segmentation protocol sets to identify neurites, which indicate the start of the in vitro neural differentiation process.

The evaluation reveals an overall increase in the number of identified neurites in cells exposed to the combination of AR-antagonist and 13-cis-RA compared to the control (13-cis-RA alone) (Figure 24). The increase in neural differentiation resulted to be AR-antagonist dose-dependent with a higher number of long protrusions per cell for 20μM dose of compounds plus retinoid with respect to lower ones (Figure 24 B). This experimental data suggest that the adrenergic receptors antagonists can augment the pro-differentiative effect of 13-cis-RA in a dose-dependent manner.

Thanks to this analysis, we confirmed that the strategy of combining 13-cis-RA with AR-antagonists is not only of value to reduce the overall cell viability but also to promote cellular differentiation which is of pivotal importance to reduce tumor aggressiveness.

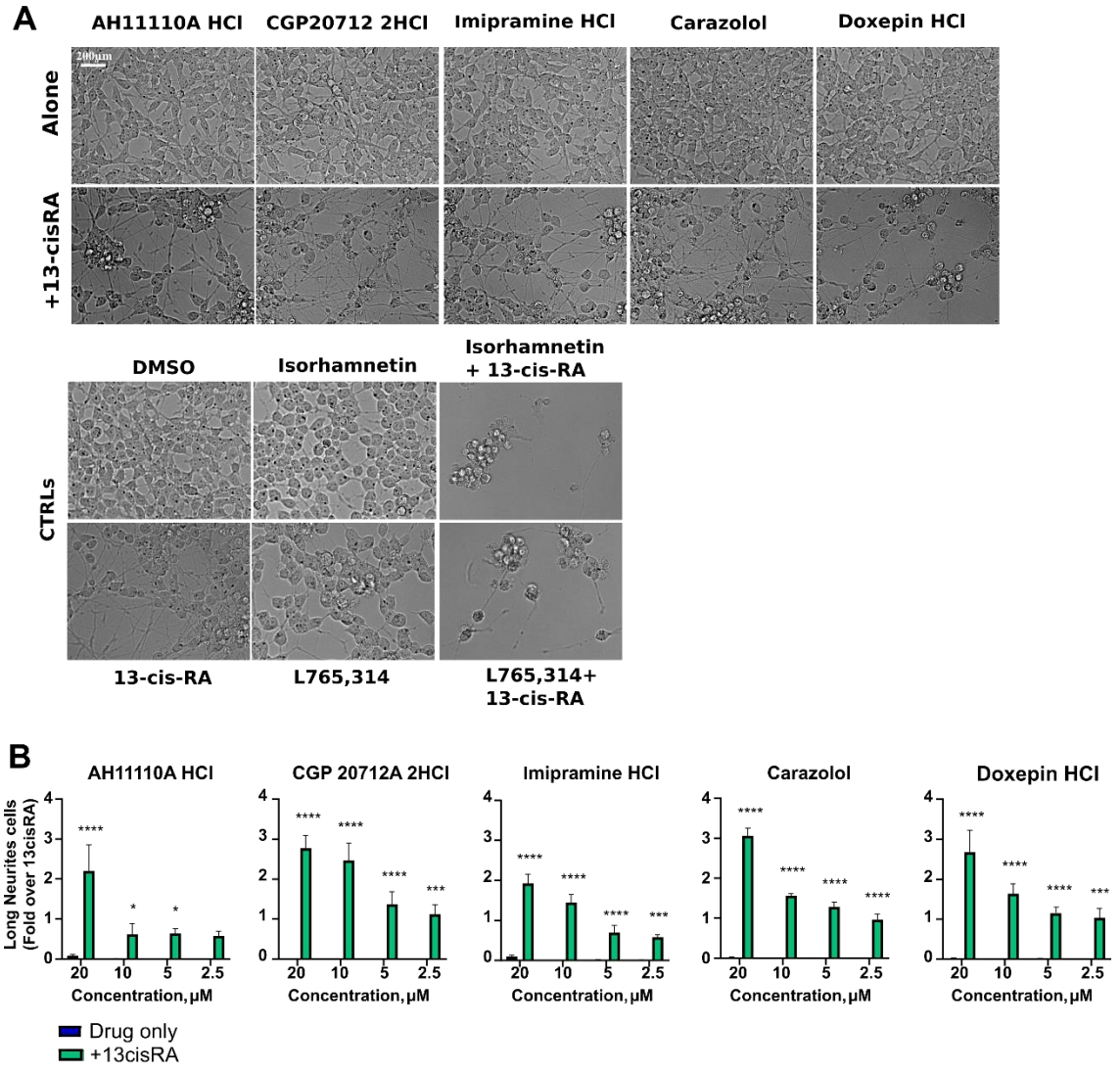

Figure 24. The presence of an ARs antagonist enhances the pro-differentiative potential of 13-cis-RA. (A) Representative images of CHP134 cells treated for 120h with 20µM of selected adrenergic receptor ligands alone or in combination with 13-cis-RA (5µM). Cells imaged by 20X LWD objective. **(B)** Quantification of lneurite number per cell (with a length above a certain threshold) by high content image analysis. For each treatment and compound concentration, the difference between the numbers of long neurite was calculated relative to the retinoid alone. Statistically significant differences between catecholamine ligand alone treatment and the combined exposure with retinoid were calculated according to two-way ANOVA followed by Dunnet's multiple comparison tests.

6. The FDA approved alpha-1-AR antagonist doxazosin combined with 13-cis-RA reduces NB cell viability

All the presented data point out the validity of alpha-adrenergic receptors as novel targets for a combinatorial therapy in NB along with 13-cis-RA. Our data indicate that the blockage of the adrenergic receptor, rather than stimulation, is the best strategy to augment the decrease of cell viability obtained by exposure of cells to 13-cis-RA. Among the subclasses of ARs, the alpha-1 receptor resulted to be the most represented target among the top 10 screening hits. From the hits-validation process, the most promising AR-ligand resulted to be AH1110A. Unfortunately, neither AH1110A HCl nor L765,314, both specific alpha-1B AR antagonists that showed good synergisms with 13-cis-RA in the reduction of NB cells viability, are routinely used as drugs. The available literature about their use *in vivo* is very limited, which is of concern for the set-up of the *in vivo* testing procedure. Some of the other alpha-1 AR antagonists selected as hits in our screening are FDA approved drugs, such as imipramine HCl and doxepin HCl, both employed primarily for the treatment of depression. The psychotropic nature of these drugs raises some worries about their potential use in children. Thus, we decide to select for our *in vivo* study a drug that: is a specific alpha-1 AR antagonist, is already used in children and is not a psychotropic molecule. Our search leads to the choice of doxazosin (commercial name: Cardura®) (Ganesh *et al*, 2009). This drug is generally prescribed to keep under control the symptoms related to benign prostate hyperplasia but is also used to manage hypertensive status in patients with NB (Seefelder *et al*, 2005).

Before the starting of the *in vivo* testing, we verified the efficacy of the doxazosin *in vitro* both on 2D and 3D cell models (Figure 25). The combination of doxazosin with 13-cis-RA resulted to be effective in the reduction of cell viability of CHP134 cells in a dose-dependent manner (Figure 25 A-B). The observed decrease of cell viability is maintained on spheroid aggregates exposed to the alpha-1 AR inhibitor and the retinoid; the formed spheres, once exposed to the combination of the compounds, stop

growing and start to disaggregate similarly to what observed in the treatment with 13-cis-RA and isorhamnetin or L765,314 (Figure 9 and Figure 25 C).

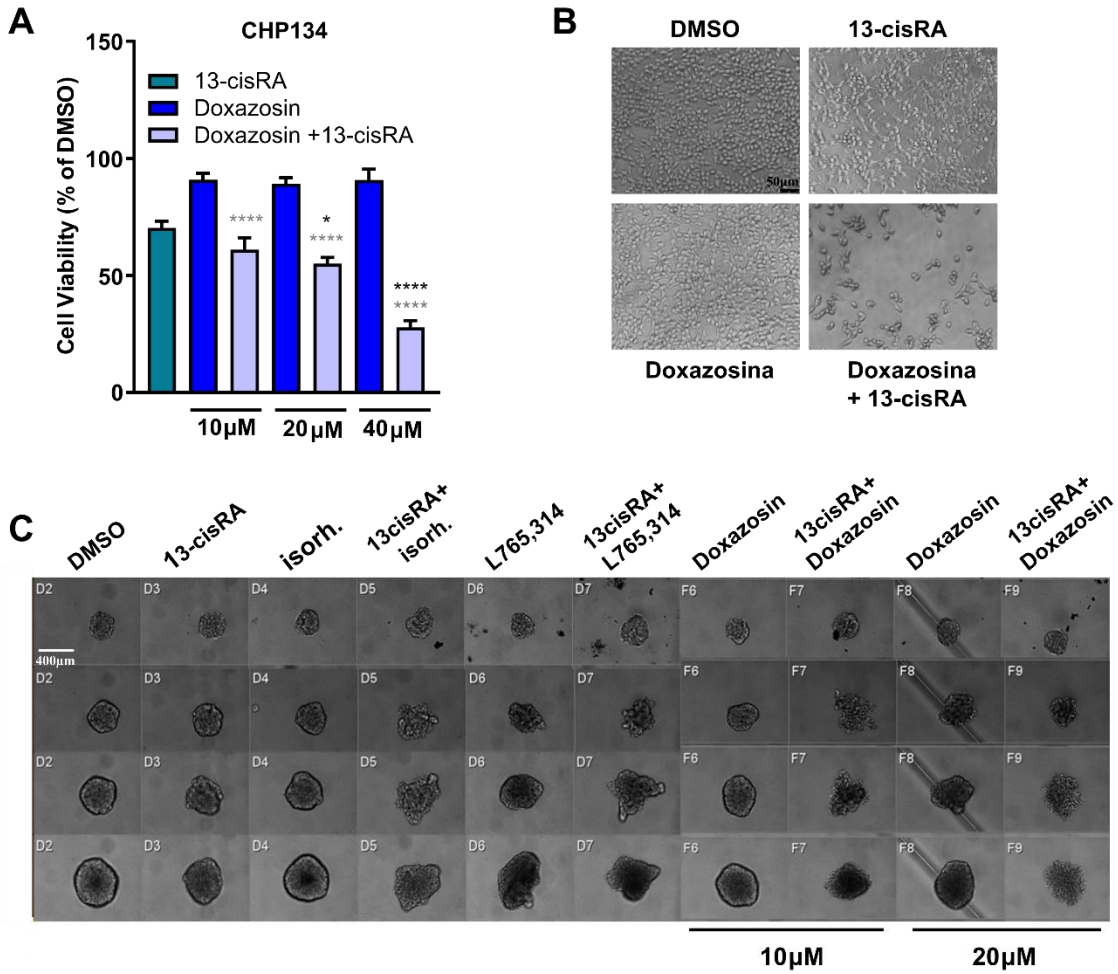

Figure 25. Doxazosin augments the anti-proliferative effect of 13-cis-RA on NB cell monolayer and spheroids. (A) Cell viability of cells treated with the indicated compounds for 72h. The data are displayed as the percentage of vehicle-treated control mean ± SD of at least three biological experiments. Statistically significant differences between double treatment and 13-cis-RA treatment (black asterisks) and doxazosin compound treatment (grey asterisks) were calculated according to one-way ANOVA followed by Dunnett's multiple comparisons tests. **(B)** Representative images of CHP134 cells treated with DMSO, doxazosin (10μM), 13-cis-RA (5μM) and the combination of the two for 72h. Cell imaged in bright filed with 10X magnification. **(C)** CHP134 spheroids were exposed to L765,314 and doxazosin alone or in combination with 13-cis-RA and imaged every 24h. Representative images of treated spheroids are reported. Spheroids imaged by 10X long WD objective.

We tested the efficacy of combinatorial treatment also on other RA sensitive NB cell lines and on SK-N-AS cells as a negative control. The tested NB cells lines resulted to be responsive to the concomitant exposure to doxazosin and 13-cis-RA, reflected by a reduction of cell viability in the combined treatment relative to single ones (Figure 26). The decrease in cell viability observed in the NB3 cell line in the treatment with 13-cis-RA and doxazosin is less striking than what was observed in the combination of the retinoid with L765,314 (Figure 16 B). This outcome can be imputed to the lower specificity of doxazosin over ADRA1B, thus indicating that the specificity over the receptor subtype is important for the sensitization of cells over 13-cis-RA.

Also, the SIMA cell line resulted to be more refractory to the combined treatment compared to the other RA-sensitive cells line (Kelly, IMR32, NB3); this is consistent with the reduced susceptibility of this cell line to the other drug combinations tested in this work (i.e. isorhamnetin Figure 8, L765,314 Figure 16 B, and AH1110A Figure 23). The SK-N-AS cells showed a slight decrease in cell viability when exposed to 20μM of doxazosin alone but without an additive effect with 13-cis-RA, again reproducing what was observed for treatment with L765,314 (Figure 16 B).

Collectively, these data indicate that the combination of the FDA approved doxazosin with 13-cis-RA is effective in reducing cell viability in different *in vitro* models of NB, thus posing the basis for further *in vivo* analysis.

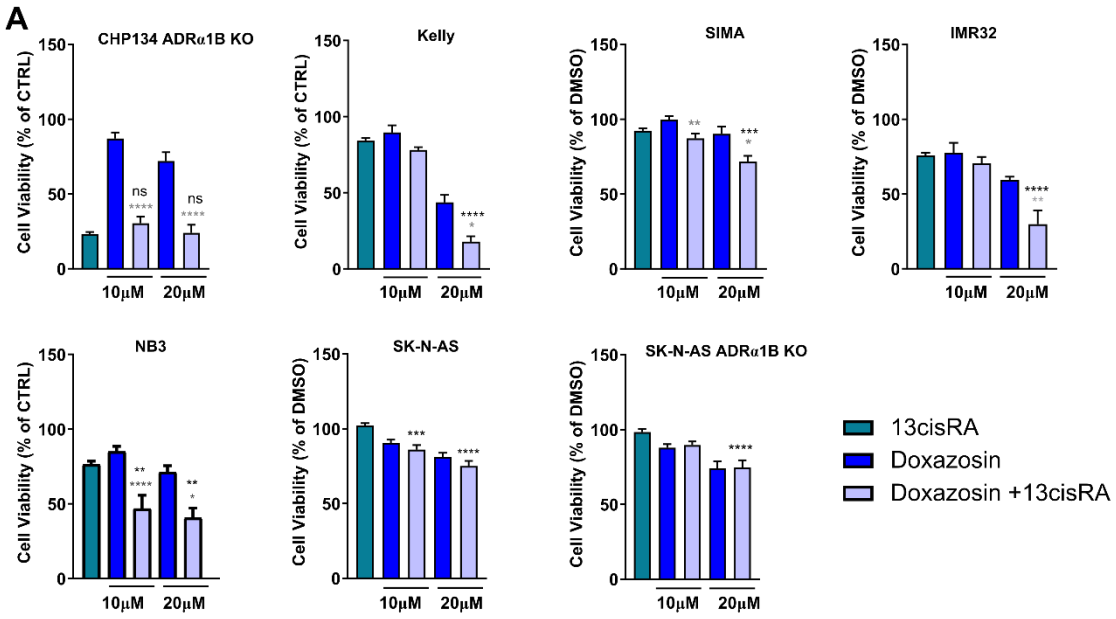

Figure 26. The combined treatment of doxazosin with 13-cis-RA is effective in the reduction of cell viability of several RA-sensitive NB cells. (A) Cell viability of different NB cell exposed to two concentrations of doxazosin alone or in combination with 13-cis-RA (5μM) for 72h. Statistically significant differences between treatments with doxazosin plus 13-cis-RA and either 13-cis-RA (black asterisks) or doxazosin alone (grey asterisks) were calculated by one-way ANOVA followed by Dunnett's multiple comparisons tests.

7. *In vivo* treatment of NB xenografts with doxazosin and 13-cis-RA blocks tumor growth

To evaluate the effectiveness of the proposed combined treatment with an alpha-1-AR agonist and 13-cis-RA *in vivo*, we decided to use a xenograft model in nude mice. We xenografted CHP134 cells, expressing luciferin, into the right flank of athymic nude mice. After the establishment of a visible tumor mass, mice were divided into four treatment groups: DMSO, 13-cis-RA, doxazosin, and 13-cis-RA plus doxazosin. We waited until the formation of the tumor mass to start the treatment to better mimic what occurs in patients where the start of the pharmacological treatment is performed after the diagnosis of the tumor.

All the compounds were given daily for two weeks. The doses for treatment has been chosen starting from those currently used in humans for both drugs and following the

indication reported by Nair *et al*. (Nair & Jacob, 2016) to translate the human doses into doses suitable for mice. Thus, we administered 10mg/kg of 13-cis-RA and 10mg/kg of doxazosin once a day for a total of 15 days. The luminescence signal from CHP134 luciferin expressing cells was used to monitor the tumor growth. Mice were live imaged on day 0, as a baseline, and then, every 7 days till the end of the treatment (15 days) and then monitored for an additional week for a total of 21 days (Figure 27 A).

The mice administered with doxazosin plus 13-cis-RA develop smaller tumors at the end of the treatment period with respect to the control and single drug groups which suggests that the drug combination slows down tumor growth. To quantify the phenomenon, we take into account two parameters: the tumor overall growth and the growth velocity both based on tumor volumes. The tumor volumes, *V*, was calculated as follows: $V = (Width^2 * Lenght)/2$, where the width and length parameters were obtained from the analysis of the acquired *in vivo* images. The overall growth of tumor masses was analysed normalizing the volume's values detected the day before the treatment start. The growth velocity evaluation, instead, was done by fitting the tumor volumes to a linear regression model *($y=\beta x+q$)*, where the unknown y is the volume and the β parameters indicate the slope of the linear model, so it is the indicator of how fast the tumor volumes varies over time. The analysis confirmed that the alpha-1-AR antagonist, doxazosin, and the retinoid, work together to slow down tumor growth (Figure 27 B). The restraints posed to the tumor growth by the double treatment led to the establishment of statistically significant smaller tumors in mice of this treatment cohort (Figure 27 C). Importantly, the double-treated tumors do not speed up their growth rate after the end of treatment periods (first 14 days) (Figure 27 B-C). This observation suggests that the treatment is effective even after the suspension of daily administration in keeping the tumor progression under control. Further analyses are needed to understand to which extent the effectiveness of the combined treatment with 13-cis-RA and doxazosin in reducing tumor aggressiveness is due to impairment of cell proliferation and malignant cells differentiation. The observations done by *in vivo* imaging has been confirmed on the day of mice suppression when the tumors were

extracted and measured: the tumors deriving from double-treated mice resulted to be smaller compared to those of all the other treatment groups (Figure 27 D).

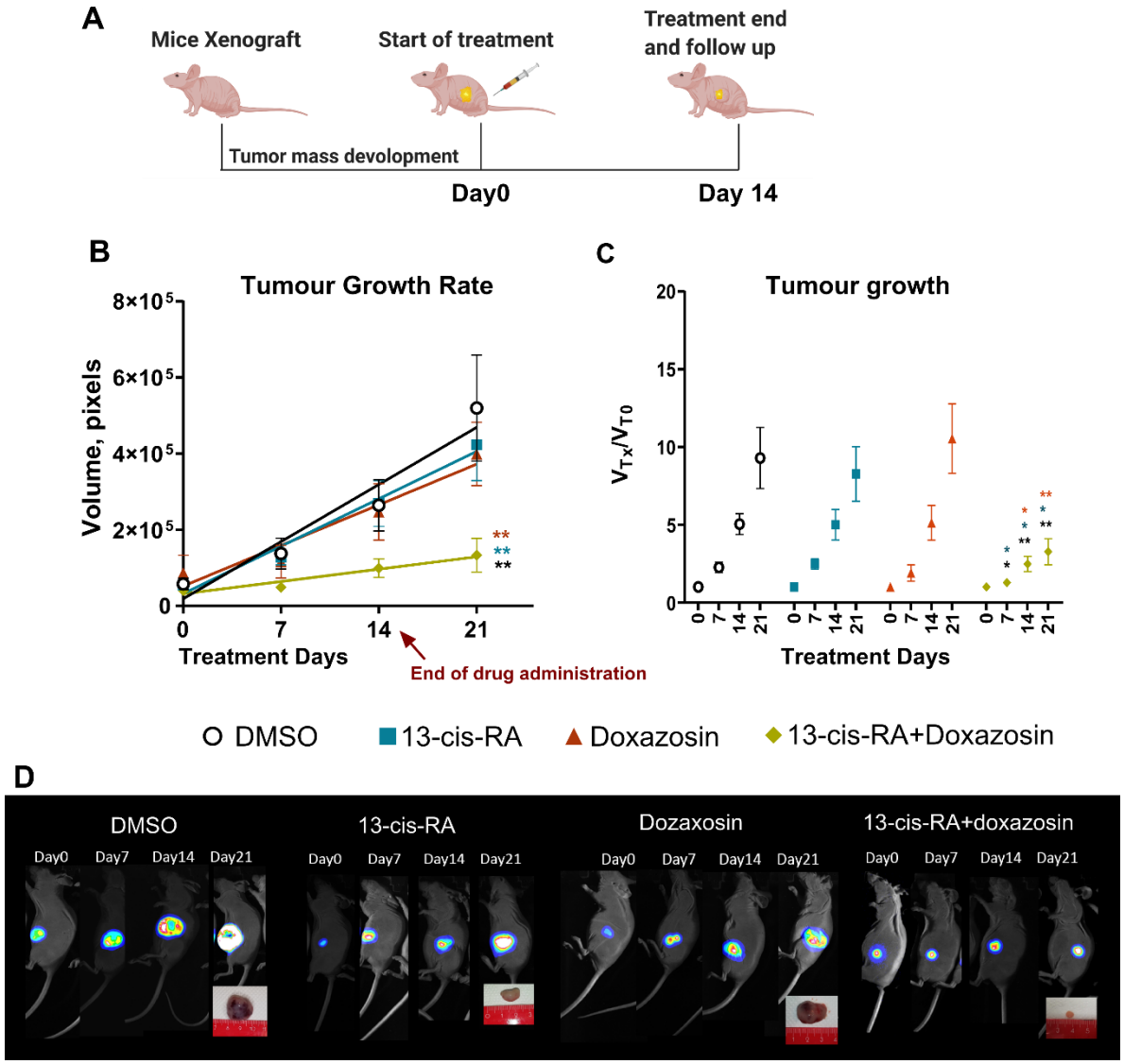

Figure 27. The co-administration of 13-cis-RA and doxazosin to mice xenograft controls tumor growth. (A) Workflow of the *in vivo* study. **(B)** Tumor xenograft volume increase. Tumor volumes were normalized on the *V* detected on day 0. Statistical analysis was performed on $\log_2 (V_t/V_0)$. **(C)** The tumor growth rate was evaluated by fitting the registered tumor volumes to a linear regression model ($y=\beta x+q$). The statistical significance was calculated comparing the β factors (i.e. the slope of the linear model) obtained for each treatment. **(D)** Representative images of *in vivo* monitoring of the differentially treated mice.

DISCUSSION AND CONCLUSIONS

Despite the aggressiveness of the treatment protocol for high-risk NB tumors, in >30% of these patients relapse occurs (Park *et al*, 2013). The tumor reoccurrence is due to the residual disease that has not been eradicated. Since the 1970s several molecules have been tested for their use as pro-differentiative agents in different types of cancer, including acute myeloid leukaemia and breast cancer (Xu *et al*, 2014). The main conceptual advantage of pro-differentiation agents over antiproliferative ones is the abrogation of malignant stem cell self-renewal by terminal maturation, which could bring to a less efficient selection of resistant clones (De Thé, 2018). For neuroblastoma, the leading drug used for this purpose is 13-cis-RA Even if the introduction of 13-cis-RA in NB therapy has contributed to the improvement of the prognosis of children diagnosed with high-risk disease, the 3-year disease-free survival rate for these patients is only about 50% (Masetti *et al*, 2012). Thus, other drugs have been proposed to ameliorate the effectiveness of 13-cis-RA in the eradication of the minimal residual disease. For example, it has been shown that the combination of retinoid and histone deacetylase inhibitors are synergistic to inhibit tumor growth in vitro (De Los Santos *et al*, 2007).

Starting from the aim of finding a novel double-drug therapy to increase the pharmacological value of 13-cis-RA, we identified the flavonoid isorhamnetin as a natural compound able to synergize with the retinoid. The exposure of NB cells to the combination of the two drugs leads to reduction of cell viability together with induction of apoptosis and stop of cell cycle progression (Figure 7, Figure 8, Figure 9, and Figure 10). Interestingly, we report that the cell viability decrease exerted by the combinatorial therapy is accompanied by the overexpression of the adrenergic receptor alpha-1B (Figure 11). The ARs are involved in the mediation of the catecholamine signalling in the peripheral sympathetic nervous system that is the anatomical location of NB. The role of catecholamines in the stimulation of proliferation is widely recognized and high levels of these neurotransmitters are present in NB patient's urine samples (Maris, 2010) Due to their role as mediators of catecholamine

signalling, also ARs have been investigated for their role in the control of pivotal signalling cascades such as control of proliferation and neural development (see sections 2.1 and 2.2). In particular, ADRA1B has been classified as an oncogene whose constant activation leads to foci formation in fibroblasts (Allen *et al*, 1991). These considerations and our data that indicate ADRA1B as an effector of the anti-cancer synergism of 13-cis-RA and isorhamnetin stimulated us to focus on ADRA1B and more generally on the class of adrenergic receptors as new targets in neuroblastoma.

To study the role of ADRA1B in NB, we started generating genetic KO cell lines for this AR. We showed that the lack of this receptor leads to sensitization of CHP134 cells to 13-cis-RA induced loss of cell viability (Figure 15 A). The observation was confirmed by incubation of cells with the ADRA1B specific inhibitor L765,314: the combination of this alpha-1B-AR antagonist with 13-cis-RA provokes a consistent fall of cell viability (Figure 15 B, C, and D) to values similar to what observed in the combination of the retinoid with isorhamnetin. This similarity of treatments outcome can be attributed to the possible role of isorhamnetin as an alpha-1-AR antagonist; the metabolic precursor of isorhamnetin, the flavonol quercetin, has been reported to be an antagonist of the alpha-1-AR (Ajay *et al*, 2003) so it is possible that also isorhamnetin works as an alpha-1-AR inhibitor.

We confirmed the effectiveness of the blockage of the alpha-1B-AR in augmentation of the anti-proliferative effect of the 13-cis-RA on a panel of different NB cell lines; the responsiveness is maintained regardless of MYNC status; the only exception is the SK-N-AS cell line, either WT or KO for the receptor (Figure 16 B). The resistance of this last cell line is due to its intrinsic refractory to 13-cis-RA therapy, indicating that retinoid responsiveness is essential to obtain a reduction of cell viability. The tested non-NB cell lines do no show to be impacted by the combination of L765,314 and 13-cis-RA (Figure 16 B).

We showed that the 13-cis-RA promoted reduction of cell viability observed in the ADRA1B KO cells is the result of high induction of apoptosis and neural differentiation. The occurrence of the differentiation process upon exposure of CHP134 cells to 13-cis-

RA was confirmed by the analysis of the expression of a selected panel of recognized markers. We observed a consistent induction of the expression of neural differentiation-associated markers, such as TH, beta3-tubulin, Sox9 and GAP43 and downregulation of MCYN (Figure 17, Figure 18 and Figure 19) that is, again, significantly more evident in cells lacking the adrenergic receptor alpha-1B. These fluctuations in expression of neural markers were not detected in SK-N-AS cells upon exposure to the retinoid alone or along with isorhamnetin, even in the SK-N-AS ADRA1B KO cells (Figure 18 A-C). This confirms that the intrinsic responsiveness to 13-cis-RA is essential to trigger the differentiation program, which is then facilitated by the lack of ADRA1B.

The direct consequence of these observations is that targeting of ARs could be beneficial to significantly potentiate the clinical effectiveness of 13-cis-RA and that such combinatorial therapy can be indicated to be applied in the post-consolidation phase of NB treatment to obtain a full differentiation of residual tumor cells, thus impacting tumor aggressiveness.

To carry out a wider validation of ARs as a new target in NB and to better understand which class of ARs in the best choice for the proposed combinatorial therapy, we performed a focused screening with ARs modulators to be administered along with 13-cis-RA looking for those combinations that augment the reduction of cell viability started by the retinoid. The high-throughput experiment leads us to the identification of 10 hits. The great majority of the hits, 8 over 10, are AR-antagonists (Figure 21, Table 5). This clearly indicates that the best option to develop a new combinatorial therapy with 13-cis-RA to affect the minimal residual disease is to inhibit rather than stimulating the AR-mediated signalling, as predicted. The most represented sub-family of ARs among the screening hits is the alpha-1-AR one. Notably, all the alpha-1 modulators that emerged from our analysis are AR-antagonist and the best hits resulted to be AH11110 HCl, with an IC50 of 10.29 μM when administered with the retinoid, that is a specific inhibitor of ADRA1B. The only AR-agonist that emerged from the screening are specific for beta-ARs, no alpha-AR agonist results to be able to potentiate the 13-cis-RA. The alpha and beta ARs are involved in different signalling cascades (Figure 6)

indicating that treatment specificity toward a particular AR family is of pivotal importance for the outcome of the proposed approach. We showed that the combination of AH11110A HCl with 13-cis-RA is effective in reducing cell viability on several NB cell lines (Figure 23). We then performed a neurite outgrowth quantitative analysis using the best AR-antagonists emerged by the hits-validation. The analysis demonstrates that the decrease in cell viability observed in the combination of the AR-antagonists with 13-cis-RA is also accompanied by augmentation of neural differentiation (Figure 24).
The overall results of the high-throughput assay on AR-ligands further confirmed the data obtained with our experiments on ADRA1B KO cells and with the specific inhibitor L765,314.

In general, from our analysis, we can confirm that the antagonization of AR, and in particular of alpha-1-AR is the most promising strategy to improve the therapeutic effects of 13-cis-RA. This approach has several advantages: the first is that being receptors the ARs are an excellent target to modulate their downstream signalling pathways; the second, the fact that on the market several FDA approved drugs are available that specifically modulate the AR; the third, the fact that thanks to the wide use of these drugs we have easy access to their pharmacokinetic properties and we are aware of possible sides effects, which is very useful for a successful drug repurposing strategy.

The first synergistic compound that we identified in the preliminary results of the thesis, the flavonoid isorhamnetin, has a pharmacokinetic profile not favourable; its bioavailability after oral intake is very low (Thilakarathna & Vasantha Rupasinghe, 2013). Studies on quercetin, the metabolic precursor of isorhamnetin, showed that its bioavailability in humans is only 1% (Gugler *et al*, 1975). The low bioavailability poses the problem of having to administer high doses to reach a therapeutically relevant dose at the target site. We tested *in vivo*, the efficacy of the combination of isorhamnetin (50mg/kg/daily) and 13-cis-RA (10mg/kg/daily) in the control of tumor growth; we

did not register any difference between the tumor's masses developed in double-treated vs single-treatment mice (data not shown). We also observe the formation of a light-yellow spot at the administration sites in mice treated with isorhamnetin either alone or together with 13-cis-RA, which is a sign of an abdominal accumulation of the flavonoid. These *in vivo* preliminary results further corroborate the choice of focusing on ARs, for the evaluation of new therapeutic approaches.

Unfortunately, AH1110A, our leading compound that emerged from the screening, is not a drug already used for therapeutic purposes. Among the other best hits, imipramine, doxepin (two tricyclic antidepressants) and carazolol (a beta-blocker used in animals) are FDA approved drugs. For their primary use, these molecules could pose some concern about safety in children, as testified by a debate (Dwyer & Bloch, 2019). Thus, we decide to look for another specific alpha-1-AR antagonist, that we can employ to perform the *in vivo* evaluation of the proposed combinatorial therapy, and that it is not used as a psychotropic drug. To this aim, we selected doxazosin which is routinely used to mitigate symptoms related to prostate hyperplasia and to treat hypertensive status in children with pheochromocytoma and neuroblastoma (Sendo *et al*, 1996; Seefelder *et al*, 2005; Ganesh *et al*, 2009). We tested the efficacy of the combination of doxazosin with 13-cis-RA in reduction of cell viability on a panel of NB cell lines (Figure 26) and 3D spheroid models, used to mimic a tumor mass (Figure 25).

Interestingly, in all the analysed drug combinations (ie. 13-cis-RA with isorhamnetin or L765,314 or AH11110A or doxazosin), we observed a range of response of the different NB cell lines tested. Being NB an heteregenous tumor, also the NB cell lines bear different somatic and genetic alterations (Table 6) that may have an impact on the degree of responsiveness to the proposed treatment. To better understand this point, we build a "response classification" ranking the cell lines on the base of the mean difference in loss of cell viability between each single treatment (i.e., 13-cis-RA or isorhamnetin or L754,314 or AH1110A or doxazosin) and the double treatment (i.e. isorhamnetin or the alpha-1-AR antagonist administered together with 13-cis-RA); the greater the mean differences were the higher ranking-score of responsiveness was

assigned to the cell lines (table 7). Interestingly the extent of reduction of cell viability experienced by the different cell lines is quite consistent among the combination of 13-cis-RA with first isorhamnetin and then the selected alpha-1-AR inhibitors (L765,314, AH1110A and doxazosin)(see table 7).

Table 6. Most common Somatic and genomic aberrations reported in letterature for the here tested neuroblastoma cell lines (Bedrnicek et al, 2005; Ordóñez et al, 2014; Harenza et al, 2017).

Cell line	**MYCN**	**1p**	**3p**	**11q**	**17q**	**ALK**	**p53**
NB-3	Amp	Loss	None	None	Gain \Loss	R1275Q	WT
CHP134	Amp	Gain\Loss	Gain	None	Gain	WT	WT
IMR-32	Amp	Loss	Loss	LOH	Gain	WT	WT
Kelly	Amp	Loss \Gain	Loss	Loss	Gain	F1174L	P177T
SiMa	Amp	Loss \Gain	Loss	Loss	Loss	R1275Q	R376Q
SK-N-AS	Non-Amp	Loss	Loss	Gain	Gain	WT	H168R

Table 7.Cell line ranking on the base of responsiveness to the indicated combined treatment with 13-cis-RA

		13-cis-RA +					
		Isorhamnetin	**L765,314**	**AH1110A**		**doxazosin**	
	Rank	**15 µM**	**20 µM**	**15 µM**	**20 µM**	**10 µM**	**20 µM**
cell line	1	CHP134	CHP134	NB3	NB3	NB3	Kelly
	2	NB3	NB3	IMR32	CHP134	CHP134	IMR32
	3	IMR32	IMR32	CHP134	IMR32	Sima	NB3
	4	Kelly	Kelly	Kelly	Kelly	Kelly	CHP134
	5	Sima	Sima	Sima	Sima	IMR32	Sima
	6	SK-N-AS	SK-N-AS	SK-N-AS	SK-N-AS	SK-N-AS	SK-N-AS

The SK-N-AS cell line showed the lowest responsive profile and never show any consistent reduction of cell viability when the retinoid is co-administered with isorhamnetin or the alpha-1-AR antagonists. This refractory behaviour can be mainly imputed to the intrinsic resistance of SK-N-AS to the 13-cis-RA, and not to the lack of MCYN amplification since the non-MYNC amplified SK-N-SH cell lines are responsive to retinoidn therapy (Bayeva *et al*, 2021) indicating that is not the only factor involved.
On the other hand, CHP134 and NB-3 reveal a great sensitivity over the proposed treatment combinations, IMR-32 and Kelly demonstrated an intermediate level of response, and SiMa resulted to be more refracotry to the analysed treatments.
Looking at the different genomic landscapes of the tested NB cell lines, CHP134 and NB-3 share some somatic and genetic alterations like the *MYCN* amplification and the presence of a WT p53 protein but differs for others like the ALK status and the loss/gain on chromosome 1p, 3p and 17q. Kelly and IMR-32, also have *MCYN* locus amplification and share aberration on chromosomes 3p, 11q and 17q. The gain on chromosome 17q is present also in the more responsive cell line CHP134 while the aberration in chromosome 11q is shared with the less sensitive SiMa cell line. This last cell line has a loss on chromosome 17q also present in NB-3 with whom also shares the same mutation on ALK gene. Of note, the three most responsive cell lines have WT p53 protein, but the presence of mutation of p53, per sè is not sufficient to abolish sensitivity over the treatments as demonstrated by Kelly and SiMa, which, even if at lower level, maintain susceptibility over the proposed synergistic treatments. CHP134 and NB-3 do not have aberration on chromosome 11q and among the tested cell lines only the CHP134 has a gain in 3p, but again the presence of loss on 11p or deletion on 3p are not enough to abolish responsiveness as demonostrated by decrease of cell vibility of IMR-32, Kelly and SiMa when exposed to proposed treatment with 13-cis-RA and alpha-1-AR anatagonists. Regarding the status of ALK; NB-3, Kelly and SiMa have a mutated locus, while CHP134, IMR-32 and SK-N-AS have a WT gene.
In general we can hypothesis that the impact on the efficacy of our treatment probably comes from a combination of somatic and genomic aberrations which need to be further investigated since the current data are not enough to pull the strings to draw a

clear picture. The heterogenicity of NB genomic landscape is for sure a pivotal aspect that need to be taken into account when proposing a new therapeutic strategy. For this purpose will be important to further expand the panel of tested NB cell lines and correlate the outcome with a deep analyse of the somatic and genetic aberrations bared by the NB cell lines used.

After validation of the selected alpha-1-AR antagonist, we moved from *in vitro* to *in vivo*. Here we report that the daily administration of doxazosin, whose bioavailability is 60-70% (https://go.drugbank.com/drugs/DB00590), together with 13-cis-RA in NB mice xenograft blocks the tumor progression. The tumors mass in mice receiving the double treatment grows at significantly lower rates than what is observed in control mice or those injected with just 13-cis-RA or doxazosin, as a consequence the tumor mass developed in these mice is significantly smaller than that on control mice. Therefore, we can conclude that the use of the specific alpha-1-AR inhibitor, doxazosin, together with 13-cis-RA is efficient in impairing the tumor growth and keep the disease progression under control in mice (Figure 27 B, C and D).

In summary, in this thesis, we demonstrated that the inhibition of the alpha-1–AR can improve the beneficial effects of 13-cis-RA therapy both in terms of reduction of tumor growth and induction of differentiation, in NB. Several other studies investigate the modulation of AR as anti-cancer therapy. For example, work on pancreatic cells showed that the blockage of β2-AR increments the inhibition of cell proliferation exerted by chemotherapeutic agent gemcitabine (Shan *et al*, 2011). Moreover, the overexpression of alpha and beta ARs has been associated with poor outcome tumors like in breast and ovarian cancer (Perez *et al*, 2011; Deutsch, 2016). Analysing publicly available data sets of NB patients samples (Molenaar *et al*, 2012), we found indication that also in NB the overexpression of alpha-1B-AR negatively correlates with overall free survival probability (Figure 28 B).

The other two members of the alpha-1-AR family, ADRA1A and ADRA1D, do not show a significant correlation between the overall survival probability and level of their

expression (Figure 28 A, C). This further indicates that specificity of treatment could be of pivotal importance for the outcome of the therapy. Our data in vitro, corroborate this consideration since we observe higher reduction of NB cell viability when we combine 13-cis-RA with the ADRA1B specific antagonist L765,314 rather than what obtained with doxazosin which is a general alpha-1-AR antagonist. Nonetheless remains the important of the positive results obtained with doxazosin both *in vitro* and *in vivo* since it is a drug already used in clinic which is of advantages for drug repositioning porpoises.

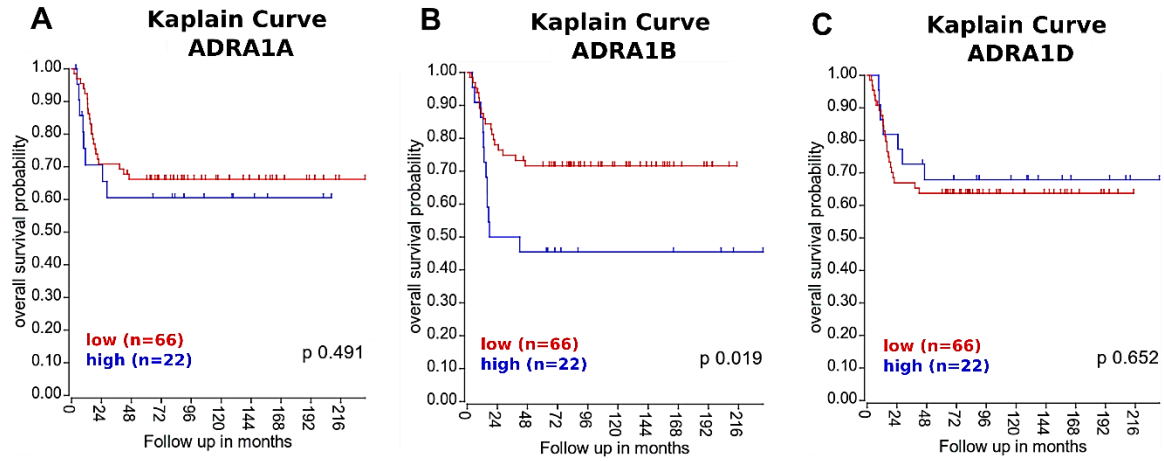

Figure 28. Kaplan Meier curve of overall survival probability of NB patients relative to ADRA1 receptor family expression. (A) ADRA1A **(B)** ADRA1B and **(C)** ADRA1D. Data of sequencing from Versteeg database composed of 88 NB patient samples (Molenaar *et al,* 2012). Data elaborated by R2 platform https://r2platfrom.com. The samples with levels of expression in the last-quartile were categorized as high-expressing and compared to all the other samples in the dataset.

The analysis on the correlation between the overall survival probability and the level of expression of the members of the alpha-1-AR was performed also on other available data-sets and we observed contrasting results: for example the analysis on the datasets from Kocak's study (GSE45547)(Kocak *et al*, 2013) gives opposite result indicating as indicator of poor prognosis the low expression of ADRA1B. On the other hand, the analysis on the expression data from Maris lab (GSE3960) (Wang *et al, 2006*) is in accordance with the results obtained with Veersteg datasets (GSE16476) *(*Molenaar *et*

al, 2012). but with less significant results. The discordance of results among the datasets indicates the need of further investigations on this point.

Taking into account that NB is a neuroendocrine catecholamine-secreting tumor, that the stress-hormone rich environment can favoure tumor progressio (Eng *et al*, 2014) (see section 2.1), that the major mediators of the stress associated signalling are the adrenergic receptors, that there is interplay between the AR and RA signalling (see section 2.3) and the evidence reported in this thesis we suggest the molecular mechanism reported in Figure 29 to explain the increase in sensitivity to 13-cis-RA following alpha-1-AR inhibition. In detail, we propose that the blockage of the catecholamine signalling via specific antagonization of alpha-1-AR frees NB cells to undergo the pro-differentiative and pro-apoptotic pathways promoted by 13-cis-RA (Figure 29). In conclusion, we indicate the alpha-1-AR as novel targets to be employed in combinatorial therapy, along with 13-cis-RA, for NB. Our work points out the ability of alpha-1-AR antagonists to potentiate the therapeutic value of 13-cis-RA for the eradication of the minimal residual disease by promotion of tumor cell apoptosis and blockage of self-renewal by inducing differentiation.

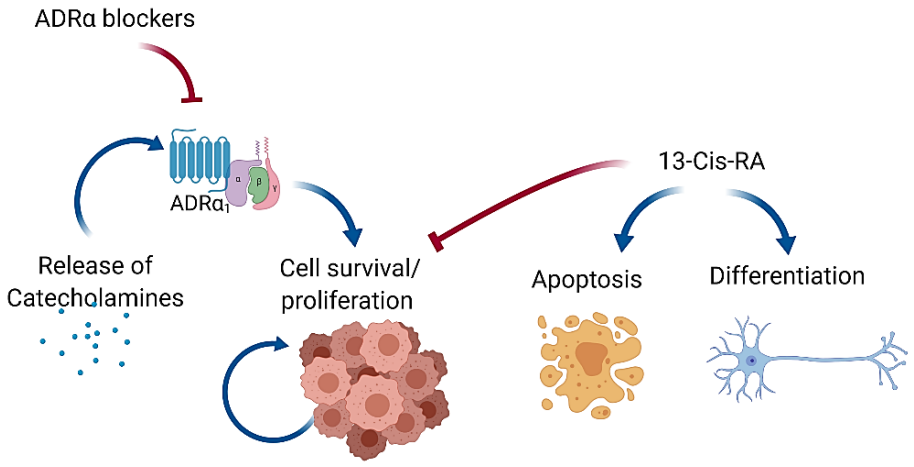

Figure 29. Proposed molecular mechanisms underneath the sensitization to 13-cis-RA of NB cells exposed to alpha-1-AR antagonist. Since NB is a catecholamine-rich tumor, we propose that the interruption, by ADRA1 blockage, of the pro-proliferative circuit generated by catecholamines restores in the cells the ability to undergo the pro-differentiative and pro-apoptotic programs promoted by 13-cis-RA.

MATERIALS AND METHODS

Cell culture

The human NB cell lines CHP134, IMR-32, Kelly were obtained from the European Collection of Cell Culture (ECACC) (Salisbury, UK), while SiMa was purchased from Deutsche Sammlung von Mikroorganismen und Zellkulturen GmbH (Braunschweig, Germany). The human NB cell line UKF-NB3 was kindly provided by the Pediatric Oncology Unit (Fondazione IRCCS Istituto Nazionale dei Tumori, Mialn, Italy). CHP134, UKF-NB3, Kelly and SiMa cells were grown in RPMI-1640 media supplemented with 10% v/v FBS, 1% v/v L-glutamine, 100U/ml penicillin and 100 U/ml streptomycin. IMR-32 cells were cultivated in EMEM supplemented with 10% v/v FBS, 1% v/v L-glutamine, 1% v/v NEAA and 100U/ml penicillin and 100 U/ml streptomycin. SK-N-AS cells were kept in DMEM medium supplemented with 10% v/v FBS, 1% v/v L-glutamine, 100U/ml penicillin and 100 U/ml streptomycin. All the cell lines were maintained at 37°C under a 5% CO_2/95% air atmosphere at constant humidity. To detach cells the Trypsin-Versene (EDTA) Mixture (1X) was used.

Generation of ADRA1B KO cells

To generate NB cell lines lacking ADRA1B we exploit the CRISPR/Cas9 technology. The gRNAs were designed using the GPP WEB Portal (Broad Institute: https://portals.broadinstitute.org/gpp/public/) (sgRNA seq: 5'-GGGCAGGTGCTGATGTGT-3') and cloned into LentiCRISPR plasmid (Addgene, #56961). For lentiviral particles production HEK 293T packaging cells were co-transfected with the lentiviral vector, the packaging plasmid psPAX2 (Addgene, #12260) and the envelope plasmid pMD2.G (Addgene, #12259). Generation of stable KO cell lines was performed transducing target cells with To generate stable cell lines, NB cells (CHP134 and SK-N-AS) were transduced with 1 RTU/ml of lentiviral particles. Positively transduced cells were selected with puromycin at 1-2µg/ml. Single clones were generated by clonal selection seeding 0,5cells/well in 96 well plate. Effective KO was

assayed by PCR amplification of the gRNA target site followed by Sanger sequencing (Eurofins Genomics) and chromatogram analysis (Synthego™).
Primers for PCR of ADRA1B: Fw 5'-TGGACCATTAAACTTGGAGCTGCCG -3', Rv 5'-AGCGGTAGAGCGATGAAGAAGGG-3'.

Chemicals

13-cis-RA (Cat. N. R3255, Sigma-Aldrich) and isorhamnetin (Cat. N. 17794, Sigma Aldrich) were dissolved in dimethyl sulfoxide (DMSO) at a concentration of 100 mM. The ADRA1B-specific inhibitor L765,314 (Ref. sc-493741, Santa Cruz Biotechnology) and the alpha-blocker doxazosin (Cat. N. D9815, Sigma-Aldrich) were dissolved at 25mM and 100mM respectively in DMSO. Stock solutions were stored at -20°C. The intermediated dilutions were performed in PBS. For ARs ligand screening, the molecules of the two libraries (Enzo Screen-Well adrenergic ligand library (#BML-28110000) and Target Mol 2700-100µl) were dissolved at 10mM in DMSO or water.

Cell viability assays/Growth inhibition assay

Cell viability was assessed using CellTiter-Glo (Promega) assay following the manufacturer's instructions. When evaluated on 3D spheroids, cell viability was assessed by the CellTiter-Glo® 3D Cell Viability Assay (Promega). The percentage of viable cells is expressed relative to control-treated cells, or to the time zero (right before the drug administration). Where indicated, IC50 of a drug was calculated by a non-linear regression model to the log (inhibitor) vs response curve (three parameters) using the GraphPad Prism Software.

Death/live cell marker staining

Live cells were stained with 0.5µM of Calcein AM green Viability Dye (Thermofisher) and with the nuclear dye Hoechst. After 1h of incubation at 37°C, cells were also stained with 5nM of Sytox Red dead cell stain (Thermofisher) and incubated for 20min at RT. Cells were imaged with Operetta (PerkinElmer) with LWD 20X objective and the appropriate filter settings; images were analyzed for positively stained cells by Harmony software (PerkinElmer).

Screening of natural compounds library in combination with 13-cis-RA treatment

$1x10^4$ CHP134 cells were seeded in 96-well plates. After 24h, cells were contemporary exposed to a sublethal dose of 13-cis-RA (0.05μM) and the library of natural compounds at 10μM final concentration in 0.1% DMSO. Every plate included the following controls: vehicle-treated control cells (0.1% DMSO v/v), 0.05μM 13-cis-RA and 20μM 13-cis-RA alone. After 48h of incubation cell viability was assessed using Cell Proliferation Reagent WST-1 (Roche). The percentage of viable cells was expressed relative to time-zero measurement. To evaluate the performance and feasibility of the screening, we determined the Z' factor. As top controls, 0.1% DMSO (the top control) and 20μM 13-cis-RA (the bottom control) leads to 100% inhibition of cell viability at 48 hours. The calculated Z'-factor of 0.568 along with a CV of 0.004 and signal to background ratio of 0.45 indicated the assay as robust and reliable. Hits validation was performed challenging cells with 10μM of selected natural compounds either used alone or in combination with 5μM of 13-cis-RA. After 24h of treatment, cell viability was assayed referred to as time zero, using Cell Proliferation Reagent WST-1 (Roche).

Polysomal RNA extraction

For polysomal RNA extraction, 24h after indicated treatment start, cells were incubated with 100 μg/ml cycloheximide for 4 min at 37°C, rinsed with PBS+10 μg/ml cycloheximide, lysed on ice with 300 μl lysis buffer [10 mM NaCl, 10 mM MgCl2, 10 mM Tris–HCl, pH 7.5, 1% Triton X-100, 1% sodium deoxycholate, 0.2 U/μl RNase inhibitor, 100 μg/ml cycloheximide and 1 mM dithiothreitol] and centrifuged at 12000g @4°C for 10min. Then, the obtained supernatants were loaded onto a 15–50% linear sucrose gradient containing 30 mM Tris–HCl, pH 7.5, 100 mM NaCl, 10 mM MgCl2, to perform fractionation by ultracentrifugation for 100 min at 180,000 g. Fractions were collected monitoring the absorbance at 254 nm. The polysomal fractions were incubated at 37°C for 2 hours in the presence of 100 μg/mL proteinase K and 1% SDS and then used to extract RNA by phenol-chloroform protocol. Polysomal RNA was resuspended in 30 μl of RNase-free water and quantified using NanoDrop ND 1000. RNA quality was assessed by the Agilent 2100 Bioanalyzer (Eukaryote Total RNA Nano kit, Agilent Technologies).

Gene expression profiling using TaqMan assay

1µg of polysomal RNA was reverse transcribed using iScript cDNA Synthesis Kit (Bio-Rad Laboratories). 10ng of cDNA was used to perform TaqMan quantitative real-time PCR in a 10µl reaction volume containing: 1x Kapa Probe Fast qPCR Universal Master Mix (Kapa Biosystems, Boston, USA) and 1x TaqMan Gene Expression assay (Life Technologies). The qPCR was performed on a CFX96 real-time PCR Detection System (Bio-Rad Laboratories) with the following cycling conditions: 3min at 95°C followed by 40 cycles at 95°C for 3sec, 60°C for 20sec, and 72°C for 1sec. The expression levels of target genes were normalized to the geometric mean of three reference genes (HPRT1 Hs99999909_m1, SDHA Hs00417200_m1, and RLPL0 Hs99999902_m1) and calibrated to the DMSO-treated control sample. The Cq values were determined by the CFX Manager 3.0 software (Bio-Rad Laboratories), applying a multi-variable, non-linear regression model to individual well's fluorescence traces.

List of analysed genes and used probes: ADRA1B Hs00171263_m1, SGK1 Hs00985035_m1, Dusp6 Hs00737962_m1, CYP26B1 Hs01011223_m1, CYP1A1 Hs00153120_m1, NFATC1 Hs00542678_m1, ADRA2A Hs01099503_m1.

Cell cycle analysis

For cell cycle analysis evaluated by high content image analysis, the newly synthesized DNA was detected utilizing Click-iT EdU Alexa Fluor 594 HCS assay (C10354, Life Technologies) following the manufacturer's instructions. The assay was multiplexed with Hoechst 33342 to counterstain the nuclei and with an anti-phosphorylated histone H3 antibody (Abcam, ab5176, 1:500) to evaluate mitotic activity. Alexa Fluor 488 goat anti-rabbit antibody (Life Technologies, A-11070, 1:1000) was used as a secondary antibody. Stained cells were imaged by Operetta (PerkinElmer) with LDW 20x objective and the appropriate filter settings and analyzed by Harmony software (PerkinElmer).

Determination of apoptosis/Apoptosis assay

$1*10^4$ CHP134 cells plated in white 96-well plates were exposed to a single dose of 13-cis-RA (5µM) and isorhamnetin (15µM) and their combination for indicated time points. At each time point for each condition, half of the wells were used to evaluate

caspase-3 and -7 activities by the Caspase-Glo 3/7 Luminescent Assay (Promega), while the other half was used to assess cell viability by Cell Titer-Glo Luminescent Cell Viability Assay (Promega). The caspase-3/7 luminescent signal was normalized to the corresponding cell viability value. Caspase-3/7 levels in the treated samples were expressed as the percentage of untreated cells.

Alternatively, the apoptosis was quantified using Cell Event™ Caspase-3/7 Green Detection Reagent (Sigma Aldrich) following manufacturer instructions. The cells were imaged by Operetta (PerkinElmer) with LDW 20x objective and the appropriate filter settings at time 0h, 3h, 6h, 12h, 18h, 24h, 36h, and 72h. Images were analysed by Harmony software (PerkinElmer) to quantify the number of positive cells. The percentage of apoptotic cells was then calculated relative to time zero.

Three-dimensional multicellular spheroids

CHP134 cell was plated in a round bottom ultra-low attachment 96-well plate (Corning) at a concentration of 1000 cells /200µl per well and centrifuged at 300g for 8min. Spheroids were let to form for 3 days and then imaged by the high-content imaging system Operetta (PerkinElmer) with LWD 10X objective (in bright-field). After imaging at day 0, the spheroids were treated with selected compounds and imaged at 24, 48 and 72 hours of treatment. Where indicated, spheroids were stained after 48h of treatment with 10nM Sytox Red dead cell stain (Thermofisher) to verify the presence of cells death. The first treatment of spheroids was done with serial dilution of 13-cis-RA (20-1.25µM) and isorhamnetin (60-3.75µM) alone or in combination. Further treatment of 3D spheroids was performed with DMSO (0,04%), 13-cis-RA (5µM), isorhamnetin (15µM), L765,314 (25µM), AH11110A HCl (20µM) or a combination of 13-cis-RA with one of the adrenergic receptor inhibitors and images were acquired at 0h, 24h, 48h, 72h after treatment. Morphological parameters such as spheroid area, roundness and dye intensity were quantified by Harmony software (PerkinElmer)(data not shown).

High-content imaging and analysis: neurites quantification

For differentiation assay, cells were seeded at a concentration of $6*10^3$ cells/well in 96 well plate and treated after 24h with 5µM of 13-cis-RA, 15µM of isorhamnetin and the

combination of the two. Images were taken every 24h for a total of 144h. For neurite quantification, images of each well were acquired by Operetta (PerkinElmer) with LWD 20X high NA objective in the digital phase contrast (DPC) channel two Z-Stack in bright field computationally processed) and analysed by Harmony software (PerkinElmer). Based on the DPC signal, cells were segmented and then neurites were detected using the building block "Find Neurites" which automatically calculated for each cell the neurite related features like total neurite length (sum of the length of all neurites attached to the cell), maximum neurite length (length of longest neurite), number of neurite segments (the number of ends of individual neurites) and number of roots (the number of starts of individual neurites in the cell body). Depending on the properties of these morphological neurite parameters, cells with neurite length above a certain threshold were further selected.

Total RNA extraction

For total RNA extraction, cells were pelleted and lysed in 1ml of Trizol (Thermo Fisher) per 5 × 10^6 cells. Briefly, after 5min incubation at RT, 0.2ml of chloroform was added and samples were centrifuged at 9000g for 15min at 4°C. The formed aqueous phase was transferred to a new tube and 0.5ml of isopropanol was added. After incubation of 10min at RT, samples were centrifuged at 12000×g for 10min at 4° C, the supernatant was removed and pellets washed with 1ml of 70% ethanol. Finally, samples were centrifuged at 5000×g for 10 min at 4° C, the supernatant removed and the RNA-containing pellet air-dry pellet for 5-10min before being dissolved in 20 µl DEPC-treated water and proceed quantified with NanoDrop.

Quantitative real-time PCR

1µg of total RNA was reverse transcribed using RevertAid RT kit (ThermoFisher, K1619) following manufacture instructions. Sybr green quantitative real-time PCR was performed in a reaction volume of 10µl containing: 20ng template cDNA, 1X ExcelTaq™ Q-PCR Master Mix (SYBR, no ROX, SMOBIO) and 0,4µM of each primer. The qPCR reaction was performed on a CFX96 real-time PCR Detection System (Bio-Rad Laboratories) with the following cycling conditions: 95°C for 2min, followed by 40

cycles at 95°C for 15sec, 60°C for 60 sec. The ΔΔCq method was used to calculate the relative mRNA levels of each gene. As a reference gene, HPRT was used. As an internal calibrator, DMSO treated samples were used.

Used qPCR primers: ADRA1B Fw 5'-TCTACCGCTTGGCTCCTTGTT-3' Rv 5'-GGAGCATGGGTAGATGATGGG-3', TH Fw 5'-CATCACCTGGTCACCAAGTT-3' Rv 5'-GGTCGCCGTGCCTGTACT-3', β3-Tubulin Fw 5'-TCAGCGTCTACTACAACGAGGC-3' Rv 5'-GCCTGAAGAGATGTCCAAAGGC-3', MCYN Fw 5'-CCGGGCATGATCTGCAA-3' Rv 5'-CCGCCGAAGTAGAAGTCATCTT-3', Sox9 Fw 5'-GTACCCGCACTTGCACAAC-3', Rv 5'-TCTCGCTCTCGTTCAGAAGTC-3', Hes1 Fw 5'-TCCTAAACTCCCCAACCCA-3', Rv 5'-AGTCCTCTTCTCTCCCAGTATTCA -3', HPRT 5'-TGACACTGGCAAAACAATGCA-3' Rv 5'-GGTCCTTTTCACCAGCAAGCT-3'.

Western Blotting

Cells were pelleted and lysed in 1X RIPA buffer (Millipore, 20-188) with 1X phosphatase and protease inhibitor. The lysates were centrifuged for 10 minutes at +4°C at the maximum speed. Supernatants were collected and quantified by BCA protein assay (Pierce). 20-30ug total proteins were boiled at 98°C for 10min, separated by SDS-PAGE and transferred to nitrocellulose membranes (Bio-Rad Laboratories). Membrane blocking was performed with 5% Milk (BioRad) in TBS-T for one hour. Primary antibodies were diluted in 5% Milk-TBS-T and incubated overnight at +4°C. Primary antibodies used were: MYCN (Cell signalling, TA150014), SOX9 (Life technologies, 702016), PHOX2B (Santa Cruz, sc-376797), GAP43 (Merk Millipore, AB5220), GPADH (Santa Cruz, sc32233), α-actinin (Santa Cruz sc17829). Incubation with secondary antibody goat anti-mouse IgG-HRP (Santa Cruz, sc-2005) or anti-rabbit IgG-HRP (Santa Cruz, sc-2005) was performed for 1 hour at room temperature. After incubation with ECL Prime detection reagent (GE Healthcare, Buckinghamshire, UK), blots were imaged with the ChemiDoc XRS1 imaging system (Bio-Rad Laboratories).

Screening with a focused library of adrenergic receptor libraries

CHP134 were seeded at a concentration of $2.5*10^2$ cells/60 µl per well in TC 384-well plates (Life Technologies, Nunc 384-well flat-bottom white TC sterile 164610). After 24h, cells were treated with 20µM and 40µM of libraries' molecules (Adrenergic Receptor Compound Library, TargetMol, L2700) (SCREEN-WELL® Neurotransmitter library, EnzoLifeScience, BML-2810-0100) in presence or absence of 13-cis-RA (5µM). The screening was performed in technical duplicates. Cell seeding and drug treatment were performed using the Tecan Evo 200 robotic platform. Cell viability was evaluated with CellTiter-Glo assay after 72h. Luminescence was measured using the Ensight plate reader (Perkin Elmer). Data analysis was performed with KNIME software (Berthold *et al*, 2008). The percentage of viable cells was expressed relative to the on plate DMSO-treated cell. For hit selection, compounds that at 20µM and 40µM alone reduced cell viability to 0- 50%, were first filtered out and then those molecules that in combination with 13-cis-RA caused a decrease of cell viability greater than that of 13-cis-RA alone of at least 30%, were selected. To validate the selected hits, serial dilution of the molecules (40µM, 20µM, 10µM, 5µM, 2.5µM) was performed in the presence or absence of 13-cis-RA (5µM) and cell viability was evaluated after 72h. Every treated plate included: vehicle-treated control cells (0,08% DMSO v/v), cells treated with 5µM 13-cis-RA alone, negative control cells treated with isorhamnetin 15µM or L765,314 20µM, and positive control cells treated with isorhamnetin or L765,314 in combination with 13-cis-RA.

In vivo treatments

$7*10^6$ CHP134 cells transduced with luciferase-expressing vector were re-suspended in a mixture 1:1 of cell medium: Matrigel (BD bioscience) and injected subcutaneously, into the right flank of crl:Nu (Ncr)-Foxn1 nu (nude mice) of 7-8 weeks old. After 10-15 days, the appearance of a palpable, subcutaneous mass indicates that the tumor has developed. The day before the treatment start, the tumor mass imaged was by live imaging with the Bruker-XTreme system after D-luciferin i.p. injection (150mg/kg, Sigma Aldrich L9504)(Dickson *et al*, 2007). Mice were divided into groups based on the pharmacological treatment. The control group was treated with DMSO (10%), the other

3 groups were treated as follows: 13-cis-RA alone (10mg/kg/day), doxazosin (10mg/kg/day) and 13-cis-RA in combination with doxazosin and doxazosin alone (10mg/kg/day). All the drugs were administered via i.p. injection every day for 15 days. All the molecules were initially suspended in DMSO 100% and then diluted in a mixture of 20% corn oil and 80% PBS (i.e., the final concentration of DMSO is 10%). The evolution of the tumor mass was followed weekly by live imaging. At the end of the treatment period, mice were further monitored for 1 week. After 21 days from the start of the treatment, mice were sacrificed, and tumor mass was extracted and measured.

Tumor volume was calculated applying the following formula modified ellipsoid formula: $V = (Width^2 * Length)/2$ based on the values obtained by *in-vivo* imaging (Jensen *et al*, 2008). The tumor growth for each mouse was calculated normalizing tumor volume with respect today 0. The tumor growth rate was evaluated using raw volume values. The tumor growth rate was evaluated by fitting the tumor volumes to a linear regression model ($y=\beta x+q$). The statistical significance was calculated by comparing the β (i.e. the slope of the linear model, which indicates how fast the tumor volume changes) of the obtained linear equations.

Statistical analysis

Cell viability assay. All presented data were normalized over DMSO treated cells and represent mean ± SD of at least three biological experiments.

- Statistically significant differences between treatments were calculated according to 1-way ANOVA followed by Dunnett's or Bonferroni's multiple comparisons tests
- Statistical analysis of cells viability on 3D spheroids was performed by a 2-way ANOVA test, followed by Dunnet's multiple comparisons tests.
- Statistical analysis to compare the impact of different treatments (13-cis-RA, isorhamnetin or the combination of the two) on non-transduced, scramble ctrl or ADRA1B KO CHP134 cells was performed, for each treatment, by one-way ANOVA followed by uncorrected Fisher's LSD multiple comparisons test.

In all the analysis the significant level was reported as follows: p-value≤ 0.0001 (****), p-value ≤ 0.001 (***), p-value≤ 0.01 (**), p-value ≤ 0.05 (*).

Apoptosis and differentiation assay. The data are represented as the mean ± SD of at least three biological replicates and normalized on DMSO treated controls. Statistically significant differences between treatments in the two different cell lines (WT and ADRA1B KO) were calculated according to two-way ANOVA followed by Bonferroni's multiple comparison test. Significant level was reported as follows: p-value ≤ 0.001 (***), p-value≤ 0.01 (**), p-value ≤ 0.05 (*).

Real-time qPCR. Gene expression data of treated samples are normalized on the mean of the non-treated control cells (DMSO). The Two-way ANOVA test followed by Bonferroni's multiple comparisons test has been used to calculate the significance of differential expression of neural differentiation markers between different treatments. Significant level was reported as follows: p-value ≤ 0.001 (***), p-value≤ 0.01 (**), p-value ≤ 0.05 (*).

AR ligand Screening Hits validation. Cell viability data were normalized on DMSO treated cells. Mean ± SD of at least three biological replicates is represented. Statistical analysis was done with a two-way ANOVA test followed by Sidak's multiple comparison test. Significant level was reported as follows: P-value ≤0.0001 (****), p-value ≤ 0.001 (***), p-value≤ 0.01 (**), p-value ≤ 0.05 (*).

In vivo experiments. The significance of the difference in tumor growth among the treatments groups was evaluated, for each time point, by multiple two-tailed t-tests on the logarithmic transformation of the fold change (= V_{tx}/V_{t0}).

The tumor growth rate was evaluated by fitting the tumor volumes to a linear regression model ($y=\beta x+q$). The statistical significance was calculated by comparing the β (i.e. the slope of the linear model) of the obtained linear equations.

All the reported statistical analyses were performed using the software graph pad version 8.4.2

BIBLIOGRAPHY

Abemayor, Elliott. 1992. "The Effects of Retinoic Acid on the in Vitro and in Vivo Growth of Neuroblastoma Cells." *Laryngoscope* 102(10):1133–49.

Afonja, Olubunmi, Bruce M. Raaka, Ambrose Huang, Sharmistha Das, Xinyu Zhao, Elizabeth Helmer, Dominique Juste, and Herbert H. Samuels. 2002. "RAR Agonists Stimulate SOX9 Gene Expression in Breast Cancer Cell Lines: Evidence for a Role in Retinoid-Mediated Growth Inhibition." *Oncogene* 21(51):7850–60.

Ajay, Machha, Anwar Ul Hassan Gilani, and Mohd Rais Mustafa. 2003. "Effects of Flavonoids on Vascular Smooth Muscle of the Isolated Rat Thoracic Aorta." *Life Sciences*.

Allen, L. F., R. J. Lefkowitz, M. G. Caron, and S. Cotecchia. 1991. "G-Protein-Coupled Receptor Genes as Protooncogenes: Constitutively Activating Mutation of the α(1B)-Adrenergic Receptor Enhances Mitogenesis and Tumorigenicity." *Proceedings of the National Academy of Sciences of the United States of America* 88(24):11354–58.

Amado, Nathália G., Bárbara F. Fonseca, Débora M. Cerqueira, Vivaldo Moura Neto, and José G. Abreu. 2011. "Flavonoids: Potential Wnt/Beta-Catenin Signaling Modulators in Cancer." *Life Sciences* 89(15–16):545–54.

Attiyeh, Edward F., Wendy B. London, Yael P. Mossé, Qun Wang, Cynthia Winter, Deepa Khazi, Patrick W. McGrady, Robert C. Seeger, A. Thomas Look, Hiroyuki Shimada, Garrett M. Brodeur, Susan L. Cohn, Katherine K. Matthay, and John M. Maris. 2005. "Chromosome 1p and 11q Deletions and Outcome in Neuroblastoma." *New England Journal of Medicine* 353(21):2243–53.

Axelson, Håkan. 2004. "The Notch Signaling Cascade in Neuroblastoma: Role of the Basic Helix-Loop-Helix Proteins HASH-1 and HES-1." *Cancer Letters* 204(2):171–78.

Bayeva, Nadiya, Erin Coll, and Olga Piskareva. 2021a. "Differentiating Neuroblastoma: A Systematic Review of the Retinoic Acid, Its Derivatives, and Synergistic Interactions." *nal of Personalized Medicine* 11(3):211.

Berry, Teeara, William Luther, Namrata Bhatnagar, Yann Jamin, Evon Poon, Takaomi Sanda, Desheng Pei, Bandana Sharma, Winston R. Vetharoy, Albert Hallsworth, Zai Ahmad, Karen Barker, Lisa Moreau, Hannah Webber, Wenchao Wang, Qingsong Liu, Antonio Perez-Atayde, Scott Rodig, Nai-Kong Cheung, Florence Raynaud, Bengt Hallberg, Simon P. Robinson, Nathanael S. Gray, Andrew D. J. Pearson, Suzanne A. Eccles, Louis Chesler, and Rani E. George. 2012. "The ALKF1174L Mutation Potentiates the Oncogenic Activity of MYCN in Neuroblastoma." *Cancer Cell* 22(1):117–30.

Bown, Nick, Simon Cotterill, Maria Łastowska, Seamus O'Neill, Andrew D. J. Pearson, Dominique Plantaz, Mounira Meddeb, Gisele Danglot, Christian Brinkschmidt, Holger Christiansen, Genevieve Laureys, Frank Speleman, James Nicholson, Alien

Bernheim, David R. Betts, Jo Vandesomple, and Nadine Van Roy. 1999. “Gain of Chromosome Arm 17q and Adverse Outcome in Patients with Neuroblastoma.” *New England Journal of Medicine* 340(25):1954–61.

Brodeur, G. M., R. C. Seeger, A. Barrett, F. Berthold, R. P. Castleberry, G. D’Angio, B. De Bernardi, A. E. Evans, M. Favrot, A. I. Freeman, G. Haase, O. Hartmann, F. A. Hayes, L. Helson, J. Kemshead, F. Lampert, J. Ninane, H. Ohkawa, and T. Philip. 1988. “International Criteria for Diagnosis, Staging, and Response to Treatment in Patients with Neuroblastoma.” *Journal of Clinical Oncology* 6(12):1874–81.

Brodeur, Garrett M. and Rochelle Bagatell. 2014. “Mechanisms of Neuroblastoma Regression.” *Nature Reviews Clinical Oncology* 11(12):704–13.

Brodeur, Garrett M., Jon Pritchard, Frank Berthold, Niels L. T. Carlsen, Victoria Castel, Robert P. Castleberry, Bruno De Bernardi, Audrey E. Evans, Marie Favrot, Fredrik Hedborg, Michio Kaneko, John Kemshead, Fritz Lampert, Richard E. J. Lee, A. Thomas Look, Andrew D. J. Pearson, Thierry Philip, Borghild Roald, Tadashi Sawada, Robert C. Seeger, Yoshiaki Tsuchida, and Paul A. Voute. 1993. “Revisions of the International Criteria for Neuroblastoma Diagnosis, Staging, and Response to Treatment.” *Journal of Clinical Oncology*.

Brodeur, Garrett M., Robert C. Seeger, Manfred Schwab, Harold E. Varmus, and J. Michael Bishop. 1984. “Amplification of N-Myc in Untreated Human Neuroblastomas Correlates with Advanced Disease Stage.” *Science* 224(4653):1121–24.

Bushue, Nathan and Yu Jui Yvonne Wan. 2010. “Retinoid Pathway and Cancer Therapeutics.” *Advanced Drug Delivery Reviews* 62(13):1285–98.

Caron, Huib, Peter Van Sluis, Jan De Kraker, Jos Bökkerink, Maarten Egeler, Geneviève Laureys, Rosalyn Slater, Andries Westerveld, P. A. Voûte, and Rogier Versteeg. 1996. “Allelic Loss of Chromosome 1p as a Predictor of Unfavorable Outcome in Patients with Neuroblastoma.” *New England Journal of Medicine* 334(4):225–30.

Cheung, Nai Kong V., Jinghui Zhang, Charles Lu, Matthew Parker, Armita Bahrami, Satish K. Tickoo, Adriana Heguy, Alberto S. Pappo, Sara Federico, James Dalton, Irene Y. Cheung, Li Ding, Robert Fulton, Jianmin Wang, Xiang Chen, Jared Becksfort, Jianrong Wu, Catherine A. Billups, David Ellison, Elaine R. Mardis, Richard K. Wilson, James R. Downing, and Michael A. Dyer. 2012. “Association of Age at Diagnosis and Genetic Mutations in Patients with Neuroblastoma.” *JAMA - Journal of the American Medical Association* 307(10):1062–71.

Ciccarone, Valentina, Barbara A. Spengler, Marian B. Meyers, June L. Biedler, and Robert A. Ross. 1989. “Phenotypic Diversification in Human Neuroblastoma Cells: Expression of Distinct Neural Crest Lineages.” *Cancer Research* 49(1):219–25.

Claviez, Alexander, Max Lakomek, Jörg Ritter, Meinolf Suttorp, Bernhard Kremens, Roswitha Dickerhoff, Dieter Harms, Frank Berthold, and Barbara Hero. 2004. “Low Occurrence of Familial Neuroblastomas and Ganglioneuromas in Five Consecutive

GPOH Neuroblastoma Treatment Studies." *European Journal of Cancer* 40(18):2760–65.

Clynes, David and Richard J. Gibbons. 2013. "ATRX and the Replication of Structured DNA." *Current Opinion in Genetics and Development* 23(3):289–94.

Cohen, Pamela S., John J. Letterio, Carlo Gaetano, Jane Chan, Kazue Matsumoto, Michael B. Sporn, and Carol J. Thiele. 1995. "Induction of Transforming Growth Factor Bl and Its Receptors during All-Trans-Retinoic Acid (RA) Treatment of RA-Responsive Human Neuroblastoma Cell Lines." *Cancer Research* 55(11):2380–86.

Cohn, Susan L., Andrew D. J. Pearson, Wendy B. London, Tom Monclair, Peter F. Ambros, Garrett M. Brodeur, Andreas Faldum, Barbara Hero, Tomoko Iehara, David Machin, Veronique Mosseri, Thorsten Simon, Alberto Garaventa, Victoria Castel, and Katherine K. Matthay. 2009. "The International Neuroblastoma Risk Group (INRG) Classification System: An INRG Task Force Report." *Journal of Clinical Oncology* 27(2):289–97.

Cotterman, Rebecca and Paul S. Knoepfler. 2009. "N-Myc Regulates Expression of Pluripotency Genes in Neuroblastoma Including Lif, Klf2, Klf4, and Lin28b" edited by J. Najbauer. *PLoS ONE* 4(6):e5799.

Degoutin, Joffrey, Nicole Brunet-de Carvalho, Carmen Cifuentes-Diaz, and Marc Vigny. 2009. "ALK (Anaplastic Lymphoma Kinase) Expression in DRG Neurons and Its Involvement in Neuron-Schwann Cells Interaction." *European Journal of Neuroscience* 29(2):275–86.

Delaune, A., C. Corbière, F. D. Benjelloun, E. Legrand, J. P. Vannier, C. Ripoll, and M. Vasse. 2007. "Promyelocytic Leukemia-Nuclear Body Formation Is an Early Event Leading to Retinoic Acid-Induced Differentiation of Neuroblastoma Cells." *Journal of Neurochemistry* 0(0):071106220615005-???

Deng, Jing, Ping Jiang, Tianyou Yang, Mao Huang, Weiwei Qi, Ti Zhou, Zhonghan Yang, Yan Zou, Guoquan Gao, and Xia Yang. 2019. "Targeting B3-Adrenergic Receptor Signaling Inhibits Neuroblastoma Cell Growth via Suppressing the MTOR Pathway." *Biochemical and Biophysical Research Communications* 514(1):295–300.

De Thé, Hugues. 2018. "Differentiation Therapy Revisited." *Nature Reviews Cancer* 18(2):117–27.

Deutsch, Dascha. 2016. "Alpha1B Adrenoceptor Expression Is a Marker of Reduced Survival and Increased Tumor Recurrence in Patients with Endometrioid Ovarian Cancer." *World Journal of Obstetrics and Gynecology* 5(1):118.

Dickson, Paxton V., Blair Hamner, Catherine Y. C. Ng, Marshall M. Hall, Junfang Zhou, Phillip W. Hargrove, M. Beth McCarville, and Andrew M. Davidoff. 2007. "In Vivo Bioluminescence Imaging for Early Detection and Monitoring of Disease Progression in a Murine Model of Neuroblastoma." *Journal of Pediatric Surgery* 42(7):1172–79.

Duester, Gregg. 2008. "Retinoic Acid Synthesis and Signaling during Early

Organogenesis." *Cell* 134(6):921–31.

Dwyer, Jennifer B. and Michael H. Bloch. 2019. "Antidepressants for Pediatric Patients." *Current Psychiatry* 18(9):26-42F.

Edsjö, Anders, Helén Nilsson, Jo Vandesompele, Jenny Karlsson, Filip Pattyn, Lloyd A. Culp, Frank Speleman, and Sven Påhlman. 2004. "Neuroblastoma Cells with Overexpressed MYCN Retain Their Capacity to Undergo Neuronal Differentiation." *Laboratory Investigation* 84:406–17.

Eng, Jason W. L., Kathleen M. Kokolus, Chelsey B. Reed, Bonnie L. Hylander, Wen W. Ma, and Elizabeth A. Repasky. 2014. "A Nervous Tumor Microenvironment: The Impact of Adrenergic Stress on Cancer Cells, Immunosuppression, and Immunotherapeutic Response." *Cancer Immunology, Immunotherapy* 63(11):1115–28.

Di Francesco, Angela Maria, Daniela Meco, Anna Rita Torella, Giuseppe Barone, Maurizio D'Incalci, Claudio Pisano, Paolo Carminati, and Riccardo Riccardi. 2007. "The Novel Atypical Retinoid ST1926 Is Active in ATRA Resistant Neuroblastoma Cells Acting by a Different Mechanism." *Biochemical Pharmacology* 73(5):643–55.

Gaelzer, Mariana Maier, Bárbara Paranhos Coelho, Alice Hoffmann De Quadros, Juliana Bender Hoppe, Silvia Resende Terra, Maria Cristina Barea Guerra, Vanina Usach, Fátima Costa Rodrigues Guma, Carlos Alberto Saraiva Gonçalves, Patrícia Setton-Avruj, Ana Maria Oliveira Battastini, and Christianne Gazzana Salbego. 2016. "Phosphatidylinositol 3-Kinase/AKT Pathway Inhibition by Doxazosin Promotes Glioblastoma Cells Death, Upregulation of P53 and Triggers Low Neurotoxicity." *PLoS ONE* 11(4):1–18.

Gaetano, C., K. Matsumoto, and C. J. Thiele. 1991. "Retinoic Acid Negatively Regulates P34cdc2 Expression during Human Neuroblastoma Differentiation." *Cell Growth & Differentiation* 2(10):487–93.

Ganesh, H. K., Shrikrishna V. Acharya, Joe Goerge, Tushar R. Bandgar, Padma S. Menon, and Nalini S. Shah. 2009. "Pheochromocytoma in Children and Adolescents." *Indian Journal of Pediatrics*.

George, Rani E., Takaomi Sanda, Megan Hanna, Stefan Fröhling, William Luther II, Jianming Zhang, Yebin Ahn, Wenjun Zhou, Wendy B. London, Patrick McGrady, Liquan Xue, Sergey Zozulya, Vlad E. Gregor, Thomas R. Webb, Nathanael S. Gray, D. Gary Gilliland, Lisa Diller, Heidi Greulich, Stephan W. Morris, Matthew Meyerson, and A. Thomas Look. 2008. "Activating Mutations in ALK Provide a Therapeutic Target in Neuroblastoma." *Nature* 455(7215):975–78.

Grupp, Ingrid L., John N. Lorenz, Richard A. Walsh, Gregory P. Boivin, and Hansjörg Rindt. 1998. "Overexpression of α_{1B} -Adrenergic Receptor Induces Left Ventricular Dysfunction in the Absence of Hypertrophy." *American Journal of Physiology-Heart and Circulatory Physiology* 275(4): H1338–50.

Grynfeld, Anna, Sven Påhlman, and Håkan Axelson. 2000. "Induced Neuroblastoma Cell

Differentiation, Associated with Transient HES-1 Activity and Reduced HASH-1 Expression, Is Inhibited by Notch1." *International Journal of Cancer* 88(3):401–10.

Gugler, R., M. Leschik, and H. J. Dengler. 1975. "Disposition of Quercetin in Man after Single Oral and Intravenous Doses." *European Journal of Clinical Pharmacology* 9(2–3):229–34.

Gupta, Manveen K., Robert S. Papay, Chris W. D. Jurgens, Robert J. Gaivin, Ting Shi, Van A. Doze, and Dianne M. Perez. 2009. "A1-Adrenergic Receptors Regulate Neurogenesis and Gliogenesis." *Molecular Pharmacology* 76(2):314–26.

Gutierrez-Merino, C., C. Lopez-Sanchez, R. Lagoa, A. K. Samhan-Arias, C. Bueno, and V. Garcia-Martinez. 2011. "Neuroprotective Actions of Flavonoids." *Current Medicinal Chemistry* 18(8):1195–1212.

Hertog, M. G. L., E. J. M. Feskens, D. Kromhout, M. G. L. Hertog, P. C. H. Hollman, M. G. L. Hertog, and M. B. Katan. 1993. "Dietary Antioxidant Flavonoids and Risk of Coronary Heart Disease: The Zutphen Elderly Study." *The Lancet* 342(8878):1007–11.

Hiyama, Eiso, Keiko Hiyama, Takashi Yokoyama, Yuichiro Matsuura, Mieczyslaw A. Piatyszek, and Jerry W. Shay. 1995. "Correlating Telomerase Activity Levels with Human Neuroblastoma Outcomes." *Nature Medicine* 1(3):249–55.

Hu, Zhuo-Wei, Xiao-You Shi, Richard Z. Lin, and Brian B. Hoffman. 1999. " Contrasting Signaling Pathways of α 1A - and α 1B -Adrenergic Receptor Subtype Activation of Phosphatidylinositol 3-Kinase and Ras in Transfected NIH3T3 Cells ." *Molecular Endocrinology* 13(1):3–14.

Huang, Xiaoke, Shan Chen, Li Xu, Yueqin Liu, Dilip K. Deb, Leonidas C. Platanias, and Raymond C. Bergan. 2005. "Genistein Inhibits P38 Map Kinase Activation, Matrix Metalloproteinase Type 2, and Cell Invasion in Human Prostate Epithelial Cells." *Cancer Research* 65(8):3470–78.

Huang, Xin-yu, Hong-Cheng Wang, Zhou Yuan, Jian Huang, and Qi Zheng. 2011. "Norepinephrine Stimulates Pancreatic Cancer Cell Proliferation, Migration and Invasion Via ß-Adrenergic Receptor-Dependent Activation of P38/MAPK Pathway." *Hepatogastroenterology* 59(115–116):889–93.

Ishibashi, Makoto, Siew Lan Ang, Kohei Shiota, Shigetada Nakanishi, Ryoichiro Kageyama, and François Guillemot. 1995. "Targeted Disruption of Mammalian Hairy and Enhancer of Split Homolog-1 (HES-1) Leads to up-Regulation of Neural Helix-Loop-Helix Factors, Premature Neurogenesis, and Severe Neural Tube Defects." *Genes and Development* 9(24):3136–48.

Iwahara, Toshinori, Jiro Fujimoto, Duanzhi Wen, Rod Cupples, Nathan Bucay, Tsutomu Arakawa, Shigeo Mori, Barry Ratzkin, and Tadashi Yamamoto. 1997. "Molecular Characterization of ALK, a Receptor Tyrosine Kinase Expressed Specifically in the Nervous System." *Oncogene* 14(4):439–49.

Janoueix-Lerosey, Isabelle, Delphine Lequin, Laurence Brugières, Agnès Ribeiro, Loïc

De Pontual, Valérie Combaret, Virginie Raynal, Alain Puisieux, Gudrun Schleiermacher, Gaëlle Pierron, Dominique Valteau-Couanet, Thierry Frebourg, Jean Michon, Stanislas Lyonnet, Jeanne Amiel, and Olivier Delattre. 2008. "Somatic and Germline Activating Mutations of the ALK Kinase Receptor in Neuroblastoma." *Nature* 455(7215):967–70.

Jansky, Selina, Ashwini Kumar Sharma, Verena Körber, Andrés Quintero, Umut H. Toprak, Elisa M. Wecht, Moritz Gartlgruber, Alessandro Greco, Elad Chomsky, Thomas G. P. Grünewald, Kai Oliver Henrich, Amos Tanay, Carl Herrmann, Thomas Höfer, and Frank Westermann. 2021. "Single-Cell Transcriptomic Analyses Provide Insights into the Developmental Origins of Neuroblastoma." *Nature Genetics* 53(5):683–93.

Jensen, Mette Munk, Jesper Tranekjæer Jørgensen, Tina Binderup, and Andreas Kjær. 2008. "Tumor Volume in Subcutaneous Mouse Xenografts Measured by MicroCT Is More Accurate and Reproducible than Determined by 18F-FDG-MicroPET or External Caliper." *BMC Medical Imaging* 8:16.

Jhaveri, Dhanisha J., Ishira Nanavaty, Boris W. Prosper, Swanand Marathe, Basma F. A. Husain, Steven G. Kernie, Perry F. Bartlett, and Vidita A. Vaidya. 2014. "Opposing Effects of A2- and β-Adrenergic Receptor Stimulation on Quiescent Neural Precursor Cell Activity and Adult Hippocampal Neurogenesis" edited by P. Gressens. *PLoS ONE* 9(6):e98736.

Johnson, Charles D., Aurora Esquela-Kerscher, Giovanni Stefani, Mike Byrom, Kevin Kelnar, Dmitriy Ovcharenko, Mike Wilson, Xiaowei Wang, Jeffrey Shelton, Jaclyn Shingara, Lena Chin, David Brown, and Frank J. Slack. 2007. "The Let-7 MicroRNA Represses Cell Proliferation Pathways in Human Cells." *Cancer Research* 67(16):7713–22.

Kang, Jung Hee, Piotr G. Rychahou, Titilope A. Ishola, Jingbo Qiao, B. Mark Evers, and Dai H. Chung. 2006. "MYCN Silencing Induces Differentiation and Apoptosis in Human Neuroblastoma Cells." *Biochemical and Biophysical Research Communications* 351(1):192–97.

Karkoulias, G., O. Mastrogianni, I. Ilias, A. Lymperopoulos, S. Taraviras, N. Tsopanoglou, N. Sitaras, And C. Flordellis. 2006. "Alpha 2-Adrenergic Receptors Decrease Dna Replication And Cell Proliferation And Induce Neurite Outgrowth In Transfected Rat Pheochromocytoma Cells." *Annals Of The New York Academy Of Sciences* 1088(1):335–45.

Karkoulias, George, Katie A. McCrink, Jennifer Maning, Celina M. Pollard, Victoria L. Desimine, Nicholas Patsouras, Miltiades Psallidopoulos, Stavros Taraviras, Anastasios Lymperopoulos, and Christodoulos Flordellis. 2020. "Sustained GRK2-Dependent CREB Activation Is Essential for A2-Adrenergic Receptor-Induced PC12 Neuronal Differentiation." *Cellular Signalling* 66:109446.

Kawahara, Tatsuo, Noriko Kawaguchi-Ihara, Yuki Okuhashi, Mai Itoh, Nobuo Nara, and

Shuji Tohda. 2009. “Cyclopamine and Quercetin Suppress the Growth of Leukemia and Lymphoma Cells.” *Anticancer Research* 29(11):4629–32.

Kholodenko, Irina V., Daniel V. Kalinovsky, Igor I. Doronin, Sergey M. Deyev, and Roman V. Kholodenko. 2018. “Neuroblastoma Origin and Therapeutic Targets for Immunotherapy.” *Journal of Immunology Research* 2018.

Kim, Sung-Eun, Jin-Hee Han, Il-Gyu Ko, Chang-Ju Kim, and Khae Hawn Kim. 2017. “Alpha $_1$ -Adrenergic Receptor Antagonist Tamsulosin Ameliorates Aging-Induced Memory Impairment by Enhancing Neurogenesis and Suppressing Apoptosis in the Hippocampus of Old-Aged Rats.” *Animal Cells and Systems* 21(6):404–11.

Kumar, Madhu S., Jun Lu, Kim L. Mercer, Todd R. Golub, and Tyler Jacks. 2007. “Impaired MicroRNA Processing Enhances Cellular Transformation and Tumorigenesis.” *Nature Genetics* 39(5):673–77.

Li, C., P. A. Einhorn, and C. P. Reynolds. 1994. “Expression of Retinoic Acid Receptors Alpha, Beta, and Gamma in Human Neuroblastoma Cell Lines.” *Progress in Clinical and Biological Research* 385:221–27.

Li, Yiwei and Fazlul H. Sarkar. 2002. “Inhibition of Nuclear Factor KB Activation in PC3 Cells by Genistein Is Mediated via Akt Signaling Pathway.” *Clinical Cancer Research* 8(7):2369–77.

Look, A. Thomas, F. Ann Hayes, Ruprecht Nitschke, Nancy B. Mcwilliams, and Alexander A. Green. 1984. “Cellular DNA Content as a Predictor of Response to Chemotherapy in Infants with Unresectable Neuroblastoma.” *New England Journal of Medicine* 311(4):231–35.

De los Santos, Maxy, Alberto Zambrano, and Ana Aranda. 2007. “Combined Effects of Retinoic Acid and Histone Deacetylase Inhibitors on Human Neuroblastoma SH-SY5Y Cells.” *Molecular Cancer Therapeutics* 6(4):1425–32.

Maris, J. M., P. S. White, C. P. Beltinger, E. P. Sulman, R. P. Castleberry, J. J. Shuster, A. T. Look, and G. M. Brodeur. 1995. “Significance of Chromosome 1p Loss of Heterozygosity in Neuroblastoma.” *Cancer Research* 55(20):4664–69.

Maris, JM. 2010. “Recent Advances in Neuroblastoma.” *New England Journal of Medicine* 362(23):2202–11.

Masetti, Riccardo, Carlotta Biagi, Daniele Zama, Francesca Vendemini, Anna Martoni, William Morello, Pietro Gasperini, and Andrea Pession. 2012. “Retinoids in Pediatric Onco-Hematology: The Model of Acute Promyelocytic Leukemia and Neuroblastoma.” *Advances in Therapy* 29(9):747–62.

Di Masi, Alessandra, Loris Leboffe, Elisabetta De Marinis, Francesca Pagano, Laura Cicconi, Cécile Rochette-Egly, Francesco Lo-Coco, Paolo Ascenzi, and Clara Nervi. 2015a. “Retinoic Acid Receptors: From Molecular Mechanisms to Cancer Therapy.” *Molecular Aspects of Medicine* 41:1–115.

Matthay, K. K., J. G. Villablanca, R. C. Seeger, D. O. Stram, R. E. Harris, N. K. Ramsay, P. Swift, H. Shimada, C. T. Black, G. M. Brodeur, and others. 1999. “Treatment of High-

Risk Neuroblastoma with Intensive Chemotherapy, Radiotherapy, Autologous Bone Marrow Transplantation, and 13-Cis-Retinoic Acid." *New England Journal of Medicine* 341(16):1165.

Mena, M. A., M. J. Casarejos, C. Estrada, and J. G. de Yebenes. 1994. "Effects of Retinoic Acid on NB 69 Human Neuroblastoma Cells and Fetal Rat Mid Brain Neurons." *Journal of Neural Transmission - Parkinsons Disease and Dementia Section* 8(1–2):85–97.

Milano, C. A., P. C. Dolber, H. A. Rockman, R. A. Bond, M. E. Venable, L. F. Allen, and R. J. Lefkowitz. 1994. "Myocardial Expression of a Constitutively Active α(1B)-Adrenergic Receptor in Transgenic Mice Induces Cardiac Hypertrophy." *Proceedings of the National Academy of Sciences of the United States of America* 91(21):10109–13.

Molenaar, Jan J., Raquel Domingo-Fernández, Marli E. Ebus, Sven Lindner, Jan Koster, Ksenija Drabek, Pieter Mestdagh, Peter Van Sluis, Linda J. Valentijn, Johan Van Nes, Marloes Broekmans, Franciska Haneveld, Richard Volckmann, Isabella Bray, Lukas Heukamp, Annika Sprüssel, Theresa Thor, Kristina Kieckbusch, Ludger Klein-Hitpass, Matthias Fischer, Jo Vandesompele, Alexander Schramm, Max M. Van Noesel, Luigi Varesio, Frank Speleman, Angelika Eggert, Raymond L. Stallings, Huib N. Caron, Rogier Versteeg, and Johannes H. Schulte. 2012. "LIN28B Induces Neuroblastoma and Enhances MYCN Levels via Let-7 Suppression." *Nature Genetics* 44(11):1199–1206.

Molenaar, Jan J., Jan Koster, Danny A. Zwijnenburg, Peter Van Sluis, Linda J. Valentijn, Ida Van Der Ploeg, Mohamed Hamdi, Johan Van Nes, Bart A. Westerman, Jennemiek Van Arkel, Marli E. Ebus, Franciska Haneveld, Arjan Lakeman, Linda Schild, Piet Molenaar, Peter Stroeken, Max M. Van Noesel, Ingrid Øra, Evan E. Santo, Huib N. Caron, Ellen M. Westerhout, and Rogier Versteeg. 2012a. "Sequencing of Neuroblastoma Identifies Chromothripsis and Defects in Neuritogenesis Genes." *Nature* 483(7391):589–93.

Mosse, Yael P., Marci Laudenslager, Deepa Khazi, Alex J. Carlisle, Cynthia L. Winter, Eric Rappaport, and John M. Maris. 2004. "Germline PHOX2B Mutation in Hereditary Neuroblastoma." *American Journal of Human Genetics* 75(4):727–30.

Mossé, Yaël P., Marci Laudenslager, Luca Longo, Kristina A. Cole, Andrew Wood, Edward F. Attiyeh, Michael J. Laquaglia, Rachel Sennett, Jill E. Lynch, Patrizia Perri, Geneviève Laureys, Frank Speleman, Cecilia Kim, Cuiping Hou, Hakon Hakonarson, Ali Torkamani, Nicholas J. Schork, Garrett M. Brodeur, Gian P. Tonini, Eric Rappaport, Marcella Devoto, and John M. Maris. 2008. "Identification of ALK as a Major Familial Neuroblastoma Predisposition Gene." *Nature* 455(7215):930–35.

Müller, Patrick, Justin D. Crofts, Ben S. Newman, Laura C. Bridgewater, Chin Yo Lin, Jan Åke Gustafsson, and Anders Ström. 2010. "SOX9 Mediates the Retinoic Acid-Induced HES-1 Gene Expression in Human Breast Cancer Cells." *Breast Cancer*

Research and Treatment 120(2):317–26.

Nair, AnroopB and Shery Jacob. 2016. "A Simple Practice Guide for Dose Conversion between Animals and Human." *Journal of Basic and Clinical Pharmacy* 7(2):27.

Nakagawara, A. and G. M. Brodeur. 1997. "Role of Neurotrophins and Their Receptors in Human Neuroblastomas: A Primary Culture Study." *European Journal of Cancer (Oxford, England : 1990)* 33(12):2050–53.

Nakagawara, Akira, Miwako Arima-Nakagawara, Nancy J. Scavarda, Christopher G. Azar, Alan B. Cantor, and Garrett M. Brodeur. 1993. "Association between High Levels of Expression of the TRK Gene and Favorable Outcome in Human Neuroblastoma." *New England Journal of Medicine* 328(12):847–54.

Nakagawara, Akira, Keiichi Ikeda, and Hideko Tasaka. 1988. "Dopaminergic Neuroblastoma as a Poor Prognostic Subgroup." *Journal of Pediatric Surgery*.

Ogawa, Seishi, Junko Takita, Masashi Sanada, and Yasuhide Hayashi. 2011. "Oncogenic Mutations of ALK in Neuroblastoma." *Cancer Science* 102(2):302–8.

Panche, A. N., A. D. Diwan, and S. R. Chandra. 2016. "Flavonoids: An Overview." *Journal of Nutritional Science* 5.

Park, Julie R., Rochelle Bagatell, Wendy B. London, John M. Maris, Susan L. Cohn, Katherine M. Mattay, and Michael Hogarty. 2013a. "Children's Oncology Group's 2013 Blueprint for Research: Neuroblastoma." *Pediatric Blood and Cancer* 60(6):985–93.

Patane, Michael A., Ann L. Scott, Theodore P. Broten, Raymond S. L. Chang, Richard W. Ransom, Jerry DiSalvo, Carlos Forray, and Mark G. Bock. 1998. "4-Amino-2-[4-[1-(Benzyloxycarbonyl)-2(s)- [[(1,1- Dimethylethyl)Amino]Carbonyl]- Piperazinyl]-6,7-Dimethoxyquinazoline (L- 765,314): A Potent and Selective α(1b) Adrenergic Receptor Antagonist." *Journal of Medicinal Chemistry* 41(8):1205–8.

Pattyn, Alexandre, Xavier Morin, Harold Cremer, Christo Goridis, and Jean François Brunet. 1999. "The Homeobox Gene Phox2b Is Essential for the Development of Autonomic Neural Crest Derivatives." *Nature* 399(6734):366–70.

Perez, Pinero C., A. Bruzzone, M. G. Sarappa, L. F. Castillo, and I. A. Luthy. 2011. "Involvement of Alpha(2) - and Beta(2) -Adrenoceptors on Breast Cancer Cell Proliferation and Tumor Growth Regulation." *Br.J.Pharmacol.* (1476-5381 (Electronic)).

Phhlman, Sven, Lars Abrahamsson, Maria E. K. Mattsson, and Thomas Esscher. 1984. "Retinoic Acid-Induced Differentiation of Cultured Human Neuroblastoma Cells : A Comparison with Phorbolester-Induced Differentiation." 14:135–44.

Piacentini, M., L. Piredda, D. T. Starace, M. Annicchiarico-Petruzzelli, M. Mattei, S. Oliverio, M. G. Farrace, and G. Melino. 1996. "Differential Growth of N- and S-Type Human Neuroblastoma Cells Xenografted into Scid Mice. Correlation with Apoptosis." *The Journal of Pathology* 180(4):415–22.

Pinto, Navin R., Mark A. Applebaum, Samuel L. Volchenboum, Katherine K. Matthay,

Wendy B. London, Peter F. Ambros, Akira Nakagawara, Frank Berthold, Gudrun Schleiermacher, Julie R. Park, Dominique Valteau-Couanet, Andrew D. J. Pearson, and Susan L. Cohn. 2015. "Advances in Risk Classification and Treatment Strategies for Neuroblastoma." *Journal of Clinical Oncology : Official Journal of the American Society of Clinical Oncology* 33(27):3008–17.

Ponthan, Frida, Per Borgström, Moustapha Hassan, Erik Wassberg, Christopher P. F. Redfern, and Per Kogner. 2001. "The Vitamin A Analogues: 13-Cis Retinoic Acid, 9-Cis Retinoic Acid, and Ro 13-6307 Inhibit Neuroblastoma Tumor Growth in Vivo." *Medical and Pediatric Oncology* 36(1):127–31.

Procházková, D., I. Boušová, and N. Wilhelmová. 2011. "Antioxidant and Prooxidant Properties of Flavonoids." *Fitoterapia* 82(4):513–23.

Qiao, Jingbo, Pritha Paul, Sora Lee, Lan Qiao, Erlena Josifi, Joshua R. Tiao, and Dai H. Chung. 2012. "PI3K/AKT and ERK Regulate Retinoic Acid-Induced Neuroblastoma Cellular Differentiation." *Biochemical and Biophysical Research Communications* 424(3):421–26.

Ramos, Sonia. 2008. "Cancer Chemoprevention and Chemotherapy: Dietary Polyphenols and Signalling Pathways." *Molecular Nutrition and Food Research* 52(5):507–26.

Reynolds, C. P., P. F. Schindler, D. M. Jones, J. L. Gentile, R. T. Proffitt, and P. A. Einhorn. 1994. "Comparison of 13-Cis-Retinoic Acid to Trans-Retinoic Acid Using Human Neuroblastoma Cell Lines." *Progress in Clinical and Biological Research* 385:237–44.

Rizk, Pamela, Julio Salazar, Rita Raisman-Vozari, Marc Marien, Merle Ruberg, Francis Colpaert, and Thomas Debeir. 2006. "The Alpha2-Adrenoceptor Antagonist Dexefaroxan Enhances Hippocampal Neurogenesis by Increasing the Survival and Differentiation of New Granule Cells." *Neuropsychopharmacology* 31(6):1146–57.

Rodríguez-García, Carmen, Cristina Sánchez-Quesada, José J. Gaforio, and José J. Gaforio. 2019. "Dietary Flavonoids as Cancer Chemopreventive Agents: An Updated Review of Human Studies." *Antioxidants* 8(5):137.

Ross, R. A., B. A. Spengler, C. Domenech, M. Porubcin, W. J. Rettig, and J. L. Biedler. 1995. "Human Neuroblastoma I-Type Cells Are Malignant Neural Crest Stem Cells." *Cell Growth and Differentiation* 6(4):449–56.

Ross, Robert A., June L. Biedler, and Barbara A. Spengler. 2003. "A Role for Distinct Cell Types in Determining Malignancy in Human Neuroblastoma Cell Lines and Tumors." Pp. 35–39 in *Cancer Letters*. Vol. 197. Elsevier Ireland Ltd.

Ross, Robert A., Barbara A. Spengler, and June L. Biedler. 1983. "Coordinate Morphological and Biochemical Interconversion of Human Neuroblastoma Cells." *Journal of the National Cancer Institute* 71(4):741–47.

Ruffolo, R. R., A. J. Nichols, J. M. Stadel, and J. P. Hieble. 1991. "Structure and Function of α-Adrenoceptors." *Pharmacological Reviews* 43(4):475–505.

Ruiz-Pérez, María Victoria, Aine Brigette Henley, and Marie Arsenian-Henriksson. 2017. "The MYCN Protein in Health and Disease." *Genes* 8(4).

Sarkar, Fazlul H., Yiwei Li, Zhiwei Wang, and Dejuan Kong. 2009. "Cellular Signaling Perturbation by Natural Products." *Cellular Signalling* 21(11):1541–47.

Schleiermacher, G., V. Mosseri, W. B. London, J. M. Maris, G. M. Brodeur, E. Attiyeh, M. Haber, J. Khan, A. Nakagawara, F. Speleman, R. Noguera, G. P. Tonini, M. Fischer, I. Ambros, T. Monclair, K. K. Matthay, P. Ambros, S. L. Cohn, and A. D. J. Pearson. 2012. "Segmental Chromosomal Alterations Have Prognostic Impact in Neuroblastoma: A Report from the INRG Project." *British Journal of Cancer* 107(8):1418–22.

Schleiermacher, Gudrun, Isabelle Janoueix-Lerosey, Agnès Ribeiro, Jerzy Klijanienko, Jérôme Couturier, Gaëlle Pierron, Véronique Mosseri, Alexander Valent, Nathalie Auger, Dominique Plantaz, Hervé Rubie, Dominique Valteau-Couanet, Franck Bourdeaut, Valérie Combaret, Christophe Bergeron, Jean Michon, and Olivier Delattre. 2010. "Accumulation of Segmental Alterations Determines Progression in Neuroblastoma." *Journal of Clinical Oncology* 28(19):3122–30.

Seefelder, Christian, J. William Sparks, Deborah Chirnomas, Lisa Diller, and Robert C. Shamberger. 2005. "Perioperative Management of a Child with Severe Hypertension from a Catecholamine Secreting Neuroblastoma." *Paediatric Anaesthesia*.

Seeger, Robert C., Garrett M. Brodeur, Harland Sather, Andree Dalton, Stuart E. Siegel, Kwan Y. Wong, and Denman Hammond. 1985. "Association of Multiple Copies of the N-Myc Oncogene with Rapid Progression of Neuroblastomas." *New England Journal of Medicine* 313(18):1111–16.

Sendo, Dai, Michihiko Katsuura, Kaori Akiba, Shinkichi Yokoyama, Saori Tanabe, Takashi Wakabayashi, Satoshi Sato, Shinsuke Otaki, Kazuya Obata, Iwao Yamagiwa, and Kiyoshi Hayasaka. 1996. "Severe Hypertension and Cardiac Failure Associated with Neuroblastoma: A Case Report." *Journal of Pediatric Surgery* 31(12):1688–90.

Shan, Tao, Qingyong Ma, Dong Zhang, Kun Guo, Han Liu, Fengfei Wang, and Erxi Wu. 2011. "B2-Adrenoceptor Blocker Synergizes with Gemcitabine to Inhibit the Proliferation of Pancreatic Cancer Cells via Apoptosis Induction." *European Journal of Pharmacology* 665(1–3):1–7.

Shen, Su Gang, Dong Zhang, Heng Tong Hu, Jun Hui Li, Zheng Wang, and Qing Yong Ma. 2008. "Effects of α-Adrenoreceptor Antagonists on Apoptosis and Proliferation of Pancreatic Cancer in Vitro." *World Journal of Gastroenterology* 14(15):2358–63.

Sidarovich, Viktoryia, Valentina Adami, and Alessandro Quattrone. 2014. "A Cell-Based High-Throughput Screen Addressing 3′UTR-Dependent Regulation of the MYCN Gene." *Molecular Biotechnology* 56(7):631–43.

Sidell, Neil, Adrienne Altman, Mark R. Haussler, and Robert C. Seeger. 1983. "Effects of Retinoic Acid (RA) on the Growth and Phenotypic Expression of Several Human

Neuroblastoma Cell Lines." *Experimental Cell Research* 148(1):21–30.
Sidell, Neil, Los Angeles, and Santa Clara. 1982. "Retinoic Acid-Induced Growth Inhibition and Morphologic Differentiation of Human Neuroblastoma Cells In Vitro". *JNCI: Journal of the National Cancer Institute* 68(4).
Smith, Valeria and Jennifer Foster. 2018b. "High-Risk Neuroblastoma Treatment Review." *Children* 5(9):114.
Souttou, Boussad, Nicole Brunet-De Carvalho, Daniel Raulais, and Marc Vigny. 2001. "Activation of Anaplastic Lymphoma Kinase Receptor Tyrosine Kinase Induces Neuronal Differentiation through the Mitogen-Activated Protein Kinase Pathway." *Journal of Biological Chemistry* 276(12):9526–31.
Spengler, B. A., D. L. Lazarova, R. A. Ross, and J. L. Biedler. 1997. "Cell Lineage and Differentiation State Are Primary Determinants of MYCN Gene Expression and Malignant Potential in Human Neuroblastoma Cells." *Oncology Research* 9(9):467–76.
Spitz, Ruediger, Barbara Hero, Karen Ernestus, and Frank Berthold. 2003. "Deletions in Chromosome Arms 3p and 11q Are New Prognostic Markers in Localized and 4s Neuroblastoma." *Clinical Cancer Research* 9(1 I):52–58.
Stein, C. Michael. 2012. "β-Adrenergic Receptors." Pp. 59–61 in *Primer on the Autonomic Nervous System*. Elsevier Inc.
Strell, Carina, Bernd Niggemann, Melanie J. Voss, Desmond G. Powe, Kurt S. Zänker, and Frank Entschladen. 2012. "Norepinephrine Promotes the B1-Integrin-Mediated Adhesion of MDA-MB-231 Cells to Vascular Endothelium by the Induction of a GROα Release." *Molecular Cancer Research* 10(2):197–207.
Strenger, Volker, Reinhold Kerbl, Hans Jürgen Dornbusch, Ruth Ladenstein, Peter F. Ambros, Inge M. Ambros, and Christian Urban. 2007. "Diagnostic and Prognostic Impact of Urinary Catecholamines in Neuroblastoma Patients." *Pediatric Blood and Cancer*.
Strother, Douglas R., Wendy B. London, Mary Lou Schmidt, Garrett M. Brodeur, Hiroyuki Shimada, Paul Thorner, Margaret H. Collins, Edward Tagge, Stanton Adkins, C. Patrick Reynolds, Kevin Murray, Robert S. Lavey, Katherine K. Matthay, Robert Castleberry, John M. Maris, and Susan L. Cohn. 2012. "Outcome after Surgery Alone or with Restricted Use of Chemotherapy for Patients with Low-Risk Neuroblastoma: Results of Children's Oncology Group Study P9641." *Journal of Clinical Oncology* 30(15):1842–48.
Thiele, Carol J. 1998. *Neuroblastoma Cell Lines -- Molecular Features.Pdf*. Vol. 1.
Thiele, Carol J., C. Patrick Reynolds, and Mark A. Israel. 1985. "Decreased Expression of N-Myc Precedes Retinoic Acid-Induced Morphological Differentiation of Human Neuroblastoma." *Nature* 313(6001):404–6.
Thilakarathna, Surangi H. and H. P. Vasantha Rupasinghe. 2013. "Flavonoid Bioavailability and Attempts for Bioavailability Enhancement." *Nutrients*

5(9):3367–87.

Trochet, Delphine, Franck Bourdeaut, Isabelle Janoueix-Lerosey, Anne Deville, Loïc De Pontual, Gudrun Schleiermacher, Carole Coze, Nicole Philip, Thierry Frébourg, Arnold Munnich, Stanislas Lyonnet, Olivier Delattre, and Jeanne Amiel. 2004. "Germline Mutations of the Paired-Like Homeobox 2B (PHOX2B) Gene in Neuroblastoma." *American Journal of Human Genetics* 74(4):761–64.

Trochet, Delphine, Seok Jong Hong, Jin Kyu Lim, Jean-François Brunet, Arnold Munnich, Kwang-Soo Kim, Stanislas Lyonnet, Christo Goridis, and Jeanne Amiel. 2005. "Molecular Consequences of PHOX2B Missense, Frameshift and Alanine Expansion Mutations Leading to Autonomic Dysfunction." *Human Molecular Genetics* 14(23):3697–3708.

Vázquez, Stella Maris, Alejandro Gustavo Mladovan, Cecilia Pérez, Ariana Bruzzone, Alberto Baldi, and Isabel Alicia Lüthy. 2006. "Human Breast Cell Lines Exhibit Functional A2-Adrenoceptors." *Cancer Chemotherapy and Pharmacology* 58(1):50–61.

Veal, Gareth J., Julie Errington, Sophie E. Rowbotham, Nicola A. Illingworth, Ghada Malik, Michael Cole, Ann K. Daly, Andrew D. J. Pearson, and Alan V. Boddy. 2013. "Adaptive Dosing Approaches to the Individualization of 13-Cis-Retinoic Acid (Isotretinoin) Treatment for Children with High-Risk Neuroblastoma." *Clinical Cancer Research* 19(2):469–79.

Verly, Iedan R. N., André B. P. van Kuilenburg, Nico G. G. M. Abeling, Susan M. I. Goorden, Marta Fiocco, Frédéric M. Vaz, Max M. van Noesel, C. Michel Zwaan, Gert Jan L. Kaspers, Johannes H. M. Merks, Huib N. Caron, and Godelieve A. M. Tytgat. 2017. "Catecholamines Profiles at Diagnosis: Increased Diagnostic Sensitivity and Correlation with Biological and Clinical Features in Neuroblastoma Patients." *European Journal of Cancer* 72:235–43.

Villablanca, J. G., A. A. Khan, V. I. Avramis, R. C. Seeger, K. K. Matthay, N. K. Ramsay, and C. P. Reynolds. 1995. "Phase I Trial of 13-Cis-Retinoic Acid in Children with Neuroblastoma Following Bone Marrow Transplantation." *Journal of Clinical Oncology : Official Journal of the American Society of Clinical Oncology* 13(4):894–901.

Wakamatsu, Yoshio, Yuko Watanabe, Harukazu Nakamura, and Hisato Kondoh. 1997. "Regulation of the Neural Crest Cell Fate by N-Myc: Promotion of Ventral Migration and Neuronal Differentiation." *Development* 124(10):1953–62.

Wang, Zhiwei, Yuxiang Zhang, Sanjeev Banerjee, Yiwei Li, and Fazlul H. Sarkar. 2006. "Inhibition of Nuclear Factor KB Activity by Genistein Is Mediated via Notch-1 Signaling Pathway in Pancreatic Cancer Cells." *International Journal of Cancer* 118(8):1930–36.

Westerlund, Isabelle, Yao Shi, Konstantinos Toskas, Stuart M. Fell, Shuijie Li, Olga Surova, and Erik Södersten. 2017. "Combined Epigenetic and Differentiation-

Based Treatment Inhibits Neuroblastoma Tumor Growth and Links HIF2 α to Tumor Suppression." 6137–46.

Wolter, Jennifer K., Nikolaus E. Wolter, Alvaro Blanch, Teresa Partridge, Lynn Cheng, Daniel A. Morgenstern, Monika Podkowa, David R. Kaplan, and Meredith S. Irwin. 2014. "Anti-Tumor Activity of the Beta-Adrenergic Receptor Antagonist Propranolol in Neuroblastoma." *Oncotarget* 5(1):161–72.

Xu, Wen Ping, Xin Zhang, and Wei Fen Xie. 2014. "Differentiation Therapy for Solid Tumors." *Journal of Digestive Diseases* 15(4):159–65.

Yang, Liqun, Xiao-Xue Ke, Fan Xuan, Juan Tan, Jianbing Hou, Mei Wang, Hongjuan Cui, and Yundong Zhang. 2016. "*PHOX2B* Is Associated with Neuroblastoma Cell Differentiation." *Cancer Biotherapy and Radiopharmaceuticals* 31(2):44–51.

Yong, Sun Lee and Anindya Dutta. 2007. "The Tumor Suppressor MicroRNA Let-7 Represses the HMGA2 Oncogene." *Genes and Development* 21(9):1025–30.

Zeineldin, Maged, Sara Federico, Xiang Chen, Yiping Fan, Beisi Xu, Elizabeth Stewart, Xin Zhou, Jongrye Jeon, Lyra Griffiths, Rosa Nguyen, Jackie Norrie, John Easton, Heather Mulder, Donald Yergeau, Yanling Liu, Jianrong Wu, Collin Van Ryn, Arlene Naranjo, Michael D. Hogarty, Marcin M. Kamiński, Marc Valentine, Shondra M. Pruett-Miller, Alberto Pappo, Jinghui Zhang, Michael R. Clay, Armita Bahrami, Peter Vogel, Seungjae Lee, Anang Shelat, Jay F. Sarthy, Michael P. Meers, Rani E. George, Elaine R. Mardis, Richard K. Wilson, Steven Henikoff, James R. Downing, and Michael A. Dyer. 2020. "MYCN Amplification and ATRX Mutations Are Incompatible in Neuroblastoma." *Nature Communications* 11(1):1–20.

Zhang, Hong Wei, Jin Jiao Hu, Ruo Qiu Fu, Xin Liu, Yan Hao Zhang, Jing Li, Lei Liu, Yu Nong Li, Qin Deng, Qing Song Luo, Qin Ouyang, and Ning Gao. 2018. "Flavonoids Inhibit Cell Proliferation and Induce Apoptosis and Autophagy through Downregulation of PI3Kγ Mediated PI3K/AKT/MTOR/P70S6K/ULK Signaling Pathway in Human Breast Cancer Cells." *Scientific Reports* 8(1):1–13.

Zhong, Hongying and Kenneth P. Minneman. 1999. "Differential Activation of Mitogen-Activated Protein Kinase Pathways in PC12 Cells by Closely Related A1-Adrenergic Receptor Subtypes." *Journal of Neurochemistry* 72(6):2388–96.

ACKNOWLEDGMENTS

I thank Professor Alessandro Quattrone for the opportunity to carry out my PhD in his laboratory. A special thanks to Dr Pamela Gatto for practical support in wet lab work, proficient discussion on data and her kindness.

Thanks to all the members of the LTG lab for being amazing colleagues. A heartfelt thanks to Chiara and Simona, you were my “partners in crime” during our PhD; I can easily say that without you everything would have been much more difficult. A further thanks to Chiara for our friendship inside and outside the laboratory, thank you because you are always there when I need you; I am very lucky to have found you on my path. Thanks to Paolo for being on my side and supporting me every day.

Finally, my most grateful thank goes out to my family. Thank you for giving me the strength and courage to not give up when I’ve fallen, thanks for being my safe place, thank you to have thaught to me to always work hard to make my dreams come true.